Towards an *in vivo* understanding of RNase H1 regulation in *Saccharomyces cerevisiae*

Dissertation

Zur Erlangung des Grades

Doktor der Naturwissenschaften

(Dr. rer. nat.)

Am Fachbereich Biologie

der Johannes Gutenberg-Universität Mainz

Carolin Birgit Wagner

Geboren am 1. September 1993 in Aschaffenburg, Deutschland

Mainz, März 2025

Dekan: Prof. Dr. Eckhard Thines

1. Berichterstatter: Prof. Dr. Brian Luke

2. Berichterstatter: Prof. Dr. Petra Beli

Datum der mündlichen Prüfung: 06.05.2025

Declaration

I, Carolin Birgit Wagner, declare that the work presented in this thesis is my own. I confirm that any information or data obtained from other sources is appropriately indicated in the thesis.

Mainz, _____ _____

Table of content

List of Publications

1. Wagner C.B. and Luke B. (2022) 'DNA–RNA Hybrids at Telomeres in Budding Yeast', *Methods in Molecular Biology*, 2528, pp. 145–157. Available at: https://doi.org/10.1007/978-1-0716-2477-7_10.

2. Misino S., Busch A., Wagner C.B., Bento F. and Luke B. (2022) 'TERRA increases at short telomeres in yeast survivors and regulates survivor associated senescence (SAS)', *Nucleic Acids Research*, 50(22), pp. 1–15. Available at: https://doi.org/10.1093/nar/gkac1125.

3. Pires V., Lohner N., Wagner T., Wagner C.B., Wilkens M., Hajikazemi M., Paeschke K., Butter F. and Luke B. (2023) 'RNA-DNA hybrids prevent resection at dysfunctional telomeres', *Cell Reports*, 42(2), p. 112077. Available at: https://doi.org/10.1016/j.celrep.2023.112077.

4. Wagner C.B., Longaretti M., Sergi S., Bento F., Wong R., Wilkens M., Butter F., Ulrich H.U. and Luke B. 'Transcription-replication conflicts drive RNase H1 expression in the absence of Sen1' (under revision with Cell Reports)

Abstract

RNA:DNA hybrids are structures, in which RNA base pairs with DNA. A special kind of RNA:DNA hybrid is called R-loop. R-loops are three-stranded structures, in which one DNA strand is displaced by the RNA portion of the hybrid. These structures have multiple functions in cells that can be beneficial, like regulating transcription or allowing error-free DNA repair, or detrimental, like stalling of the replication fork or mutagenesis of the displaced ssDNA strand. Due to the positive and negative functions of RNA:DNA hybrids, these structures have to be tightly regulated. Different kinds of enzymes exist for preventing or resolving RNA:DNA hybrids. Ribonucleases H (RNases H) for example can degrade the RNA portion of the hybrids, while Sen1 helicase and the human homologue Senataxin can unwind RNA:DNA hybrids and prevent their formation.

While RNase H2's regulation has been studied, little is known about RNase H1 regulation. It has been shown that RNase H1 mainly acts in genomic regions with a high RNA:DNA hybrid density. The enzyme also binds to RNA:DNA hybrids outside these regions of high RNA:DNA hybrid density, but the probability for degradation is low in these regions.

The aim of this study is to gain a broader understanding of RNase H1 regulation. I could show, that RNase H1 does not influence regulatory RNA:DNA hybrids in the budding yeast *S. cerevisiae* as overexpression of the enzyme or the catalytic inactive allele does not change the transcriptome. Furthermore, in the absence of Sen1, RNase H1 function is important for viability. This importance of RNase H1 most likely is the reason for the upregulation of the enzyme. Sen1 is traveling with the replisome and there preventing transcription-replication conflicts. In this work I showed that RNase H1 is acting together with Sen1 in this function. If Sen1 is gone or a loss of function mutant was used, RNase H1 served as a backup. As transcription-replication conflicts arise during replication, it is not surprising, that for upregulation of RNase H1 cells have to go through S-phase. Furthermore, transcription-replication conflicts favor the formation of R-loops. I showed that these R-loops are triggering a higher expression of RNase H1. In summary, I found a new function of RNase H1 in the prevention and resolution of transcription-replication conflicts in this study that impacts the regulation of RNase H1.

Zusammenfassung

RNA:DNA Hybride sind natürlich vorkommende Strukturen, bei deren Bildung RNA mit DNA hybridisiert. Eine Sonderform, R-loop genannt, zeichnet sich dadurch aus, dass der durch RNA ersetzte DNA Strang als einzelsträngige DNA erhalten bleibt. Diese Strukturen haben einige vorteilhafte Funktionen in der Zelle. Beispielsweise regulieren sie die Transkription und sind wichtig für die korrekte Reparatur von DNA Doppelstrangbrüchen. Andererseits können R-loops jedoch zu DNA Defekten und Mutationen führen, zum Beispiel durch erleichterte Basenmutation in einzelsträngiger DNA oder durch das Blockieren der Replikations-maschinerie. Da diese Strukturen viele positive und negative Eigenschaften haben müssen sie gut reguliert werden. Hierfür gibt es verschiedene Enzyme. Ein Prominentes Beispiel sind Ribonukleasen H (RNase H). Diese können die RNA des RNA:DNA Hybrids verdauen und so eine Hybridisierung der beiden DNA Stränge begünstigen. Während die Regulation von RNase H2 bereits erforscht wurde, ist wenig über die Regulation von RNase H1 bekannt. Es konnte bereits gezeigt werden, dass sie bevorzugt dort im Genom RNA:DNA Hybride verdaut, wo eine hohe Dichte dieser Strukturen vorhanden ist, während lokal niedrige RNA:DNA Hybrid Konzentrationen zu einer Bindung durch RNase H1 führt, die katalytische Aktivität jedoch nicht einsetzt.

Ziel dieser Studie ist es die Regulation von RNase H1 besser zu verstehen. Ich konnte zeigen, dass das Enzym keinen Einfluss auf regulatorische RNA:DNA Hybride hat, da die Überexpression des Enzyms oder des katalytisch inaktiven Allels das Transkriptom nicht verändert. Des Weiteren wird es in Abwesenheit der RNA:DNA Helikase Sen1 höher exprimiert. Sen1 hat in der Zelle verschiedene Funktionen. Sie liegen in der Transkriptionstermination sowie in der Vorbeugung von Transkriptions-Replikations Konflikten. Ich konnte zeigen, dass RNase H1 spezifisch auf die Akkumulation von Transkriptions-Replikations Konflikten reagiert und wichtig für das Überleben der Zellen ist, wenn sich diese häufen. Da für diesen Prozess aktive Replikation von Nöten ist, ist der Durchlauf der S-Phase des Zellzyklus Voraussetzung für die erhöhten RNase H1 Expression in den Zellen. Transkriptions-Replikations Konflikte begünstigen die Entstehung von R-loops. Ich konnte zeigen, dass diese als Signal für die erhöhte Expression von RNase H1 dienen. Zusammenfassend habe ich eine neue Funktion von RNase H1 in der Prävention und Auflösung von Transkriptions-Replikations Konflikten gefunden, die maßgeblich mit der Regulation des Enzyms zusammenhängt.

List of Figures

Abbreviations

3’RACE
3’ rapid amplification of cDNA-ends.
5-Ph-IAA
5-Phenyl-1H-indole-3-acetic acid.
AID*
auxin-inducible degron.
ALT
Alternative lengthening of telomeres.
AOA2
Ataxia with oculomotor apraxia type 2.
ATP
Adenosine triphosphate.
bp
Base pair.
BRCA1
Breast Cancer 1.
BSA
Bovine serum albumin.
CAT
Catalytic domain.
CD
Co-directional.
cDNA
Complementary DNA.
ChIP
Chromatin immunoprecipitation.
CHX
Cycloheximide.
ddH_20
Double distilled water.
ddH_2O
Double destilled water.
ddPCR
Digital droplet PCR.
DDR
DNA damage response.
DMSO
Dimethyl sulfoxide.
DNA
Deoxyribonucleic acid. ,
dNMP
Deoxyribonucleoside Monophosphate.
DRIP
DNA:RNA immunoprecipitation.
DSB
Double strand break.
dsDNA
Double-stranded DNA.
EDTA
Ethylenediaminetetraacetic acid.
EtOH
Ethanol.
FACS
Fluorescence Activated Cell Sorting.
FL
Full length.
HB
Hybrid binding domain.
HDR
homology-directed repair.
HO
Head-on.
HR
Homologous recombination.
HU
Hydroxyurea.
IAA
indole-3-acetic acid.
IP
immunoprecipitation.
kb
Kilo base pair.
LB
Luria broth.
MATa
Mating type a.
MATalpha
Mating type alpha.
MES
2-(N-Morpholino)ethansulfonic acid.
MMS
Methyl methanesulfonate.
mRNP
Messenger Ribonucleoprotein.
mtDNA
Mitochondrial DNA.
NaN3
Sodium azide.

NHEJ
non-homologous end joining.
NNS
Nrd1-Nab3-Sen1.
nt
Nucleotide.
OD_{600}
Optical density at 600 nm.
PBS-T
Phosphate buffered saline with Tween-20.
PCR
Polymerase Chain Reaction.
PFA
Paraformaldehyde.
qDRIP
Quantitative DRIP.
qPCR
quantitative PCR.
rDNA
Ribosomal DNA.
RER
Ribonucleotide Excision Repair.
RNA
Ribonucleic acid. ,
RNAP I
RNA polymerase I.
RNAP II
RNA polymerase II.
RNAP III
RNA polymerase III.
RNase H
Ribonuclease H.
RNAseq
RNA sequencing.
rNMP
Ribonucleoside Monophosphate.
ROI
Region of interest.
RPA
Replication protein A complex.
RT
Reverse transcription.
Room temperature.
SC
Synthetic complete.
SDS
Sodium dodecyl sulfate.
SDS-PAGE
SDS polyacrylamide gel electrophoresis.
SETX
Senataxin.
snoRNA
Small nucleolar RNA, 2
SOD
Sodium deoxycholate.
SPO
Sporulation.
ssDNA
Single-stranded DNA.
ssRNA
Single stranded RNA.
TCA
Trichloroacetic acid.
TGIRT-seq
Thermostable group II intron reverse transcriptases sequencing.
Top1
Topoisomerase 1.
TRC
transcription-replication conflict.
tRNA
Transfer RNA.
VE
Voll entsalzt.
YPD
Yeast Extract Peptone Dextrose.

1. Introduction

1.1 RNA:DNA hybrids

RNA:DNA hybrids (Figure 1 A) are abundant structures that arise within the genome when RNA (ribonucleic acid) base pairs with DNA (deoxyribonucleic acid). A special form of RNA:DNA hybrid is the R-loop (Figure 1 B). In this three-stranded structure, one strand of dsDNA (double-stranded DNA) is opened up and displaced by RNA. In this thesis I will refer to RNA:DNA hybrids in cases I cannot rule out that only R-loop structures are participating in a process. About 8 % of the budding yeast genome is prone to the formation of RNA:DNA hybrids (Wahba *et al.*, 2016), while about 5 % of the human genome form these structures (Sanz *et al.*, 2016). Furthermore, the expression level of a gene correlates positively with the amount of RNA:DNA hybrids detectable (Wahba *et al.*, 2016). R-loop structures usually range between 100 bp and about 450 bp, but exceptionally long structures can reach up to 2.7 kb in length (Malig *et al.*, 2020).

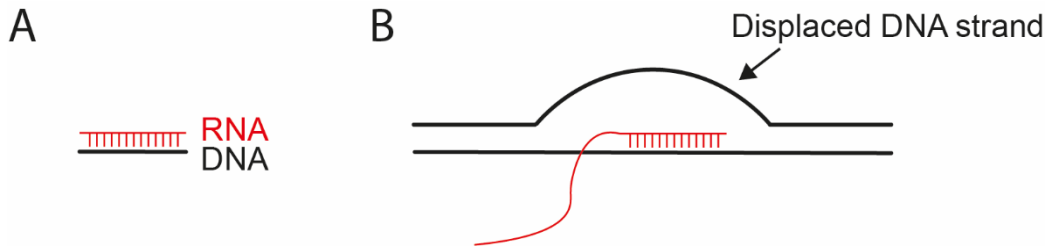

Figure 1 – RNA:DNA hybrid vs. R-loop – what is the difference? ***(A)*** *An RNA:DNA hybrid is a structure consisting of hybridized RNA and DNA. The term RNA:DNA hybrid does not give any information about the context the hybrid is in.* ***(B)*** *An R-loop refers to a RNA:DNA hybrid that results in an displaced DNA strand.*

1.1.1 The different kinds of RNA:DNA hybrids

Different kinds of RNA:DNA hybrids, including R-loops, exist and were reviewed by Niehrs and Luke (2020). They are classified into multiple groups which are illustrated in Figure 2. Incorporations of single ribonucleoside monophosphates (rNMPs) are the most abundant form of RNA:DNA hybrids. They arise during replication when an rNMP is incorporated into the newly synthesized DNA strand instead of a dNMP (Deoxyribonucleoside monophosphate) (reviewed by Cerritelli and El Hage, 2020; Niehrs and Luke, 2020). Longer RNA:DNA hybrid stretches can be, for example, found as RNA primers during lagging strand synthesis and have to be removed during Okazaki fragment maturation (reviewed by Sun *et al.*, 2023). Another form of RNA:DNA hybrid arises during telomere elongation (Greider

and Blackburn, 1989). Telomeres are the ends of linear chromosomes that protect the coding regions from erosion. In budding yeast, telomere elongating enzyme telomerase uses the RNA template *TLC1*, which base pairs to telomeric DNA for elongation of the telomeres (Singer and Gottschling, 1994).

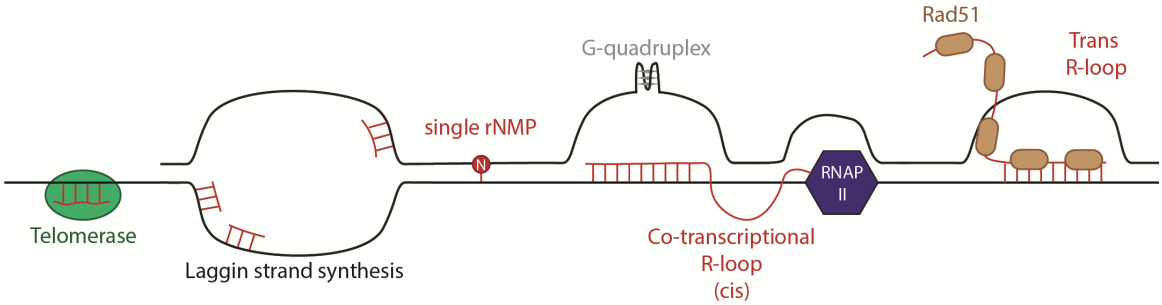

Figure 2 - Different classes of RNA:DNA hybrids and R-loops. Figure adapted from Niehrs and Luke (2020).

A special form of RNA:DNA hybrid are R-loop structures with their displaced DNA strand. These structures can arise co-transcriptional and downstream of the transcribing RNA polymerase ('cis' R-loop). Furthermore, R-loops can arise in 'trans' when RNA that is bound to different RNA binding proteins, like Rad51 or RPA, invades the dsDNA strand (Skourti-Stathaki, Proudfoot and Gromak, 2011; Wahba, Gore and Koshland, 2013; Feretzaki *et al.*, 2020; Lafuente-Barquero *et al.*, 2020; Mazina *et al.*, 2020).

A common feature of R-loops with G-rich displaced ssDNA is the formation of G-quadruplexes on the displaced strand (Zheng *et al.*, 2017; De Magis *et al.*, 2019). G-quadruplexes are very stable structures that can form in guanine-rich ssDNA strands. These structures can lead to a further stabilization of the R-loop. Genome stability is threatened by R-loops that associate with G-quadruplexes due to their high stability especially at tRNA (transfer RNA) genes (Tran *et al.*, 2017). The formation of G-quadruplexes can be prevented by coating of the ssDNA with the ssDNA binding protein RPA, while existing G-quadruplexes can be unwound by Pif1 helicase (Maestroni *et al.*, 2020).

1.1.2 RNA:DNA hybrid localization in the genome

R-loops have been mapped at ribosomal DNA (rDNA) loci, Ty elements, telomeres, snoRNAs (small nucleolar RNAs), tRNAs and in the mitochondrial genome, with 50 % of the R-loops mapping to rDNA loci (Chan *et al.*, 2014; El Hage *et al.*, 2014; Wahba *et al.*, 2016; Chen *et al.*, 2017). Furthermore, in budding yeast, hybrids often form at genes that are prone to antisense transcription (Chan *et al.*, 2014). Additionally, Wahba and colleagues (2016)

could show that RNA:DNA hybrids preferentially form at sequences with Poly-A tracts that are longer than 21 nt or that have an A/T skew, while most other publications associate R-loop formation with a G/C skew on the displaced DNA strand (Chan *et al.*, 2014; Chen *et al.*, 2017). Furthermore, it was shown that the RNA portion of an RNA:DNA hybrid can be a transcript that is transcribed by all RNA polymerases, especially at highly transcribed genes (Chan *et al.*, 2014; El Hage *et al.*, 2014). In budding yeast, RNA:DNA hybrids accumulate in the context of active transcription (El Hage *et al.*, 2014). Depending on the study, hotspots of RNA:DNA hybrids in yeast are at the second exon in case the gene is spliced, at promotors, at transcription start sites (5' end of the gene) and the most prominent at the transcription termination site at the 3' end of the gene (El Hage *et al.*, 2014; Sanz *et al.*, 2016; Wahba *et al.*, 2016; Chen *et al.*, 2017). Accumulation of RNA:DNA hybrids at promotors is caused by stalling of RNA polymerase II at the transcription start side. This stalling of the polymerase cannot be reversed by degradation of the R-loop (Chen *et al.*, 2017).

1.1.3 Cellular localization of RNA:DNA hybrids

The cellular location of RNA:DNA hybrids was for a long time clear to be in the nucleus and the mitochondria, but recently it could be shown by the Cimprich lab that in human cells cytoplasmic RNA:DNA hybrids exist (Crossley *et al.*, 2023). These hybrids are stable products that arise during the excision of R-loops in cells lacking Senataxin or BRCA1 (Breast Cancer 1), a protein that mediates binding of SETX helicase to termination regions (Hatchi *et al.*, 2015; Crossley *et al.*, 2023). Consequently, this class of RNA:DNA hybrids leads to the activation of an innate immune response. This is mediated by phosphorylation of Interferon regulatory factor 3, which leads to an upregulation of Interferon-β and in a consequence autophagy and cell death (Crossley *et al.*, 2023).

1.1.4 RNA:DNA hybrids – the timing matters

RNA:DNA hybrids are highly abundant in the cells and have an impact on several cellular processes. The outcome of the RNA:DNA hybrid can be good or bad for the cells. Whether the RNA:DNA hybrid is harmful to the cell or not depends mainly on the timing of the formation and resolution of the structure. Scheduled RNA:DNA hybrids ('Good' RNA:DNA hybrids) for example have implications in transcription regulation, epigenetic modification, class switch recombination, and DNA repair (Figure 3 A), while unscheduled RNA:DNA

hybrids ('Bad' RNA:DNA hybrids) cause DNA instability, interfere with transcription and block DNA replication (Figure 3 A; Yu *et al.*, 2003; Costantino and Koshland, 2015; Ohle *et al.*, 2016; Grunseich *et al.*, 2018; Ribeiro De Almeida *et al.*, 2018; Crossley, Bocek and Cimprich, 2019; Tan-Wong, Dhir and Proudfoot, 2019; Ortega *et al.*, 2021; Xu *et al.*, 2021). It has been described, that harmful RNA:DNA hybrids mostly form in 'cis' and in an Rad51-independent manner (Lafuente-Barquero *et al.*, 2020).

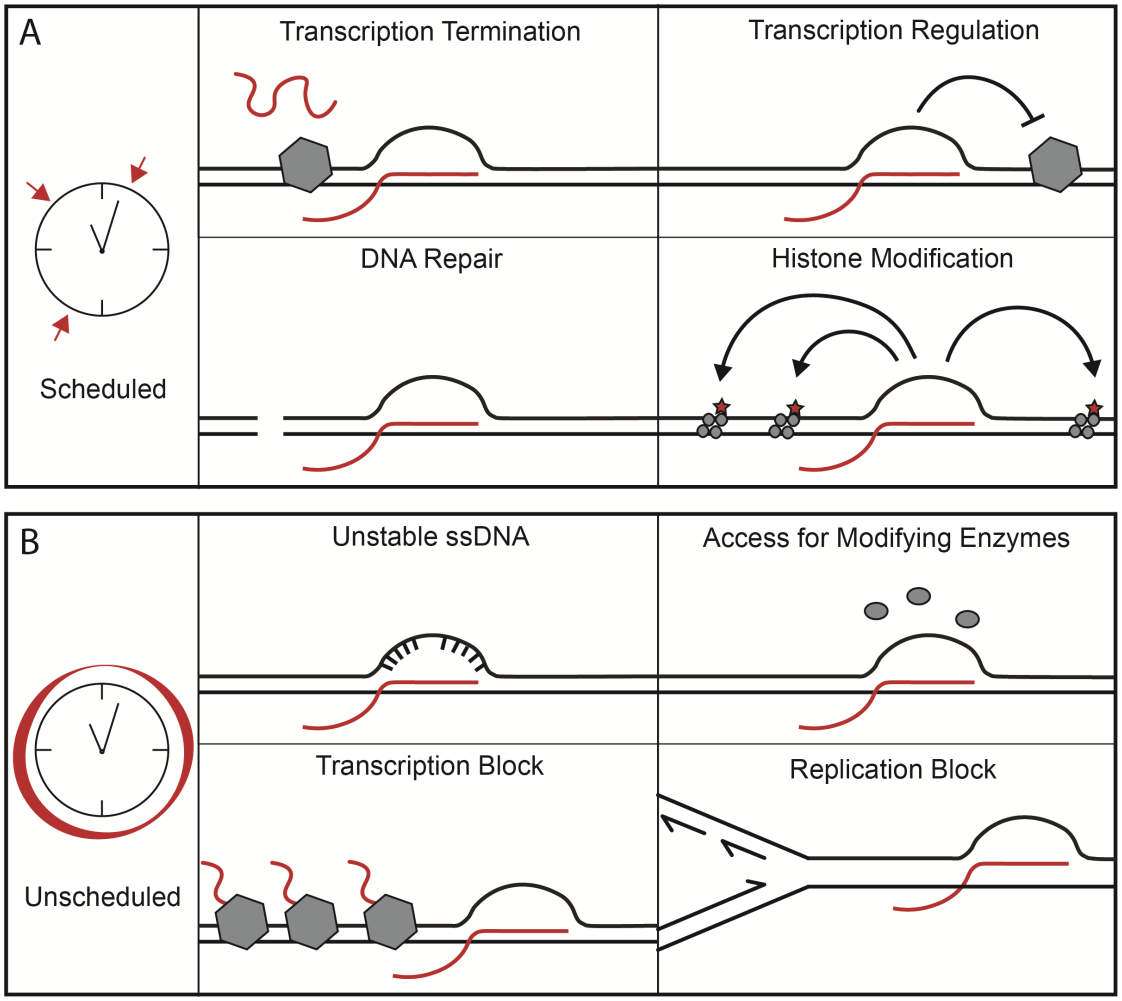

Figure 3 – Consequences of scheduled and unscheduled RNA:DNA hybrids. ***(A)*** *Scheduled RNA:DNA hybrids influence the cells by signaling transcription termination, inhibiting transcription, allowing DNA repair and mediating histone modification.* ***(B)*** *Unscheduled RNA:DNA hybrids have detrimental outcomes like instability of ssDNA, accessibility for modifying enzymes and blockage of transcription and replication. Figure modified from Costantino and Koshland (2015).*

1.1.5 Regulation of RNA:DNA hybrids

RNA:DNA hybrids are helpful regulators but can also have a detrimental outcome when they arise unscheduled. For this reason, they have to be tightly regulated for optimal cell survival and growth progression. Different proteins and enzymes are evolutionarily

conserved and either prevent the formation of RNA:DNA hybrid formation or resolve existing RNA:DNA hybrids. An important role in prevention of RNA:DNA hybrids is taken over by multiple RNA binding proteins that cover the newly synthesized RNA and, with this, prevent the hybridization of the nascent RNA to the DNA template. Consequently, also factors involved in RNA biogenesis that bind the RNA after transcription, like splicing factors (Figure 4 A) or factors important for RNA export to the cytoplasm, are important for restricting the RNA from hybridizing to DNA (Wahba *et al.*, 2011). An example for RNA export factors that prevent RNA:DNA hybrid formation is the THO/TREX complex (Figure 4 B). The THO/TREX complex is involved in the formation of messenger Ribonucleoproteins (mRNPs) and the mutation of complex members leads to an accumulation of co-transcriptional R-loops (Wellinger, Prado and Aguilera, 2006; San Martin-Alonso *et al.*, 2021). The complex consists of the proteins Hpr1, Mft1, Tho2 and Thp2 (Peña *et al.*, 2012). In the literature, often mutants of *HPR1* or *MFT1* are used for studying the impact of the THO/TREX complex on RNA:DNA hybrids. Especially deletion of *HPR1* leads to an increase of RNA:DNA hybrid levels over longer genes (Chan *et al.*, 2014). Additionally, in HPR1 mutants RNA:DNA hybrids accumulate in G1 and S-phase, causing a delay in replication progression (Gómez-González *et al.*, 2011; San Martin-Alonso *et al.*, 2021).

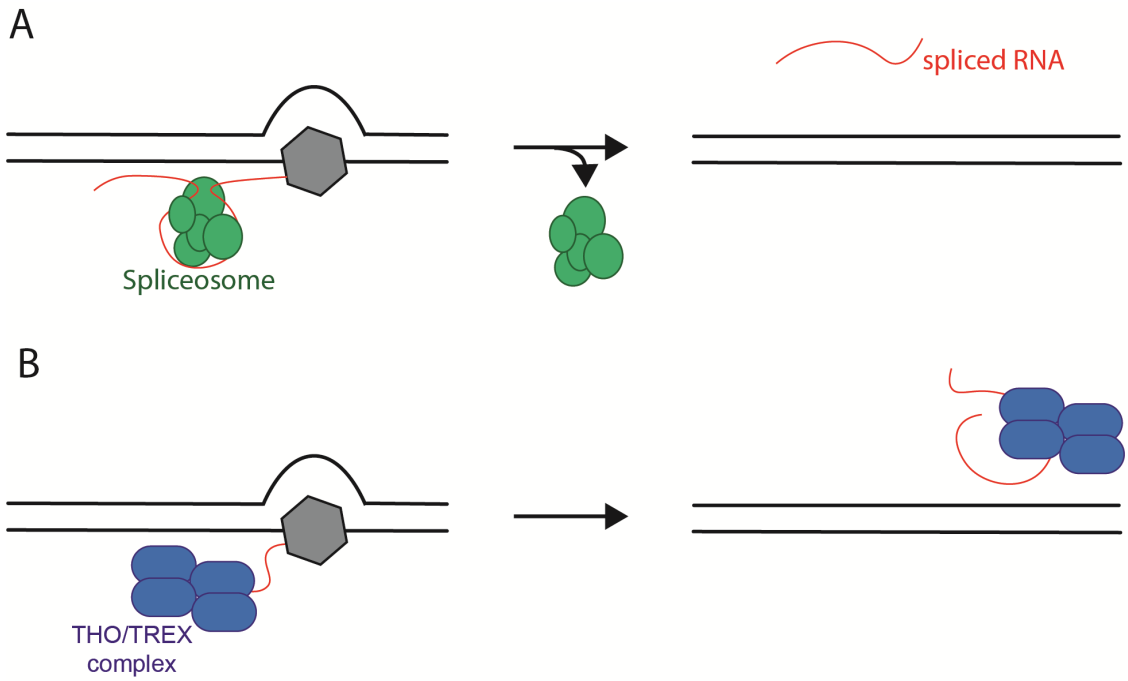

Figure 4 – Prevention of RNA:DNA hybrids by RNA binding proteins. ***(A)*** *The spliceosome binds the newly synthesized RNA co-transcriptionally and prevents the reannealing of it to the template DNA. This process results in spliced RNA.* ***(B)*** *The THO/TREX complex binds to newly transcribed RNA, preventing the hybridization of the RNA to the template DNA. Furthermore, the THO/TREX complex leads the RNA to the nuclear pores and mediated RNA export.*

Topological stress can stimulate RNA:DNA hybrid formation. This can be prevented for example by topoisomerase 1 (Top1). Top1 is known to resolve topological stress that arises during DNA unwinding in order to allow transcription. Additionally, this function prevents the formation of co-transcriptional R-loops because it limits the more open chromatin state behind the RNA polymerase (negative supercoiling) that is caused by polymerase movement along the DNA (Figure 5; reviewed by Kim and Jinks-Robertson, 2017). Nonetheless, besides reduction of RNA:DNA hybrid formation topoisomerase can favor R-loops in human cells (Manzo *et al.*, 2018).

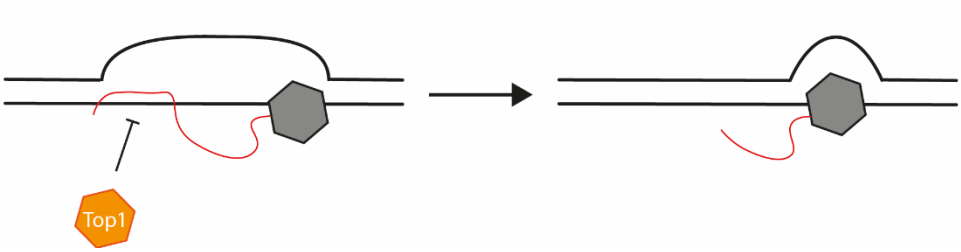

Figure 5 – Prevention of RNA:DNA hybrids by Top1. Top1 resolves torsional stress caused by the negative supercoiling behind the transcription machinery. This prevents the RNA from hybridizing to the template strand.

Even if multiple mechanisms inhibit RNA:DNA hybrid formation, RNA:DNA hybrids still arise and have to be removed in a timely manner. For this, two classes of enzymes exist: Ribonucleases and Helicases. Due to their importance for this work, these enzymes and their mode of action will be described in depth under 1.2 and 1.3.

1.2 Ribonucleases H

Ribonucleases H (RNases H) are enzymes that are conserved from bacteria to humans. These enzymes are non-essential in yeast, but essential in mice and human. In eukaryotes, RNase H1 and RNase H2 share their RNA:DNA hybrid degradation capability, while only RNase H2 is able to excise single rNMPs that are incorporated into the genomic DNA (Figure 6). In contrast to RNase H1, RNase H2 is a trimeric protein in yeast, encoded by the genes *RNH201, RNH202* and *RNH203.* With Rnh201 being the catalytic subunit of the enzyme. The absence of RNase H1 and RNase H2 leads to increased RNA:DNA hybrid levels and genome instability (Conover *et al.*, 2015; O'Connell, Jinks-Robertson and Petes, 2015; Wahba *et al.*, 2016; Sui *et al.*, 2022). This instability is mainly caused by the instability that the incorporated rNMP brings into the DNA strand. In alkaline conditions, the presence of the rNMP leads to hydrolysis and as a consequence to a single strand break in the DNA (McElhinny *et al.*, 2010). Furthermore, budding yeast cells are more sensitive to DNA

damage caused by genotoxic drugs like Hydroxyurea (HU) and Methyl methanesulfonate (MMS) that favor RNA:DNA hybrids in these conditions (Arudchandran *et al.*, 2000; Lockhart *et al.*, 2019; Cerritelli and El Hage, 2020; Heuzé *et al.*, 2023). After the resolution of this genotoxic stress caused by drugs, RNases H are essential for fork restart by stimulating RPA-coating of ssDNA (Heuzé *et al.*, 2023).

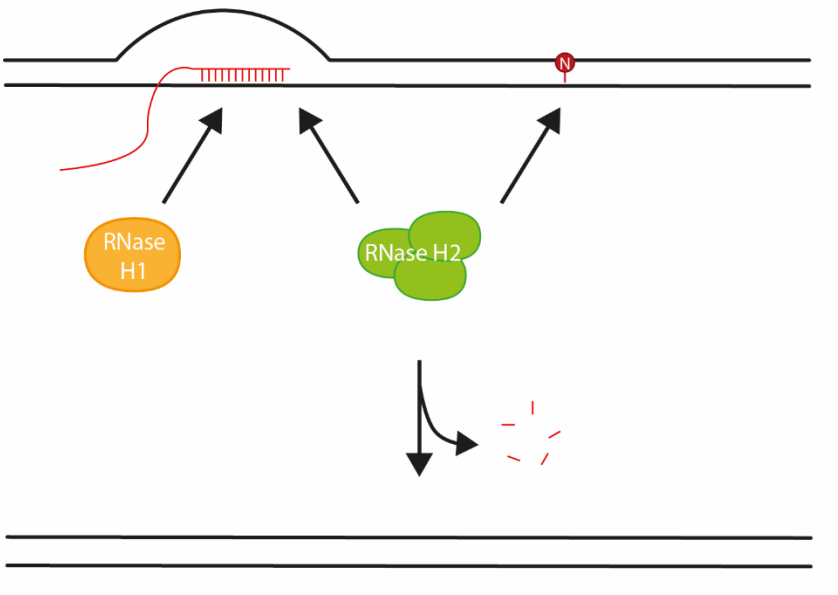

Figure 6 – Degradation of RNA:DNA hybrids by RNase H1 and RNase H2. Both RNases H are able to degrade RNA:DNA hybrids, while only RNase H2 is able to excise single rNMPs that were incorporated during replication.

Both RNases H especially target RNA:DNA hybrids transcribed by RNA polymerase III (RNAP III) (Chan *et al.*, 2014; El Hage *et al.*, 2014; Wahba *et al.*, 2016; Sagi *et al.*, 2024). RNase H1 and RNase H2 prevent RNA:DNA hybrid accumulation over long and highly transcribed genes (Chan *et al.*, 2014). Here, an accumulation would lead to genome instability, especially at the rDNA loci (Wahba *et al.*, 2011; O'Connell, Jinks-Robertson and Petes, 2015). Moreover, deletion of RNases H reduces the expression levels of tRNAs (El Hage *et al.*, 2014). In fission yeast, these RNA:DNA hybrids were shown to accumulate in S-phase and correlate with Rad52 foci, indicating the RNases H are important for resolving transcription-replication conflicts (Sagi *et al.*, 2024). Besides the accumulation in S-phase, RNA:DNA hybrids form over the whole cell cycle in *RNH1 RNH201* deletion mutants and cause DNA damage, indicating functions for RNA:DNA hybrid removal for RNase H1 and RNase H2 also outside of S-phase (Wahba *et al.*, 2011).

RNase H2 association to the chromatin is upregulated in late S-phase and G2/M-phase, where rNMP removal peaks. Removal of stretches of RNA:DNA hybrids can nonetheless be

performed during the whole cell cycle by RNase H2. For removal of rNMPs, RNase H2 travels with the replisome, where it binds to PCNA *via* its PIP-box and is recruited to it by Rtf2 (Bubeck *et al.*, 2011; Conti *et al.*, 2024). Furthermore, a recent study showed that RNase H2 activity is promoted by Smc5/6, ensuring removal of RNA:DNA hybrids at highly transcribed regions and the linear ends of the chromosomes, called telomeres (Roy *et al.*, 2024). In contrast to RNase H2, RNase H1 is important throughout the cell cycle in stressful situations where RNase H2 cannot handle the amount of RNA:DNA hybrids anymore (Lockhart *et al.*, 2019). While the regulation of RNase H2 is well studied, not much is known about RNase H1 regulation.

Besides RNA:DNA hybrid degradation *per se*, RNases H were also implicated to be involved in transcription termination after RNAP II stalling. Here the enzymes start degrading the RNA:DNA hybrid forming behind RNAP II, allowing Rat1 to enter and terminate the stalled transcription. Like this, new transcription cycles can start and transcription-replication conflicts are avoided (Mérida-Cerro *et al.*, 2024). In summary, RNases H are important enzymes for regulating RNA:DNA hybrid levels and preventing DNA damage.

1.2.1 Ribonuclease H1

Ribonuclease H1 (RNase H1 or Rnh1) is a monomeric enzyme that, in budding yeast, consists of two hybrid binding domains, a catalytic domain and connecting unstructured linker domains (Figure 7). Human RNase H1 has only one hybrid binding domain (Cerritelli and Crouch, 2009). The enzyme is important for degrading RNA:DNA hybrids genome-wide (Wahba *et al.*, 2011, 2016), but has a special role in replication of mitochondrial DNA (Holt, 2019). In budding yeast and humans, RNase H1 can be targeted to the mitochondria if translation is started from an alternative start codon, encoding a mitochondrial leading sequence (Suzuki *et al.*, 2010; Monteuuis *et al.*, 2019). Furthermore, RNase H1 can deplete co-transcriptional R-loops in the mitochondrial genome (El Hage *et al.*, 2014). In higher eukaryotes the deletion of RNase H1 is lethal due to this function in mitochondrial biogenesis (Cerritelli *et al.*, 2003), while lower eukaryotes like *S. cerevisiae* are viable without RNase H1.

Human RNase H1 has a cleavage preference for the sequence CA|AG (vertical line indicates cut site), following G-rich sequences (Kielpinski *et al.*, 2017). The catalytic activity can be

abolished by a single point mutation, which is D210N for human RNase H1 and D193N for budding yeast (Wu, Lima and Crooke, 2001; Zimmer and Koshland, 2016).

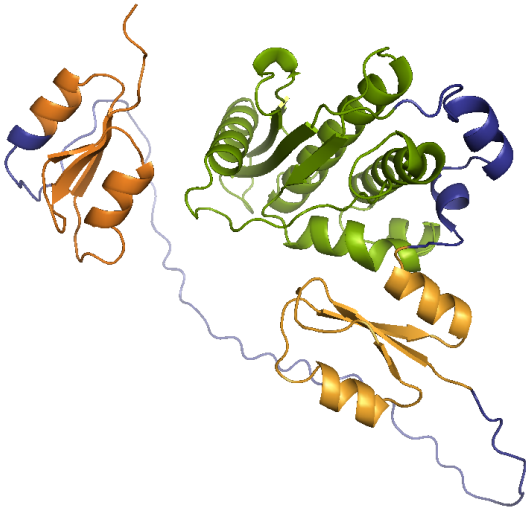

Figure 7 – Structure of RNase H1. The structure depicted was calculated by AlphaFold (Jumper et al.*, 2021). Orange/yellow: Hybrid binding domains, blue: Linker domains and green: catalytic domain.*

For a long time, RNases H1 have been seen as pure endonuclease (Hyjek, Figiel and Nowotny, 2019), but recently this view changed. First, it was shown in *E. coli* that RNase HI (bacterial RNase H1) can act as an exo- or endoribonuclease, depending on the substrate (Lee *et al.*, 2021). In case a 3' DNA overhang is present, RNase HI acts as a processive exoribonuclease *in vitro*, but as a distributive endonuclease on 5' DNA overhangs (Lee *et al.*, 2021). Furthermore, junctions between dsDNA and ssDNA can help the enzyme finding the R-loop, but blunt ends abolish the binding. Interestingly, the switch between exo- and endoribonuclease in budding yeast relies on another factor than in *E. coli*. Budding yeast RNase H1 starts degrading R-loops acting as an endonuclease and processes the RNA:DNA hybrid as an exonuclease once the degradation is started. Upon depletion, Replication Protein A complex (RPA) covers the ssDNA strand, promoting RNase H1 to act bidirectional, speeding up R-loop degradation (Li *et al.*, 2024). Furthermore, in human cells, RPA is an important stimulator for RNase H1 binding and activity towards R-loops when binding to the displaced ssDNA strand (Nguyen *et al.*, 2017). Additionally, the chromatin remodeler Smc5/6 promotes RPA binding during homologous recombination, indirectly influencing RNase H1 recruitment (Roy *et al.*, 2024).

In contrast to RNase H2 (Ribonuclease H2), RNase H1 in budding yeast does not act genome-wide, but in RNase H1 hot spot areas where a high density of RNA:DNA hybrids leads to genotoxic stress, while it is binding genome-wide (Zimmer and Koshland, 2016).

Furthermore, work from our lab could confirm that RNase H1 reacts to stress triggered by a high density of RNA:DNA hybrids and as a consequence accumulates on the chromatin (Lockhart *et al.*, 2019). Additionally, it was shown, that RNase H1 most likely acts as a backup mechanism for RNase H2 (O'Connell, Jinks-Robertson and Petes, 2015).

How budding yeast RNase H1 is recruited to chromatin in a stress-dependent manner is not clear. For human RNase H1 it is known, that the recruitment is mediated by m6A modification of the RNA. This modification is integrated by METTL3/14, which is recruited by the R-loop recognizing enzyme ARID1A (Zhang *et al.*, 2024). Furthermore, in an *in vitro* study it could be shown that human RNase H1 activity is decreased if the RNA portion of the RNA:DNA hybrid is modified with 2'OMe or inosine (Doxtader Lacy *et al.*, 2022). Besides RNA modifications, also DNA modifications can impair RNase H1 recruitment. It has been shown, that 8-oxoguanine accumulation in mitochondrial DNA (mtDNA) due to oxidative stress impairs RNase H1 recruitment, leading to higher RNA:DNA hybrid levels (Renaudin *et al.*, 2021). As RNase H1 is essential for the initiation of mitochondrial replication, this leads to the inhibition of mtDNA replication (Holt, 2019; Renaudin *et al.*, 2021). The influence of RNA and DNA modifications on RNase H1 activity could be an explanation of how the enzyme discriminates between RNA:DNA hybrids it is binding to and those it binds to and also degrades.

Expression of human RNase H1 is repressed by Sirt1 (Sir2 in budding yeast) and CHCHD2 and activated by G9a. G9a can methylate the RNase H1 promotor and with this inhibit the binding of CHCHD2 and Sirt1 (Li *et al.*, 2023). For yeast RNase H1 no direct activators or repressors are known.

Mutations in human RNase H1 have been implicated in cancer. 19 different cancer types show a significant upregulation of RNase H1, which correlates with a fatal outcome for the patients (Yi *et al.*, 2023). In summary, RNase H1 is important for avoidance of genotoxic stress and its mutations are implicated in cancer. Little is known about RNase H1 regulation, making it an important enzyme to study for getting a better understanding of these diseases.

1.2.2 RNase H in DNA damage

RNA:DNA hybrids are sources of DNA damage. Not only is the ssDNA strand of an R-loop prone to mutations, but the structure can also be a block for replication. Furthermore, co-

transcriptional R-loops can cause transcription-replication conflicts, which can lead to DNA damage (Alzu *et al.*, 2012; Costantino and Koshland, 2015; San Martin-Alonso *et al.*, 2021). In mammalian cells RNase H1 has a role in the resolution of transcription-replication conflicts. As a consequence, depletion of RNase H1 leads to increased RNA:DNA hybrid levels, slowed down fork progression and as a result DNA damage response (Parajuli *et al.*, 2017). Overexpression of RNase H1 reverses the effect of RNase H1 depletion, leading to an increased fork speed (Jones *et al.*, 2013). Furthermore, in bacterial cells, RNase HI is known to be recruited to transcription-replication conflicts in order to remove the R-loop moiety of the conflict (Wolak *et al.*, 2020) and the eukaryotic parasite *Leishmania major* shows changes in replication timing and increased DNA damage in the absence of RNase H1 (Damasceno *et al.*, 2025).

Not only can RNA:DNA hybrids be the cause of DNA damage, it was additionally shown in yeast that RNA:DNA hybrids accumulate at DSBs and need to be removed for efficient homologous recombination (HR) by recruiting RPA and inducing resection (Ohle *et al.*, 2016; Ortega *et al.*, 2021). On the contrary, if RNA:DNA hybrid levels are too low at DSBs, this can lead to loss of repeated sequence elements. This is the reason why the right amount of RNase H has to be present at the DSB, and both, deletion of *RNH1* and *RNH201* as well as overexpression of *RNH1* inhibit HR (Amon and Koshland, 2016; Ohle *et al.*, 2016; Ortega *et al.*, 2021). In the absence of RNase H, DSB repair is still possible. In these conditions, RNA:DNA hybrids accumulate and the S-phase checkpoint is activated, leading to DSB repair in a Mus81-dependent manner (Zhao *et al.*, 2018). Furthermore, depletion of Top1 in the absence of *RNH1* and *RNH201* activates the Rad9 checkpoint, leading to a G2/M arrest of the cells, but one of both RNases H is sufficient to prevent checkpoint activation and cell cycle arrest (Amon and Koshland, 2016). Moreover, in the absence of both RNases H, Top1 becomes essential during S-phase in order to prevent R-loop stress by preventing topological stress in G2/M-phase (Amon and Koshland, 2016). In summary, RNA:DNA hybrids have to be tightly regulated to allow for DNA damage and repair, which makes RNases H important enzymes for preventing DNA damage and allowing DNA repair. For this reason, RNase H1 is an especially interesting enzyme to study as its regulation is not well characterized.

1.3 Sen1 helicase

In addition to the degradation by RNases H, RNA:DNA hybrids can also be unwound by helicases. The most prominent example is Sen1, an Upf1-like helicase (Figure 8; Aiello, Porrua and Libri, 2025). Mutations in the human homologue to Sen1, Senataxin (SETX; belonging to Super Family 1B group of helicases) are associated with the neurodegenerative diseases amyotrophic lateral sclerosis 4 (ALS4) and ataxia with oculomotor apraxia type 2 (AOA2; Groh *et al.*, 2017; Giannini and Porrua, 2024). These diseases have been implicated with protein aggregation caused by dysregulated non-coding RNA expression, which is a feature of SETX depletion (Wen *et al.*, 2024). Furthermore, altered SETX levels have been found in human cancers (reviewed by Gatti *et al.*, 2023). Further helicases known to unwind RNA:DNA hybrids in human cells are for example Aquarius and Bloom, which are not conserved in budding yeast (Yang *et al.*, 2023).

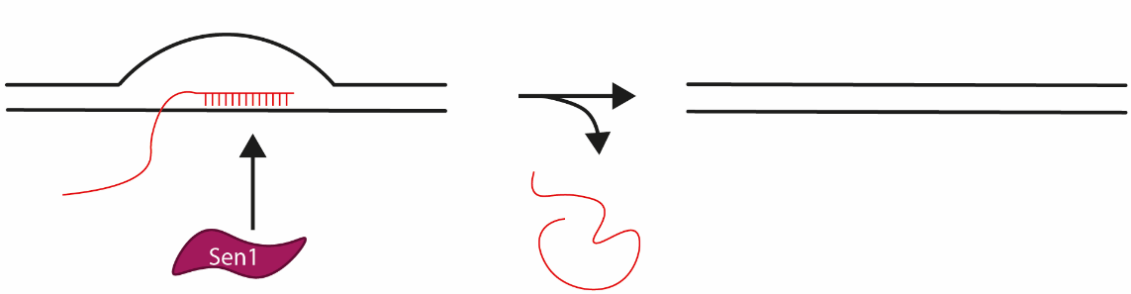

Figure 8 – Resolution of RNA:DNA hybrids by Sen1. Sen1 helicase unwinds the RNA:DNA hybrids, releasing the RNA.

Sen1 and Senataxin are nucleic acid dependent ATPases that unwind duplex substrates in a 5’ to 3’ directionality. Furthermore, both can translocate along single-stranded DNA or RNA in an ATP-dependent manner in the same directionality. Both enzymes are more efficient in unwinding dsDNA than dsRNA (Hasanova *et al.*, 2023). When it comes to loop structures, both enzymes need a 5’ RNA overhang for efficient unwinding. While SETX unwinds RNA:DNA hybrids more efficiently than DNA:DNA duplexes, Sen1 shows a higher activity for DNA:DNA duplexes than RNA:DNA hybrids (Hasanova *et al.*, 2023). Importantly, loss of function of Sen1 (*sen1-1* temperature sensitive mutant) leads RNA:DNA hybrids accumulation over short genes in general and tRNA genes in specific, which are also targeted by RNases H (Chan *et al.*, 2014). In human cells depletion of SETX leads to increased RNA:DNA hybrid levels over rDNA genes, peri-centromeric and intergenic regions, while protein coding regions are not influenced (Wen *et al.*, 2024).

Besides unwinding of RNA:DNA hybrids, Sen1 has multiple functions in the cells. Sen1 is known to be part of the Nrd1-Nab3-Sen1 (NNS) complex, in which Nrd1 and Nab3 recruit Sen1 to pausing RNAP II transcripts, releasing RNAP II and the transcript (Figure 9 A). In this process, Nrd1 binds to transcripts with the motives GUAA or GUAG, while Nab3 binds to UCUU(G). This is why AU-rich sequences are important for functional NNS mediated RNAP II transcription termination (Porrua *et al.*, 2012). For mediating transcription termination, Sen1 translocates along the ssRNA (single-stranded RNA) until RNAP II is in close proximity. There it can move RNAP II forward by acting on the nascent transcript. The subsequent reannealing of upstream DNA in the transcription bubble favors Sen1 to terminate transcription by releasing RNAP II. In this mechanism mainly non-coding transcription is terminated (Han, Libri and Porrua, 2017). Termination defects in these non-coding transcripts can regulate expression of coding genes downstream of the non-coding gene. Additionally, phosphorylation of amino acid residue T1623 can reduce the termination efficiency of Sen1, influencing its gene regulatory function. This process is especially important in zinc homeostasis (Haidara, Giannini and Porrua, 2022).

Sen1 transcription termination of RNAP II limits accumulation of RNA:DNA hybrids and is mediated by the Sen1 helicase domain (Mischo *et al.*, 2011). Sen1's function in termination of RNAP II transcription and RNA:DNA hybrid prevention is conserved in SETX (Skourti-Stathaki, Proudfoot and Gromak, 2011; Hasanova *et al.*, 2023). It has been proposed, that SETX's function in transcription termination is dependent on RNAP II pausing (Skourti-Stathaki, Proudfoot and Gromak, 2011).

Besides transcription termination of RNAP II, Sen1 is terminating transcription of RNA polymerases I and III in a NNS independent manner (Figure 9 C). In the case of RNA polymerase I (RNAP I), rDNA transcription is paused once RNAP I approaches the DNA binding protein Nsi1. Nsi1 interacts with Fob1, which is binding downstream at the replication fork barrier and acts as a backup in case transcription is not successfully terminated at the Nsi1 binding site. Transcription can then be either terminated by Sen1 or Rat1, releasing RNAP I (Xie, Libri and Porrua, 2023).

Sen1 is also involved in transcription termination of RNAP III, which is mediated by polymerase pausing at T-tracts or G-tracts (Rivosecchi *et al.*, 2019; Xie *et al.*, 2022). RNAP III transcripts are mainly short, structured RNAs that form secondary structures, like tRNAs (Rivosecchi *et al.*, 2019; Xie *et al.*, 2022). These structures help terminating transcription of

RNAP III transcribed genes. In case a T-tract is short (<5 nt), secondary structures or protein aided mechanisms apply, in which Sen1 releases the polymerase (Xie *et al.*, 2022). For this function, Sen1 physically interacts with RNAP III (Rivosecchi *et al.*, 2019; Xie *et al.*, 2022). Due to its functions in termination of transcription of all three RNA polymerases, degradation of Sen1 leads to genome-wide changes in the transcriptome, especially upregulating stress response genes and downregulating rDNA loci (Aiello *et al.*, 2022).

Besides its functions in transcription termination, Sen1 travels with the replisome in order to coordinate replication and transcription (Alzu *et al.*, 2012). This interaction is mediated *via* Ctf4 and Mrc1 (Appanah *et al.*, 2020). Loss of Sen1's interaction with the replisome or loss of function of Sen1 leads to increased genome instability and recombination events that depend on ongoing transcription (Mischo *et al.*, 2011; Appanah *et al.*, 2020). Furthermore, the interaction with the replisome is necessary for resolving transcription-replication conflicts at the 5' end of genes (Aiello *et al.*, 2022). In budding yeast, this is especially important if the replication fork approaches highly transcribed RNAP II genes in a head-on (transcription on the lagging strand) confirmation (Alzu *et al.*, 2012). Furthermore, in the absence of Sen1 in these loci RNA:DNA hybrids form, which can lead to genome instability and checkpoint activation. The checkpoint activation is mediated by high amounts of ssDNA that is covered by the replication protein A (RPA) complex (Alzu *et al.*, 2012). Sen1 mutants accumulate RNA:DNA hybrids mainly in S-phase and slow down replication speed (Alzu *et al.*, 2012; San Martin-Alonso *et al.*, 2021). In human cells Senataxin is important for the restart of replication forks after stalling, preventing MUS81-dependent fork degradation (Rao *et al.*, 2024).

As depicted in Figure 9 B and D, Sen1 is an important resolvase of different conflicts between transcription and the replisome or between two transcription bubbles thet approach each other in a head-on confirmation (Aiello *et al.*, 2022). For mediating conflict resolution Sen1 is able to remove RNAP II at conflict sites within genes and at rDNA loci. Upstream of these stalled RNAP II enzymes R-loops form which partake in the transcription-replication conflict. In order to release these stalled RNAP II, Sen1 has to be able to interact with the replisome. During replisome association, Sen1 in not suppressing the R-loop formed in the conflict. Here come RNases H into play. They can remove the R-loop portion of the conflict, releasing RNAP II. This feature of RNase H seems to be a phenomenon during non-coding RNAP II transcription at rDNA loci. (Aiello *et al.*, 2022).

The absence of Sen1 leads to DNA damage at transcription-replication conflicts, which slow down S-phase progression (San Martin-Alonso *et al.*, 2021). Besides transcription-replication conflicts, Sen1 can also resolve conflicts between RNAP II and RNAP III at tRNA loci. This process is R-loop independent as RNases H do not play a role in it (Aiello *et al.*, 2022).

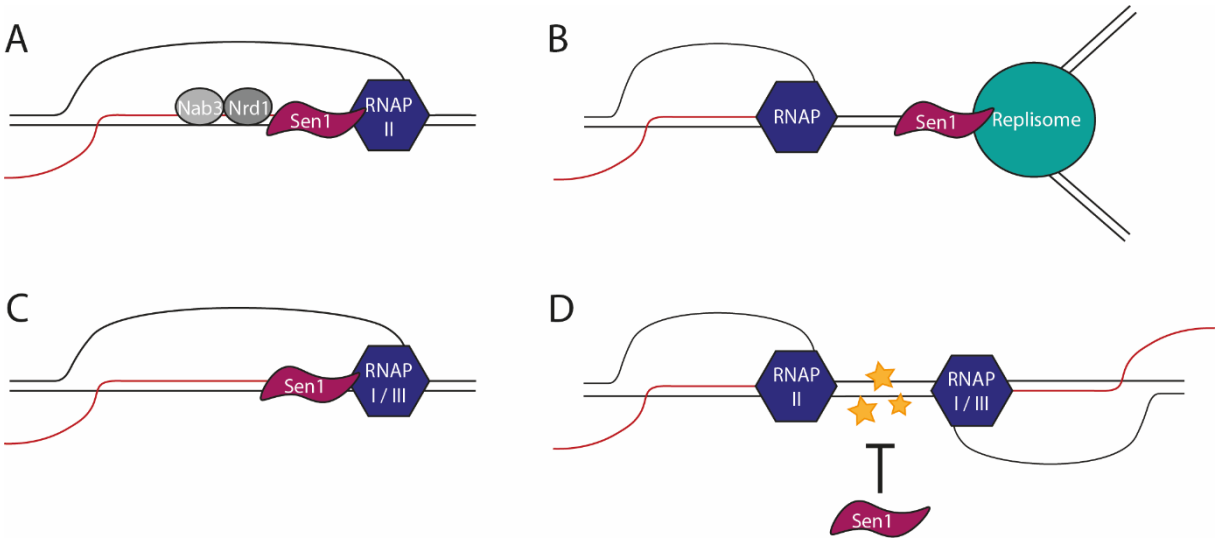

Figure 9 – Functions of Sen1 in budding yeast. ***(A)*** *In the NNS complex, Sen1 terminates non-coding transcription of RNAP II.* ***(B)*** *Sen1 resolves transcription-replication conflicts independent of the RNA polymerase.* ***(C)*** *Sen1 terminates RNAP I and RNAP III transcription in a NNS independent manner.* ***(D)*** *Sen1 prevents conflicts between RNAP II and RNAP I or RNAP III.*

Recently, Sen1 was implicated in termination of replication, where it is important for prevention of topological stress. This is the case when two replication forks approach each other and replication has to be terminated or if replication is terminated at the telomeres. Furthermore, Sen1 reduces the topological stress even more by terminating RNAP II transcription at sites of replication termination (Choudhary *et al.*, 2023). In summary it can be concluded, that Sen1 is important in preventing transcription-replication conflicts and that it has redundant functions with RNase H at the rDNA.

The manifold functions of Sen1 are the reason, why the protein has to be tightly regulated. Due to the important functions of Sen1 in the prevention of transcription-replication conflicts, it is highest expressed in S-phase and G2/M phase (Mischo *et al.*, 2018). While depletion of Sen1 causes DNA damage (San Martin-Alonso *et al.*, 2021), overexpression of the protein causes enhanced transcription termination at alternative transcription sites, impairing cell growth (Mischo *et al.*, 2018).

1.3.1 Sen1/SETX in DNA damage repair

Sen1 is important for the prevention of DNA damage caused by replication conflicts. Besides the prevention of DNA damage, it also plays an important role in DNA damage repair. Budding yeast Sen1 is recruited to double strand breaks (DSBs) in a Mre11-dependent manner (Rawal *et al.*, 2020). The presence of Sen1/SETX at DSBs gets important in case DSB resection occurs at transcriptionally active loci that form R-loops (Cohen *et al.*, 2018; Rawal *et al.*, 2020). Importantly, RNA:DNA hybrids that were formed during transcription before the DSB, can block the repair (Costantino and Koshland, 2018). In contrast, RNA:DNA hybrids, which arise at the DSB after it has been formed promote resection (Ohle *et al.*, 2016). Recruitment of Sen1 is important for canonical resection in order to allow error free repair by homology-directed repair (HDR) (Rawal *et al.*, 2020). Furthermore, Sen1 is preventing error prone non-homologous end joining (NHEJ).

In human cells, SETX is not required for resection, but it promotes Rad51 recruitment, allowing HR and preventing error prone rejoining events, which prevents translocations (Cohen *et al.*, 2018). No influence of RNase H1 could be found in Sen1's functions during DNA damage, while fork restart defects after deletion of *RNH1* and *RNH201* can be rescued by overexpression of Sen1 helicase (Rawal *et al.*, 2020; Heuzé *et al.*, 2023). In summary, Sen1 and SETX are important factors for allowing error free repair of DNA damage in cases RNA:DNA hybrids are involved.

1.4 Transcription-replication conflicts

Transcription-replication conflicts (TRCs) arise when replication approaches transcribing RNAPs. This can happen in a head-on (HO) orientation in case the lagging strand template is transcribed (Figure 10 A) or in a co-directional (CD) orientation when the leading strand template is transcribed (Figure 10 B). Both, HO- and CD-conflicts can cause DNA damage (Kumar *et al.*, 2021). Due to the nature of the conflicts, HO-conflicts cause more genotoxic stress (Stars in Figure 10 A), as both, replication and transcription create supercoiling downstream of the process, creating torsional stress. In bacteria the torsional stress at this kind of conflict requires topoisomerase 2 for resolution (Lang and Merrikh, 2021). On the other hand, CD-conflicts cause lower or no torsional stress, due to the cancelation between the positive supercoiling downstream of replication and the negative supercoiling upstream of transcription (Figure 10 B).

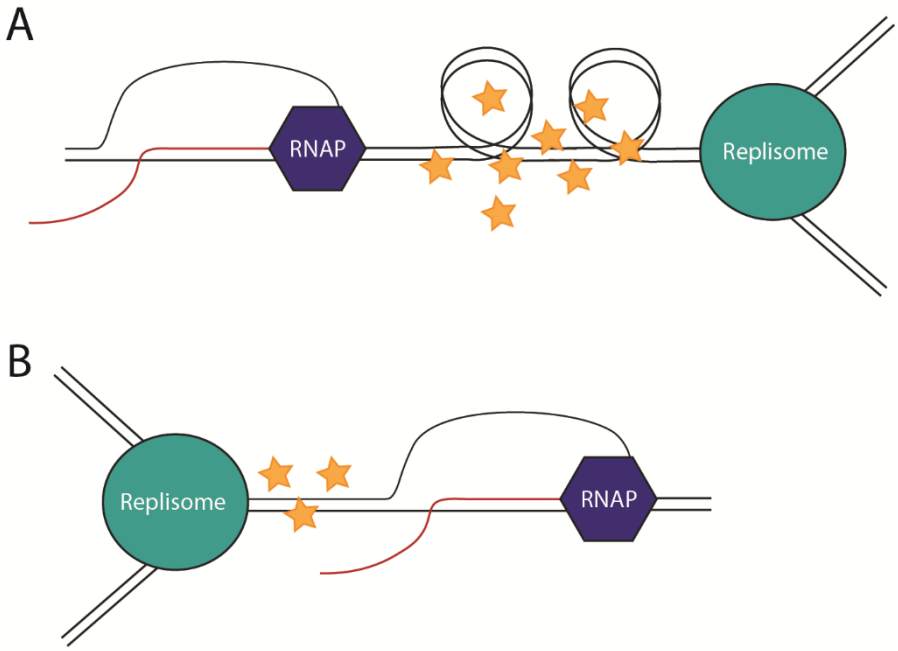

Figure 10 – Transcription-replication conflicts. ***(A)*** *Head-on (HO) transcription-replication conflict.* ***(B)*** *Co-directional (CD) transcription-replication conflict. Stars indicate genotoxic stress*

In the absence of Sen1 helicase, especially HO-conflicts lead to the accumulation of RNA:DNA hybrids and DNA damage due to defects in terminating RNAP II transcription and releasing of the RNA polymerase. In this scenario replication and transcription are inhibited (San Martin-Alonso *et al.*, 2021; Zardoni *et al.*, 2021). These phenotypes can be rescued by depletion of the transcription elongation factor *SPT2* (Zardoni *et al.*, 2021). If RNAP II in a TRC is engaged with an R-loop, DNA damage arises and the DNA damage response (DDR) is activated (Hamperl *et al.*, 2017). In general, proteins bound to the RNA portion of the conflict can aggravate the TRC, as well as R-loop stabilization by G-quadruplex formation on the displaced ssDNA strand (Brüning and Marians, 2020; Kumar *et al.*, 2021).

The directionality of the TRC primes the DNA damage response pathway in mammalian cells. While HO-conflicts can be caused by deregulated origin firing, promote R-loop formation and induce replication stress that leads to the activation of the DDR kinase ATR (activated through RPA), CD-conflicts lead to the resolution of R-loops and promote ATM activation, which is activated at DSBs (Hamperl *et al.*, 2017). It has been shown in bacteria that stalled replication forks that encounter transcription disassemble their replisome. The replisome has to be rebuilt in order to restart fork progression (reviewed by Browning and Merrikh, 2024). These ‘naked’ replication forks are coated with Rad51 in eukaryotic cells at the fork junction. In order to prevent Rad51-mediated fork reversal, RECQ5 DNA helicase

displaces Rad51 and promotes fork cleavage by Mus81. Fork cleavage by Mus81 can be prevented by SETX in cases replication stalling was caused by an TRC (Rao *et al.*, 2024). Mus81 dependent fork cleavage relieves the torsional stress arising between the transcription bubble and the replication fork in HO-conflicts. Transcription is restarted and the fork is repaired in a Rad52-dependent manner, followed by replication restart, mediated by POLD3 (Chappidi *et al.*, 2020).

TRCs can be reduced by overexpression of RNase H1 in human and yeast cells (Hamperl *et al.*, 2017; Brown *et al.*, 2022). RNase H1 promotes fork passage, especially at CD-conflicts (Kumar *et al.*, 2021). In line with this the combined deletion of RNase H1 and RNase H2 leads to increased DNA damage during S-phase, indicating both enzymes are involved in resolving or preventing TRCs (Costantino and Koshland, 2018; Sagi *et al.*, 2024). This effect can be increased if Sen1 is additionally depleted (Costantino and Koshland, 2018). Furthermore, in the absence of RNases H, the RNA:DNA hybrid portion of the conflict can be passed behind the fork, leaving a gap in the newly synthesized DNA that is filled with the hybrid RNA. These RNA:DNA hybrids interfere with fork progression and fork restart (Heuzé *et al.*, 2023; Stoy *et al.*, 2023). Interestingly, also the increased RNA:DNA hybrid levels after depletion of THO/TREX complex member Hpr1 lead to a slowdown in S-phase progression. Only a small portion of this is caused by direct TRCs, but by the persistent R-loops in these conditions that block replication (San Martin-Alonso *et al.*, 2021).

Interestingly, two replication forks starting from the same origin of replication stay linked in budding yeast and are called sister forks. Linked in this context means that if one of the replication forks encounters transcription and gets stalled, also the second fork gets arrested. This is different from stalling due to DSBs where the sister fork is not stalled. For completion of replication upon sister fork stalling, dormant replication origins fire, which is not inhibited by the replication checkpoint. In the absence of Sen1, these arrested forks are protected from Exo1 mediated cleavage by Mre11 and the Mrc1-Ctf4 complexes (Brambati *et al.*, 2018). In summary, the RNA:DNA hybrid regulating enzymes RNase H1, RNase H2, and Sen1/SETX are very important in the prevention and solvation of transcription-replication conflicts. The possible interplay of the three enzymes in prevention and resolution of TRCs is not clear yet.

1.5 RNA:DNA hybrids in DNA damage repair and disease

DSBs can serve as promoters for *de novo* RNAP II transcription. This transcription leads to accumulation of RNA:DNA hybrids at resected DNA ends, which are important for efficient DNA repair (Ohle *et al.*, 2016; Michelini *et al.*, 2017; D'Alessandro *et al.*, 2018). Another model discussed at DSBs is that RNA:DNA hybrids do not arise because of transcription promotion, but due to the slowdown of already ongoing transcription once a proximal DSB happens (Marnef and Legube, 2021). These RNA:DNA hybrids at DSB are resolved by helicases like Sen1/SETX, DHX9, and DDX5 and are implicated in regulating resection (Cohen *et al.*, 2018; Matsui *et al.*, 2020; Rawal *et al.*, 2020; Yu *et al.*, 2020). Furthermore, repair by homologous recombination requires the formation of Rad51 filaments, which is regulated by RNA:DNA hybrids at the DSB (D'Alessandro *et al.*, 2018). Additionally, a role for DSB proximal RNA:DNA hybrids as an alternative, Rad51-independent but Rad52-dependent RNA-templated repair mechanism was described. In this mechanism, the RNA of the hybrid can serve as a template for initiation of DNA syntheses at DSBs (Mazina *et al.*, 2017).

Furthermore, in budding yeast in the absence of Sen1 and RNases H, when RNA:DNA hybrids accumulate, DSB are mainly repaired by break-induced replication (Amon and Koshland, 2016; Costantino and Koshland, 2018). A special form of break-induced replication is alternative lengthening of telomeres (ALT), which happens at short telomeres (Dilley *et al.*, 2016). Break-induced replication is a homologous recombination pathway in which only one end of the DSB is available for repair. This problem is counteracted by resection of the strand and subsequent RPA coating of the 3' overhang. After Rad51 recruitment, a homologous sequence is searched that is used as replication template (Kramara, Osia and Malkova, 2018). The pathway choice for break-induced replication is due to RNA:DNA hybrids at the second end of the DSB, that does not allow for a repair pathway that includes both ends (Amon and Koshland, 2016). This is especially happening at the rDNA, where RNA:DNA hybrid levels are highest in yeast (Amon and Koshland, 2016; Wahba *et al.*, 2016).

1.6 Detection methods for RNA:DNA hybrids

Modern detection of RNA:DNA hybrids can be classified in two branches of methods. Those that are based on an antibody raised against RNA:DNA hybrids, called S9.6, and those that

use the catalytically inactive version of RNase H1. These methods bypassed older approaches like bisulfide sequencing and are the state of the art methods.

1.6.1 S9.6 antibody-based methods

S9.6-based methods range from microscopy over chromatin spreads to chromatin precipitation methods. The S9.6 antibody directly targets the RNA:DNA hybrid (Figure 11 A), but has the disadvantage, that it not only binds to RNA:DNA hybrids, but also to ssRNA and dsRNA. This has to be controlled for with enzymatic digestion using RNase III (degrades dsRNA) and RNase T1 (degrades ssRNA), which is not reliable for a microscopy approach when cells are intact (Chédin *et al.*, 2021; Smolka *et al.*, 2021). This is the reason why microscopy experiments using the S9.6 antibody need to be well controlled, for example by overexpression of RNase H1. The overexpression of RNase H1 has the disadvantage that it has been shown to alter transcription termination in human cells, leading to read-through with a possible impact on the experimental outcome (Skourti-Stathaki, Proudfoot and Gromak, 2011). For quantification of RNA:DNA hybrids it is hence better to use genomic DNA out of the cellular context in methods like chromatin spreading, where ssRNA and dsRNA are washed off and only RNA:DNA hybrids in the genomic DNA and mitochondrial DNA can be detected. Also here a control overexpressing RNase H1 is necessary. Quantification of RNA:DNA hybrids can also be done with Slot- and Dot-blots where the genomic DNA has to be pretreated with RNase T1 and RNase III and a control with *in vitro* digest with bacterial RNase H is necessary. These methods allow the genome-wide quantification of RNA:DNA hybrids. The weakness of the Slot- and Dot-blot is in the low sensitivity and challenges in the quantification that reduce the reproducibility (Chédin *et al.*, 2021). Chromatin precipitation with the S9.6 antibody is called DRIP (DNA:RNA immunoprecipitation; Figure 11 A) (Ginno *et al.*, 2012). It can be coupled to qPCR (quantitative polymerase chain reaction) or sequencing, for either getting a fast gene specific read-out or a genome-wide map of RNA:DNA hybrids. Specific adaptations of this method have been published in order to answer specific questions. For example, in DRIPc, the RNA fraction of the hybrid is reverse transcribed and the cDNA is sequenced instead of the DNA portion of the RNA:DNA hybrid (Sanz *et al.*, 2016). In qDRIP, external spike ins are added to the immunoprecipiatation in order to quantify RNA:DNA hybrid levels between samples (Figure 11 B, Crossley *et al.*, 2020). Another approach for improving the signal in

DRIP is digestion of the ssDNA portion of an R-loop in order to avoid reannealing during sonication (Figure 11 C). This method is calles S1-DRIP (Wahba *et al.*, 2016).

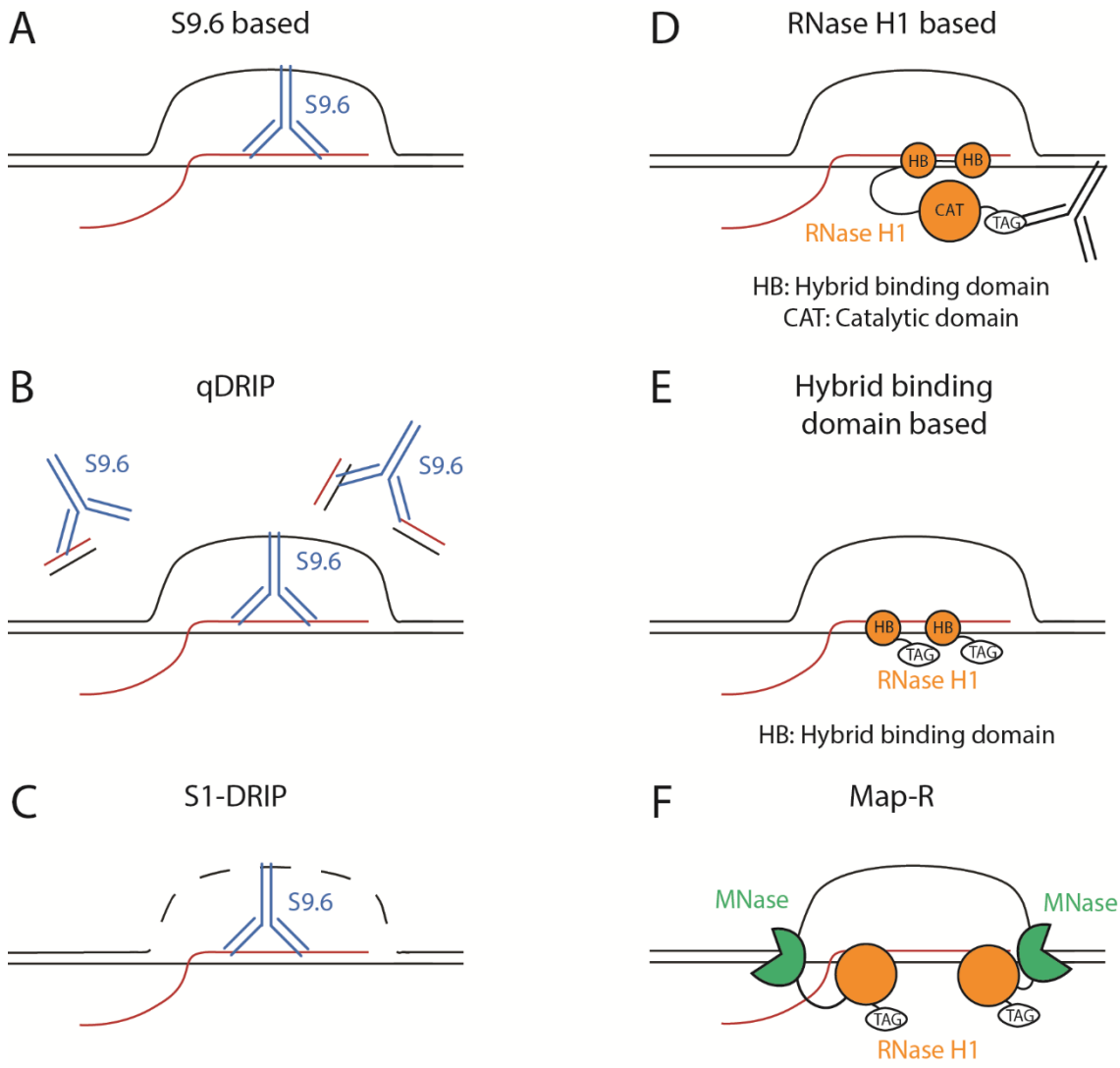

Figure 11 – Methods for mapping RNA:DNA hybrids. ***(A)*** *Methods based on binding of the S9.6 antibody to the RNA:DNA hybrid.* ***(B)*** *qDRIP, a method that uses the S9.6 antibody in DRIP and allows for absolute quantification of R-loops by using external spike-in RNA:DNA hybrids.* ***(C)*** *S1-DRIP increases the signal output of S9.6-based ChIP methods by degradation of the displaced ssDNA.* ***(D)*** *RNase H1 based methods, like R-ChIP, that detect catalytic inactive RNase H1 that binds RNA:DNA hybrids.* ***(E)*** *Methods based on the hybrid binding domain of RNase H1.* ***(F)*** *Map-R methods, coupling MNase to catalytic inactive RNase H1 for cutting out the RNA:DNA hybrid and purifying. Map-R scheme adapted from Yan et al. (2019).*

1.6.2 Methods based on catalytic inactive RNase H1

Due to the problem of the S9.6 antibody binding to ssRNA and dsRNA, multiple methods exist that use the catalytic inactive variant of RNase H1 (D193N in yeast and D210N in

human) in order to detect RNA:DNA hybrids. One of them is R-ChIP, a method for immunoprecipitation of RNA:DNA hybrids by overexpressing tagged, catalytic inactive RNase H1 and pulling it down with an antibody against the tag (Figure 11 D, Chen *et al.*, 2017). We have published, that especially at the telomeres R-ChIP is more sensitive than DRIP (Wagner and Luke, 2022). The analysis of the pull down can, like for DRIP, be performed with qPCR or sequencing. A critic to this method is, that the overexpression of catalytic dead RNase H1 can lead to stabilization of RNA:DNA hybrids and falsify the result (Chédin *et al.*, 2021). This effect could also be shown in this work. In a similar approach to R-ChIP, the hybrid binding (HB) domain of RNase H1 (Figure 11 E) is used for pulling down RNA:DNA hybrids (Wang *et al.*, 2021). Additionally, it is also used for staining RNA:DNA hybrids in microscopy (Silva, Guillén-Mendoza and Aguilera, 2022). Another method exploiting the catalytic inactive version of RNase H1 is called MapR. In this case, a recombinant fusion protein consisting of micrococcal nuclease (MNase), catalytic inactive RNase H1 and a tag for purification is used for *in vitro* cut out of the RNA:DNA hybrid, followed by a pull down, allowing to purify only RNA:DNA hybrids without adjacent dsDNA (Yan *et al.*, 2019).

When designing an experiment in order to study RNA:DNA hybrid levels, the advantages and disadvantages of S9.6- and RNase H1-based methods have to be evaluated carefully. While the S9.6 antibody is known for its binding to ssRNA and dsRNA and its sequence preference for GC-rich RNA:DNA hybrids (König, Schubert and Längst, 2017), RNase H1 might be biased to specific kinds of RNA:DNA hybrids that it preferentially degrades in a physiological context. Furthermore, *in vivo*, overexpression of RNase H1 or the catalytic inactive allele can cause changes to RNA:DNA hybrid levels and transcription read-through, changing the experimental outcome (Skourti-Stathaki, Proudfoot and Gromak, 2011; Chédin *et al.*, 2021).

1.7 Rationale

The two RNA:DNA hybrid degrading nucleases RNase H1 and RNase H2 were long seen as redundant in their function. While RNase H2 degrades RNA:DNA hybrids throughout the whole genome, RNase H1 is binding RNA:DNA hybrids genome-wide, but only degrades them in hybrid dense genomic regions. These regions are more prone to genotoxic stress due to the high RNA:DNA hybrid load (Zimmer and Koshland, 2016). Furthermore, RNase H1 accumulates at the chromatin in case genotoxic stress arises (Lockhart *et al.*, 2019). Starting from this knowledge, the question of how RNase H1 determines which RNA:DNA hybrids to degrade arose. A possible mode of activation can be the high density of RNA:DNA hybrids in combination with the naturally high density of RPA at R-loops. This theory is favored by the change in processivity RNase H1 goes through in the presence of RPA (Li *et al.*, 2024).

Furthermore, it is not known how budding yeast RNase H1 is regulated with regards to protein levels and activity. It is only known that it is important for regulating RNA:DNA hybrids. Dysregulated RNA:DNA hybrids can be detrimental to the cells, making it important to understand how the major regulators of RNA:DNA hybrids are regulated themselves.

RNA:DNA hybrids can be threats for genome stability. A major source of R-loop dependent DNA damage arises during transcription-replication conflicts (TRCs). Sen1 helicase can displace the transcribing RNA polymerases and unwind the RNA:DNA hybrid portion of the conflict. Human Sen1 homologue SETX is mutated in diseases like ALS or AOA2. How these mutations affect SETX function is not known yet. A link between Sen1 dysfunction in yeast with RNase H1 accumulation at the chromatin (Lockhart *et al.*, 2019) is worth investigating further in order to better understand the human diseases and for gaining a better understanding of how TRCs are regulated in general.

2. Material and Methods

2.1 Material

2.1.1 Yeast strains

Yeast strains used in this study were derived from the S288C backgrounds BY4741 (haploid, mating type a), BY4742 (haploid, mating type alpha) or BY4743 (diploid).

Strain name	Genotype	Source
yAL637	*MATa his3Δ1 leu2Δ0 ura3Δ0 met15Δ0 sen1-1::KAN rnh201::HYG*	This study
yCW3, 4 and 5	*MATa his3Δ1 leu2Δ0 ura3Δ0 met15Δ0*	This study
yCW13, 19, 25, 1603, 1604 and 1605	*MATa his3Δ1 leu2Δ0 ura3Δ0 met15Δ0 + pBL211*	This study
yCW15, 21, 27	*MATa his3Δ1 leu2Δ0 ura3Δ0 met15Δ0 + pBL352*	This study
yCW17, 23, 28	*MATa his3Δ1 leu2Δ0 ura3Δ0 met15Δ0 + pBL633*	This study
yCW70, 71, 244 and 250	*MATa his3Δ1 leu2Δ0 ura3Δ0 met15Δ0 sen1-1::KAN + pBL211*	This study
yCW72, 73, 246 and 252	*MATa his3Δ1 leu2Δ0 ura3Δ0 met15Δ0 sen1-1::KAN + pBL352*	This study
yCW74, 75, 248 and 254	*MATa his3Δ1 leu2Δ0 ura3Δ0 met15Δ0 sen1-1::KAN + pBL633*	This study
yCW78, 79 and 80	*MATalpha his3Δ1 leu2Δ0 ura3Δ0 lys2Δ0 rad52::KAN + pBL211*	This study
yCW340, 341 and 342	*MATa his3Δ1 leu2Δ0 ura3Δ0 met15Δ0 rnh1::KAN*	This study
yCW347, 348 and 349	*MATa his3Δ1 leu2Δ0 ura3Δ0 met15Δ0 rnh201::HYG*	This study
yCW354, 355 and 356	*MATa his3Δ1 leu2Δ0 ura3Δ0 met15Δ0 rnh1::KAN rnh201::HYG*	This study
yCW372, 373	*MATa his3Δ1 leu2Δ0 ura3Δ0 met15Δ0 rnh1::KAN rnh201::HYG + pBL211*	This study
yCW374, 375	*MATa his3Δ1 leu2Δ0 ura3Δ0 met15Δ0 rnh1::KAN rnh201::HYG + pBL352*	This study
yCW376, 377	*MATa his3Δ1 leu2Δ0 ura3Δ0 met15Δ0 rnh1::KAN rnh201::HYG + pBL633*	This study

Strain name	Genotype	Source
yCW540, 541 and 542	*MATa his3Δ1 leu2::pGDP-AFB2-LEU2 met15Δ0 ura3Δ0 RNH1-6xHA-KAN RNH201-AID*-9xMYC-HIS3*	This study
yCW545, 546 and 547	*MATa his3Δ1 leu2::pGDP-AFB2-LEU2 met15Δ0 ura3Δ0 RNH1-6xHA-KAN SEN1-AID*-9xMYC-HIS3*	This study
yCW550, 551 and 552	*MATa his3Δ1 leu2::pGDP-AFB2-LEU2 ura3Δ0 RNH1-6xHA-KAN TOP1-AID*-9xMYC-HIS3*	This study
yCW694 and 695	*MATalpha his3Δ1 leu2Δ0 met15Δ0 ura3Δ0 HPR1-AID*-9xMYC-HIS3 trp1::GDP-OsTIR1(F74G)-Nat RNH1-6xHA-KAN*	This study
yCW696	*MATa his3Δ1 leu2Δ0 met15Δ0 ura3Δ0 HPR1-AID*-9xMYC-HIS3 trp1::GDP-OsTIR1(F74G)-Nat RNH1-6xHA-KAN*	This study
yCW702, 703 and 704	*MATa his3Δ1 leu2::pGDP-AFB2-LEU2 met15Δ0 ura3Δ0 RNH1-6xHA-KAN RNH201-AID*-9xMYC-HIS3 SEN1-AID*-9xMYC-HIS3*	This study
yCW730, 731 and 732	*MATa his3Δ1 leu2Δ0 met15Δ0 ura3Δ0 met15Δ0 LYS2 top1::HYG + pBL211*	This study
yCW733, 734 and 735	*MATa his3Δ1 leu2Δ0 met15Δ0 ura3Δ0 met15Δ0 LYS2 top1::HYG + pBL352*	This study
yCW736, 737 and 738	*MATa his3Δ1 leu2Δ0 met15Δ0 ura3Δ0 met15Δ0 LYS2 top1::HYG + pBL633*	This study
yCW775 and 776	*MATalpha his3Δ1 leu2Δ0 ura3Δ0 met15Δ0 lyp1Δ::GPD-OsTIR1(F74G)-NAT CDC20-AID*-9xMYC-HYG RNH1-6xHA::KAN*	This study
yCW828	*MATalpha his3Δ1 leu2Δ0 ura3Δ0 met15Δ0 lyp1Δ::GPD-OsTIR1(F74G)-NAT NAB3-AID*-9xMYC-HYG*	This study
yCW829	*MATa his3Δ1 leu2Δ0 ura3Δ0 met15Δ0 lyp1Δ::GPD-OsTIR1(F74G)-NAT NAB3-AID*-9xMYC-HYG*	This study
yCW831, 832 and 833	*MATa his3Δ1 leu2Δ0 ura3Δ0 met15Δ0 lyp1Δ::GPD-OsTIR1(F74G)-NAT NAB3-AID*-9xMYC-HYG RNH1-6xHA-KAN*	This study

Strain name	Genotype	Source
yCW834	*MATalpha his3Δ1 leu2Δ0 ura3Δ0 met15Δ0 lyp1Δ::GPD-OsTIR1(F74G)-NAT NRD1-AID*-9xMYC-HYG*	This study
yCW835	*MATa his3Δ1 leu2Δ0 ura3Δ0 met15Δ0 lyp1Δ::GPD-OsTIR1(F74G)-NAT NRD1-AID*-9xMYC-HYG*	This study
yCW837 and 838	*MATalpha his3Δ1 leu2Δ0 ura3Δ0 met15Δ0 lyp1Δ::GPD-OsTIR1(F74G)-NAT NRD1-AID*-9xMYC-HYG RNH1-6xHA-KAN*	This study
yCW839	*MATa his3Δ1 leu2Δ0 ura3Δ0 met15Δ0 lyp1Δ::GPD-OsTIR1(F74G)-NAT NRD1-AID*-9xMYC-HYG RNH1-6xHA-KAN*	This study
yCW919, 920 and 921	*MATa his3Δ1 leu2Δ0 ura3Δ0 rnh1::HYG*	This study
yCW922, 923 and 924	*MATa his3Δ1 leu2Δ0 ura3Δ0 sen1-1::KAN*	This study
yCW925, 926 and 927	*MATa his3Δ1 leu2Δ0 ura3Δ0 rnh1::HYG sen1-1::KAN*	This study
yCW929, 930 and 931	*MATa his3Δ1 leu2Δ0 met15Δ0 ura3Δ0 mft1::KAN + pBL211*	This study
yCW932, 933 and 934	*MATa his3Δ1 leu2Δ0 met15Δ0 ura3Δ0 mft1::KAN + pBL352*	This study
yCW935, 936 and 937	*MATa his3Δ1 leu2Δ0 met15Δ0 ura3Δ0 mft1::KAN + pBL633*	This study
yCW967, 968 and 969	*MATa his3Δ1 leu2::pGDP-AFB2-LEU2 ura3Δ0 RNH201-6xMYC-URA3 SEN1-AID*-9xMYC-HIS3*	This study
yCW971, 972 and 973	*MATa his3Δ1 leu2::pGDP-AFB2-LEU2 ura3Δ0 RNH202-3xMYC-URA3 SEN1-AID*-9xMYC-HIS3*	This study
yCW977, 978 and 979	*MATalpha his3Δ1 leu2Δ0 met15Δ0 ura3Δ0 trp1::GDP-OsTIR1(F74G)-NAT RNH1-6xHA-KAN SEN1-AID*-9xMYC-HIS3 + pBL211*	This study
yCW980, 981 and 982	*MATalpha his3Δ1 leu2Δ0 met15Δ0 ura3Δ0 trp1::GDP-OsTIR1(F74G)-NAT RNH1-6xHA-KAN SEN1-AID*-9xMYC-HIS3 + pBL1117*	This study
yCW1013, 1014, 1015	*MATa his3Δ1 leu2Δ0 ura3Δ0 met15Δ0 top1::HYG*	This study

Strain name	Genotype	Source
yCW1019, 1020, 1021	*MATa his3Δ1 leu2Δ0 ura3Δ0 met15Δ0 top1::HYG sen1-1::KAN*	This study
yCW1029, 1030 and 1033	*MATa his3Δ1 leu2Δ0 ura3Δ0 met15Δ0 sen1-1::HYG NAT-G2-RNH1-TAP-HIS3*	This study
yCW1031, 1032 and 1035	*MATa his3Δ1 leu2Δ0 ura3Δ0 met15Δ0 NAT-G2-RNH1-TAP-HIS3*	This study
yCW1034	*MATalpha his3Δ1 leu2Δ0 ura3Δ0 met15Δ0 NAT-G2-RNH1-TAP-HIS3*	This study
yCW1036, 1037 and 1040	*MATa his3Δ1 leu2Δ0 ura3Δ0 met15Δ0 G1-RNH1-6xHA-NAT/KAN*	This study
yCW1038, 1039	*MATa his3Δ1 leu2Δ0 ura3Δ0 met15Δ0 sen1-1::HYG G1-RNH1-6xHA-NAT/KAN*	This study
yCW1049, 1050 and 1051	*MATa his3Δ1 leu2Δ0 met15Δ0 ura3Δ0 mft1::HYG rnh1::KAN*	This study
yCW1052, 1053 and 1054	*MATa his3Δ1 leu2Δ0 met15Δ0 ura3Δ0 mft1::HYG*	This study
yCW1061, 1062 and 1063	*MATa his3Δ1 leu2::pGDP-AFB2-LEU2 ura3Δ0 RNH1-6xHA-KAN SEN1-AID*-9xMYC-HIS3 bar1::NAT*	This study
yCW1069, 1070 and 1071	*MATa his3Δ1 leu2Δ0 ura3Δ0 met15Δ0 rnh1::KAN top1::HYG*	This study
yCW1080 and 1082	*MATa his3Δ1 leu2Δ0 ura3Δ0 S-RNH1-6xHA-NAT/KAN sen1-1::HYG*	This study
yCW1081	*MATalpha his3Δ1 leu2Δ0 ura3Δ0 S-RNH1-6xHA-NAT/KAN sen1-1-HYG*	This study
yCW1083	*MATalpha his3Δ1 leu2Δ0 ura3Δ0 S-RNH1-6xHA-NAT/KAN*	This study
yCW1084 and 1085	*MATa his3Δ1 leu2Δ0 ura3Δ0 S-RNH1-6xHA-NAT/KAN*	This study
yCW1239, 1240 and 1241	*MATa his3Δ1 leu2Δ0 ura3Δ0 met15Δ0 lyp1Δ::GPD-OsTIR1(F74G)-NAT RPO31-AID*-9xMYC-HYG RNH1-6xHA-KAN*	This study
yCW1243, 1244 and 1245	*MATa his3Δ1 leu2Δ0 ura3Δ0 met15Δ0 lyp1Δ::GPD-OsTIR1(F74G)-NAT RPO31-AID*-9xMYC-HYG RNH1-6xHA-KAN SEN1-AID*-9MYC-HIS3*	This study
yCW1306, 1307 and 1308	*MATa his3Δ1 leu2::pGDP-AFB2-LEU2 ura3Δ0 RNH1-6xHA-KAN rpa190-1-URA*	This study

Strain name	Genotype	Source
yCW1309	*MATalpha his3Δ1 leu2::pGDP-AFB2-LEU2 ura3Δ0 RNH1-6xHA-KAN SEN1-AID*-9xMYC-HIS3 rpa190-1-URA*	This study
yCW1310 and 1311	*MATa his3Δ1 leu2::pGDP-AFB2-LEU2 ura3Δ0 RNH1-6xHA-KAN SEN1-AID*-9xMYC-HIS3 rpa190-1-URA*	This study
yCW1314, 1315 and 1316	*MATa his3Δ1 leu2::pGDP-AFB2-LEU2 ura3Δ0 RNH1-6xHA-KAN RPB1-AID*-6xFLAG-HYG*	This study
yCW1318, 1319 and 1320	*MATa his3Δ1 leu2::pGDP-AFB2-LEU2 ura3Δ0 RNH1-6xHA-KAN SEN1-AID*-9xMYC-HIS3 RPB1-AID*-6xFLAG-HYG*	This study
yCW1380, 1381 and 1382	*MATa his3Δ1 leu2::pGDP-AFB2-LEU2 ura3Δ0 rnh1(D913N)-6xHA-KAN SEN1-AID*-9xMYC-HIS3*	This study
yCW1384, 1385 and 1386	*MATa his3Δ1 leu2::pGDP-AFB2-LEU2 ura3Δ0 rnh1(D913N)-6xHA-KAN RNH201-AID*-9xMYC-HIS3*	This study
yCW1429, 1430 and 1431	*MATa his3Δ1 leu2Δ ura3Δ0 HPR1-AID*-9xMYC-HIS3 rnh1(D913N)-6xHA-KAN trp1::GDP-OsTIR1(F74G)-NAT*	This study
yCW1433, 1434 and 1435	*MATa his3Δ1 leu2Δ0 ura3Δ0 met15Δ0 sen1-1::HYG mft1::KAN*	This study
yCW1506, 1507 and 1508	*MATa his3Δ1 leu2::pGDP-AFB2-LEU2 ura3Δ0 SEN1-AID*-9xMYC-HIS3*	This study
yCW1509, 1510 and 151	*MATa his3Δ1 leu2::pGDP-AFB2-LEU2 ura3Δ0 SEN1-AID*-9xMYC-HIS3 rnh1::KAN*	This study
yCW1609, 1610 and 1611	*MATalpha his3Δ1 leu2Δ0 ura3Δ0 met15Δ0 rnh1::HIS3 + pBL211*	This study
yCW1615, 1616 and 1617	*MATa his3Δ1 leu2Δ0 ura3Δ0 rnh1::KAN trp1::GDP-OsTIR1(F74G)-NAT SEN1-AID*-9xMYC-HIS3 + pBL211*	This study
yCW1618, 1619 and 1620	*MATa his3Δ1 leu2Δ0 ura3Δ0 trp1::GDP-OsTIR1(F74G)-NAT SEN1-AID*-9xMYC-HIS3 rnh1::KAN + pBL352*	This study
yCW1621, 1622 and 1623	*MATa his3Δ1 leu2Δ0 ura3Δ0 trp1::GDP-OsTIR1(F74G)-NAT SEN1-AID*-9xMYC-HIS3 + pBL211*	This study

Strain name	Genotype	Source
yFB405 and 406	*MATa his3Δ1 leu2Δ0 ura3Δ0 rnh201::NAT sen1-1::KAN*	This study
yFB1091, 2066 and 2430	*MATa his3Δ1 leu2Δ0 met15Δ0 ura3Δ0 RNH1-6xHA::KAN*	This study
yFB1175	*MATa his3Δ1 leu2Δ0 met15Δ0 ura3Δ0 rnh1::KAN rnh201::HYG + pBL906*	This study
yFB1355 and 1356	*MATa his3Δ1 leu2Δ0 met15Δ0 ura3Δ0 rnh1::KAN rnh201::HYG + pBL797*	This study
yFB1364	*MATa his3Δ1 leu2Δ0 met15Δ0 ura3Δ0 rnh1::KAN rnh201::HYG + pBL804*	This study
yFB1367	*MATa his3Δ1 leu2Δ0 met15Δ0 ura3Δ0 rnh1::KAN rnh201::HYG + pBL808*	This study
yFB1424 and 1425	*MATa his3Δ1 leu2Δ0 met15Δ0 ura3Δ0 + pBL906*	This study
yFB1426 and 1427	*MATa his3Δ1 leu2Δ0 met15Δ0 ura3Δ0 + pBL797*	This study
yFB1428 and 1429	*MATa his3Δ1 leu2Δ0 met15Δ0 ura3Δ0 + pBL837*	This study
yFB1492 and 1493	*MATa his3Δ1 leu2Δ0 met15Δ0 ura3Δ0 rnh1::KAN rnh201::HYG + pBL837*	This study
yFB1541 and 1542	*MATa his3Δ1 leu2Δ0 met15Δ0 ura3Δ0 rnh1::KAN rnh201::HYG + pBL906*	This study
yFB2426	*MATa his3Δ1 leu2Δ0 ura3Δ0 met15Δ0 RNH1-6xHA-KAN SEN1-AID*-9xMYC-HIS3 LEU2::pGDP-AFB2-LEU2*	This study
yFB2427	*MATalpha his3Δ1 leu2::pGDP-AFB2-LEU2 ura3Δ0 met15Δ0 RNH1-6xHA-KAN SEN1-AID*-9xMYC-HIS3*	This study
yFB2433	*MATalpha his3Δ1 leu2::pGDP-AFB2-LEU2 ura3Δ0 met15Δ0 RNH1-ΔHB1-6xHA-KAN SEN1-AID*-9xMYC-HIS3*	This study
yFB2434	*MATa his3Δ1 leu2::pGDP-AFB2-LEU2 ura3Δ0 met15Δ0 RNH1-ΔHB1-6xHA-KAN SEN1-AID*-9xMYC-HIS3*	This study
yFB2450	*MATalpha his3Δ1 leu2::pGDP-AFB2-LEU2 ura3Δ0 met15Δ0 RNH1-ΔHB2-6xHA-KAN SEN1-AID*-9xMYC-HIS3*	This study

Strain name	Genotype	Source
yFB2451	*MATalpha his3Δ1 leu2::pGDP-AFB2-LEU2 ura3Δ0 met15Δ0 RNH1-ΔHB2-6xHA-KAN SEN1-AID*-9xMYC-HIS3*	This study
yML199 and 201	*MATalpha his3Δ1 leu2Δ0 ura3Δ0 SEN1-9xMYC-His3*	This study
yML203 and 105	*MATalpha his3Δ1 leu2Δ0 ura3Δ0 rnh1::KAN SEN1-9xMYC-HIS3*	This study
ySGS20 and 21	*MATa his3Δ1 leu2Δ0 met15Δ0 ura3Δ0 RNH1-6xHA-KAN sen1-3-9xMYC-HIS3 rnh201::NAT*	This study
ySGS22	*MATalpha his3Δ1 leu2Δ0 met15Δ0 ura3Δ0 RNH1-6xHA-KAN sen1-3-9xMYC-HIS3 rnh201::NAT*	This study
ySGS23 and 24	*MATalpha his3Δ1 leu2Δ0 met15Δ0 ura3Δ0 RNH1-6xHA-KAN sen1-3-9xMYC-HIS3*	This study
ySGS25	*MATa his3Δ1 leu2Δ0 met15Δ0 ura3Δ0 RNH1-6xHA-KAN sen1-3-9xMYC-HIS3*	This study
ySGS26 and 27	*MATa his3Δ1 leu2Δ0 met15Δ0 ura3Δ0 RNH1-6xHA-KAN rnh201::NAT*	This study
ySGS28	*MATalpha his3Δ1 leu2Δ0 met15Δ0 ura3Δ0 RNH1-6xHA-KAN rnh201::NAT*	This study
ySGS29	*MATalpha his3Δ1 leu2Δ0 met15Δ0 ura3Δ0 LYS2 RNH1-6xHA-KAN*	This study
ySGS30 and 31	*MATa his3Δ1 leu2Δ0 met15Δ0 ura3Δ0 RNH1-6xHA-KAN*	This study

2.1.2 Oligonucleotides

Name	5'-3' Sequence	Target gene	Direction	Application	Source
oAL8	GGACACGATGGTGATCCAGG	*RNH1*	Forward	Confirmation of C-terminal AID*-tag, 3'RACE	This study
oAL31	ATGGACAGCAGGAAGAACG	*RNH201*	Forward	3'RACE	This study
oAL76	CCTTGATACGAGCGTAACCATCA	*PDC1*	Forward	qPCR	This study
oAL78	GAAGGTATGAGATGGGCTGGTAA	*PDC1*	Reverse	qPCR	This study
oBL29	CTGCAGCGAGGAGCCGTAAT	*pTEF*	Reverse	Knock out confirmation	This study
oBL292	CCCAGGTATTGCCGAAAGAATGC	*ACT1*	Forward	ddPCR	This study
oBL293	TTTGTTGGAAGGTAGTCAAAGAAGCC	*ACT1*	Reverse	ddPCR	This study
oCW1	CAGGAAATGAAATGGCAGATTTTCTGGCGAAGAAAGGAGCATCTAGACGACGTACGCTGCAGGTCGAC	*RNH1*	Forward	C-terminal tagging with AID*	This study
oCW2	TTCTATTACAGGTACAACAGGTCCAGTAAGAAGCCAAGCAAAAAACAGCAATCGATGAATTCGAGCTCG	*RNH1*	Reverse	C-terminal tagging with AID*	This study
oCW8	CTGCAGCGAGGAGCCGTAAT	KAN_B	Reverse	Confirmation of strains from ORF collection	This study
oCW57	CAATGCAGCTACTTCGAACATTTCTAATGGTTCATCTACCCAAGATATGAAACGTACGCTGCAGGTCGAC	*HPR1*	Forward	C-terminal tagging with AID*	This study
oCW58	CTATGCATGAATTTCTTATCAGTTTAAAATTTCTATTAAGAGGATAATTTAATCGATGAATTCGAGCTCG	*HPR1*	Reverse	C-terminal tagging with AID*	This study

Name	Sequence	Target gene	Direction	Application	Source
oCW59	GAGATGAGTTGAAGAG CGAACAGACGC	*HPR1*	Forward	Confirmation of C-terminal AID tag	This study
oCW68	TACGCGGTTAGAAAGG GCAG	*RNH1*	Forward	ddPCR	This study
oCW69	CCAGCATGCGTTGAACT TCC	*RNH1*	Reverse	ddPCR	This study
oCW117	AACCCGGGGATCCGTCG ACC	*TAP*-Tag	Reverse	Confirmation TAP tagging	This study
oCW118	AGTTCCCACCGACGAGA AAC	*RNH201*	Forward	ddPCR	This study
oCW119	ATGCAGTAGAGCGAGTC TGC	*RNH201*	Reverse	ddPCR	This study
oCW120	CACTTTTACACTGCCGCC AC	*RNH202*	Forward	ddPCR	This study
oCW121	GGCCCTTTGCCGAATTG AAA	*RNH202*	Reverse	ddPCR	This study
oCW122	GCCATCCTCTCGGGAAA CAC	*RNH203*	Forward	ddPCR	This study
oCW123	CGCCAATTCGTTGCGAT CAG	*RNH203*	Reverse	ddPCR	This study
oCW128	TTCGTATACCCGGGTAC CAATTTTTTTTTTTTTTT T	Poly-A	Reverse	3'RACE RT	(Mischo *et al.*, 2011)
oCW129	TTGGTACCCGGGTATAC GAA	3'RACE adaptor	Reverse	3'RACE adaptor primer	(Mischo *et al.*, 2011)
oCW130	GTGGTGACACTGCCACT GTC	*PGK1*	Forward	3'RACE	This study
oCW137	GTGCCATGAATGTAGGC CTAAATTC	*RNH202*	Forward	3'RACE	This study
oCW139	CGAATTGGCGCGATTGC AAG	*RNH203*	Forward	3'RACE	This study
oCW140	GATGAATATGAGTGCAT TTGGCTCG	*SNR13*	Forward	3'RACE	This study
oCW184	GTCAGAGGCTATATTTC ACTGGAGAA	*PDR5*	Reverse	qPCR	(San Martin-Alonso *et al.*, 2021)

Name	Sequence	Target gene	Direction	Application	Source
oCW185	TACGTCTTGTTTCGGCCTTAATC	*PDR5*	Forward	qPCR	(San Martin-Alonso *et al.*, 2021)
oFB171	TATGATTCTCGCTTAGGGTGCGGGAGG	*SUF2*	Forward	qPCR	(Chan *et al.*, 2014)
oFB172	CATTAACATTGGTCTTCTCCAGCTTACTC	*SUF2*	Reverse	qPCR	(Chan *et al.*, 2014)
oLP178	TTGTGCCCGAATCCAGTGA	*GCN4*	Forward	qPCR	(Santos-Pereira *et al.*, 2013; San Martin-Alonso *et al.*, 2021)
oLP179	TGGCGGCTTCAGTGTTTCTA	*GCN4*	Reverse	qPCR	(Santos-Pereira *et al.*, 2013; San Martin-Alonso *et al.*, 2021)
oSM16	GGTTGCGGCCATATCTACCA	5s rDNA	Forward	qPCR	(Misino *et al.*, 2022)
oSM17	ACCTGAGTTTCGCGTATGGT	5s rDNA	Reverse	qPCR	(Misino *et al.*, 2022)

2.1.3 Plasmids

Plasmid identifier	Name	Source
pBL211	pRS425 pGAL1	Gift from M. Peter
pBL352	pRS425 pGAL1-RNH1-HA	(Graf et al., 2017)
pBL633	pRS425 pGAL1-rnh1(D193N)-HA	(Wagner and Luke, 2022)
pBL797	pRS416 pGAL1-RNH1-HA	This study
pBL804	pRS416 pGAL1-rnh1(D193N)-HA delta52	This study
pBL808	pRS416 pGAL1-rnh1(D193N)-HA delta53-168	This study
pBL837	pRS416 pGAL1-rnh1(D193N)-HA	(Misino *et al.*, 2022)
pBL906	pRS416 pGAL1-3HA	(Misino *et al.*, 2022)
pBL1117	pRS425 pGAL1-RNH1-3Myc	This study

2.1.4 Reagents

Name	Supplier and order number
Acetone	Merck KGaA
Agar	Merck KGaA
Agarose	Merck KGaA
Alpha-factor	Zymo Research
β-Mercaptoethanol	Merck KGaA
Bacto tryptone	BD Biosciences
Bacto yeast	BD Biosciences
Boric acid	Merck KGaA
Bovine serum albumin (BSA, lyophylized)	Merck KGaA
Bovine serum albumin (20 mg/ml) molecular biology grade	NEB
Bradford reagent	AppliChem
Broad range molecular weight marker	NEB
Bromophenol blue	Merck KGaA
Carbenicillin disodium salt	Merck KGaA
Complete™ Mini EDTA-free protease inhibitor cocktail tablets	Roche
ddPCR™ Droplet Reader Oil	BioRad
DMSO	Merck KGaA
dNTPs	Invitrogen
DPEC treated water	Merck KGaA
EDTA	Merck KGaA
Ethanol	Merck KGaA
Ficoll Type 400	AppliChem
5x First Strand buffer	NEB
Formaldehyde (37 %)	Merck KGaA
G418 disulfate solution	AppliChem
Galactose	AppliChem
Glucose	Merck KGaA
Glycerol	Fisher Scientific
Glycine	Merck KGaA
HEPES-KOH	AppliChem
High Sensitivity RNA ScreenTape sample buffer	Agilent
Hydroxyurea (HU)	Merck KGaA
Hygromycin B Gold	InvivoGen
K_2HPO_4	Merck KGaA
KCl	Merck KGaA
KH_2PO_4	Merck KGaA

Name	Supplier and order number
LiAc	Merck KGaA
LiCl	Merck KGaA
Methyl methanesulfonate (MMS)	Merck KGaA
$MgCl_2$	Merck KGaA
NaCl	Merck KGaA
NaN_3	Merck KGaA
NaOH	Merck KGaA
Nonident© P40	AppliChem
Nourseothricin-dihydrogen sulfate (ClonNAT)	Werner BioAgents
Orange G	AppliChem
Peptone	AppliChem
Phenol	Merck KGaA
Phenol : Chloroform : Isoamylalcohol (25 : 24 : 1)	AppliChem
PhosSTOP	Roche
Ponceau solution	Merck KGaA
Potassium acetate	Merck KGaA
QX200™ Droplet generation Oil for EvaGreen	BioRad
Raffinose	AppliChem
Random hexamers	Invitrogen
RDD buffer	Qiagen
Ribonucleotide Solution Mix	NEB
SC-His	MP Biomedicals
SC-Leu	MP Biomedicals
SC-Ura	MP Biomedicals
Sodium acetate	Merck KGaA
Sodium deoxycholate (SOD)	Merck KGaA
Sodium dodecyl sulfate (SDS, 20% w/v)	AppliChem
Sodium azide	Merck KGaA
Sorbitol	Merck KGaA
Skim milk	Merck KGaA
Standard nutrient broth No.1	Merck KGaA
Supersignal West Pico Plus	Fisher Scientific
SYBR safe DNA Gel stain	Invitrogen
Sytox green	Thermo Scientific
Sucrose	Merck KGaA
Tergitol-type NP-40	AppliChem
5x Turboblot transfer buffer	Bio-Rad
Trichloroacetic acid	Merck KGaA

Name	Supplier and order number
Tris base	Merck KGaA
Tris-HCl	AppliChem
Triton X-100	Merck KGaA
Urea	Merck KGaA
Yeast maker carrier DNA	Takara
Yeast Nitrogen Base without amino acids	Difco
YPD agar	Merck KGaA
Zinc acetate	Merck KGaA

2.1.5 Buffers and Solutions

Name	Composition
AE-buffer	50 mM Na-Acetate pH 5.3 10 mM EDTA (Ethylenediaminetetraacetic acid)
Buffer III	10 mM Tris-HCl pH 8.0 1 mM EDTA 250 mM LiCl 1 % Tergitol-type NP-40 (v/v) 1 % SOD (Sodium deoxycholate, w/v)
DNA loading dye	10 mM EDTA pH 8.0 15 % Ficoll Type 400 (w/v) Orange G
DTT	0.1 M Dithiotreitol
Elution buffer B	50 mM Tris-HCl pH 7.5 1 % SDS (w/v) 10 mM EDTA
Extraction buffer (CBA)	50 mM Tris-HCl pH 7.4 100 mM KCL 2.5 mM $MgCl_2$
FA 500/lysis buffer	50 mM HEPES-KOH pH 7.5 500 mM NaCl 1 mM EDTA 1 % Triton X-100 (v/v) 0.1 % SOD (w/v)
FA lysis buffer minus SOD	50 mM HEPES-KOH pH 7.5 140 mM NaCl 1 mM EDTA 1 % Triton X-100 (v/v)
FA lysis buffer plus SOD	50 mM HEPES-KOH pH 7.5 140 mM NaCl 1 mM EDTA 1 % Triton X-100 (v/v) 0.1 % SOD (w/v)
LiAc Mix	0.1 M Tris-HCL pH 8.0 0.05 M EDTA 0.1 M LiAc

Name	Composition
MES solution	0.1 M MES pH 6.5 (2-(N-Morpholino)ethansulfonic acid) 1 M Sorbitol 1 mM EDTA 0.5 mM $MgCl_2$
6x Orange loading dye	10 mM EDTA pH 8.0 15 % (w/v) Ficoll Type 400 Orange G
PFA (Paraformaldehyde) solution	3 % (w/v) Paraformaldehyde pH 7.0 3.4 % Sucrose
Phenole Chloroform Isoamylalcohol	50 % (v/v) Phenol 48 % (v/v) Chloroform 2 % (v/v) Isoamylalcohol
Phosphate buffered saline (PBS)	11.8 mM Phosphate buffer pH 7.4 137 mM NaCl 2.7 mM KCl
Phosphate buffered saline with Tween-20 (PBS-T)	11.8 mM Phosphate buffer pH 7.4 137 mM NaCl 2.7 mM KCl 0.1 % (v/v) Tween-20
PEG Mix	0.1 M Tris-HCL pH 8.0 0.05 M EDTA 0.1 M LiAc 0.1 M Polyethylene glycol 4000
10x SDS running buffer	0.25 M Tris-HCl pH 8.3 1 % (v/v) SDS 1.92 M Glycine
SDS solution	20 % (w/v) Sodium dodecyl sulfate
Sodium acetate stock	3 M Sodium acetate pH 5.3
Solution 1	1.85 N NaOH 7.6 % (v/v) β-Mercaptoethanol
Solution 2	50 % (v/v) Trichloroacetic acid
Spheroblsting buffer (CBA)	50 mM Potassium phosphate buffer pH 7.4 1 M Sorbitol 1 mM DTT
1x TBE buffer	89 mM Tris base pH 8.0 89 mM Boric acid 2 mM EDTA
1x TBS buffer	50 mM Tris-HCl pH 7.6 150 mM NaCl

Name	Composition
1x TE buffer	0.1 M Tris-HCL pH 8.0 0.05 M EDTA
Tris-HCl	50 mM Tris-HCl pH 7.4
1x TurboBlot transfer buffer	20 % (v/v) 5x TransBlot transfer buffer 20 % (v/v) Ethanol
Urea buffer	120 mM Tris-HCl pH 6.8 5 % (v/v) Glycerol 8 M Urea 143 mM β-Mercaptoethanol 8 % (v/v) SDS Bromophenol blue
ZK buffer	25 mM Tris-HCl pH 7.5 800 mM KCl

2.1.6 Media

Name	Composition
LB agar	10 g/L NaCl 10 g/L Bacto tryptone 5 g/L Bacto yeast extract 15 g/L Agar
LB medium	10 g/L NaCl 10 g/L Bacto tryptone 5 g/L Bacto yeast extract
preSPO plates	30 g/L Standard nutrient broth No.1 10 g/L Bacto yeast extract 20 g/L Agar 2 % (w/v) Glucose
SC-His	1.9 g/L SC-His 6.7 g/L Yeast Nitrogen Base without amino acids 2 % (w/v) Glucose
SC-Leu	1.67 g/L SC-Leu 6.7 g/L Yeast Nitrogen Base without amino acids 2 % (w/v) Glucose or Raffinose
SC-Leu agar	1.67 g/L SC-Leu 6.7 g/L Yeast Nitrogen Base without amino acids 24 g/L Agar 2 % (w/v) Glucose or Galactose
SC-Ura	1.9 g/L SC-Ura 6.7 g/L Yeast Nitrogen Base without amino acids 2 % (w/v) Glucose or Raffinose
SPO medium	1 % (w/v) Potassium acetate 0.005 % (w/v) Zinc acetate
YPD	8.8 g/L Bacto yeast 17.6 g/L Peptone 2 % (w/v) Glucose
YPD agar	65 g/L YPD agar (Sigma Aldrich)

Concentrations of antibiotics:

Nat: 100 µg/mL Nourseothricin-dihydrogen sulfate (ClonNAT)

Kan: 300 µg/mL G418 disulfate solution (Kanamycin)

Hyg: 300 µg/mL Hygromycin B Gold

Carb: 100 µg/mL Carbenicillin disodium salt

2.1.7 Antibodies

Antigen	Host	Dilution	Supplier
Anti-alpha-Tubulin	Rabbit	Western blot: 1:20000	Abcam
Anti-HA (clone 3F10)	Rat	ChIP: 2 µg/mL (final)	Roche
Anti-HA (clone 12CA5)	Mouse	Western blot: 1:3000	IMB core facility
Anti-Histone H3	Rabbit	Western blot: 1:1000	Abcam
Anti-Pgk1	Mouse	Western blot: 1:20000	Invitrogen
Anti-pS2-RNAPII	Rabbit	ChIP: 1:200	Abcam
Anti-Mouse-HRP	Goat	Western blot: 1:3000	BioRad
Anti-Mouse-IRDye 800CW	Goat	Western blot: 1:2000	Li-COR
Anti-Myc (Clone 9E10)	Mouse	Western blot: 1:1000	IMB core facility
Anti-Rabbit-HRP	Goat	Western blot: 1:3000	BioRad
Anti-Rabbit-IRDye 680RD	Goat	Western blot: 1:2000	Li-COR
Anti-Rad53 (Clone EI7.E1)	Mouse	Western blot: 1:1000	Abcam
Anti-Rnr3	Rabbit	Western blot: 1:1000	Agrisera Antibodies
Anti-Mouse-Cy3	Goat	Chromatin spread: 1:666	Jackson Immuno
S9.6	Mouse	Chromatin spread: 1:100 ChIP: 1:250	IMB core facility

2.1.8 Enzymes

Name	Supplier and order number
Eva green master mix	IMB core facility
DNase I from RNase free DNase Set	Qiagen
Lyticase from Arthrobacter	Merck KGaA
Proteinase K	Biofroxx
QX200™ ddPCR™ EvaGreen Supermix	BioRad
RNase A	Life Technologies
RNaseOut	Thermo Scientific
SM nuclease	IMB core facility
Superscript III	Thermo Scientific
T4 PNK	NEB
Zymolyase T20	Zymo Research

2.1.9 Electronic devices

Name	Supplier
2100 Bioanalyzer	Agilent Technologies
Bioruptor Pico	Diagenode
C1000 Touch™ Thermal Cycler with 96–Deep Well Reaction Module	BioRad
Cellometer X1	Nexcelom
CFX384 Touch Real-TIME PCR Detection System	BioRad
ChemiDoc	BioRad
Climo-Shaker ISF-x	Kuhnner
Echo Revolve	Echo
Excella 24 Incubator	New Brunswick Scientific
FACS Fortessa	BD Biosciences
Homogenizer Fastprep-24	MP Biomedicals
NextSeq 500	Illumina
Odyssey® XF imaging system	Li-Cor
PowerPacTM Basic Power Supply	BioRad
PX1 PCR Plate Sealer	BioRad
Qubit 2.0 Fluorometer	Life Technologies
QX200™ Droplet Generator	BioRad
QX200™ Droplet Reader	BioRad
Test-tube rotator	Labinco
ThermoMixer	Eppendorf
Sonifier 450	Branson
SW22 water bath shaker	Julabo
TapeStation	Agilent
Trans-Blot Turbo Transfer System	BioRad

2.1.10 Software

Name	Supplier
CFX manager (3.1)	BioRad
Microsoft Office Professional Plus 2016	Microsoft
Fiji/ImageJ (1.54f)	NIH
FlowJo (10.10)	BD Life Sciences
GraphPad Prism (10.1.4)	GraphPad Software
Illustrator (27.8)	Adobe
Image lab (6.1.0)	Bio-Rad
Image studio (3.1)	Li-COR
Quantasoft™ Analysis Pro (1.0.596)	BioRad
TapeStation analysis software (4.1.1.)	Agilent

2.1.11 Additional materials

Name	Supplier
15 ml Bioruptor pico tubes	Diagenode
4–15 % Mini-PROTEAN™ TGX Stain-Free™ Protein Gels, 15 well	BioRad
4–15 % Mini-PROTEAN™ TGX Stain-Free™ Protein Gels, 10 well	BioRad
7.5 % Mini-PROTEAN™ TGX Stain-Free™ Protein Gels, 15 well	BioRad
7.5 % Mini-PROTEAN™ TGX Stain-Free™ Protein Gels, 10 well	BioRad
Bioruptor sonication beads	Diagenode
ddPCR Plates 96-well, semi-skirted	BioRad
DG8TM Cartridges for QX200TM Droplet Generator	BioRad
DG8TM Gaskets for QX200TM Droplet Generator	BioRad
DH5α competent E.coli cells 'Mix & Go!'	Zymo research
DynabeadsTM Protein G	Invitrogen
FC tubes – 5 ml round bottom tubes	VWR
High Precision Microscope Cover Glasses 24x50 mm	Paul Marienfeld GmbH & Co.KG
High Sensitivity DNA screen tape	Agilent Technologies
High Sensitivity RNA screen tape	Agilent Technologies
Magnetic rack for 1.5 ml centrifugation tubes DynaMag^{TM}-2	Invitrogen
Magnetic rack for 15 ml centrifugation tubes MSR50151	Permagen
Microseal® 'B' PCR Plate Sealing Film, adhesive, optical	BioRad
NEXTflex Small RNA-Seq Kit V3	Bioo Scientific
NextSeq 500/550 High output Flowcell	Illumina
NextSeq 500 Midoutput Flowcell	Illumina
Optical tube stripe cap	Agilent
Optical tube stripes	Agilent
PCR Plate Heat Seal foil	BioRad
Petri dishes	Falcon
Photoflo	Kodak
QIAquick PCR purification kit	Qiagen
qPCR plates	BioRad
qPCR sealing tape	BioRad
Qubit dsDNA HS Assay Kit	Life Technologies
riboPool kit	siTOOLs
RNeasy MinElute Kit	Qiagen
Superfrost^{TM}Plus Adhesion Microscope Slides	Epredia
Trans-Blot Turbo RTA Midi 0.2 µm LF PVDF Transfer Kit	BioRad
TruSeq stranded mRNA LT Sample Prep Kit	Illumina
TruSeq stranded Total RNA LT Sample Prep Kit	Illumina

2.2 Methods

2.2.1 Yeast cell culture

If not stated otherwise, liquid yeast cell cultures were incubated in YPD (Yeast Extract Peptone Dextrose) medium or synthetic complete (SC) medium (if necessary without specific amino acids and/or with raffinose instead of glucose) at 30 °C (25 °C for temperature-sensitive strains), shaking at 200 rpm. For cultivation of yeast on agar plates, the cells were streaked on the respective YPD or SC agar plate (with or without antibiotics) and incubated at 30 °C (25 °C for temperature-sensitive strains).

2.2.2 Yeast mating and sporulation

In order to mate two haploid yeast strains, the strains need to have the opposite sex. Mating type a (MATa) can only be crossed to mating type alpha (MATalpha). A small patch (0.5 cm x 0.5 cm) of a mix from a MATa and a MATalpha strain was streaked onto an YPD agar plate. The plate was incubated for 5 h to 6 h at 30 °C (25 °C for temperature-sensitive strains). If both strains carried different antibiotic or auxotrophic markers, diploids were selected by streaking the crossed cells on a suitable agar plate that selects for one selection marker of each strain. If selection by streaking on a selective plate was not possible, diploids were picked using the Singer Sporeplay micromanipulator microscope. The diploids were incubated for 2 d to 3 d at 30 °C (25 °C for temperature-sensitive strains).

For sporulation, the diploid strain was patched on preSPO plates and incubated at 30 °C (25 °C for temperature-sensitive strains) overnight. The patch was used to inoculate sporulation (SPO) cultures in 3 ml SPO medium. The cultures were incubated at 23 °C and 220 rpm for at least four days, up to four weeks. 10 µl of the sporulated cells were treated with 10 µl Lyticase (2.5 mg/mL; digestion of the cell wall) for 15 min at room temperature (RT). A stripe of treated cells were applied to an YPD plate in the middle of the plate. Once dried, tetrads of spores were picked and split into single cells using the Singer Sporeplay micromanipulator microscope. The cells were incubated for 2 d to 3 d at 30 °C (25 °C for temperature-sensitive strains).

2.2.3 Yeast transformation

For transforming budding yeast with either plasmids or Polymerase chain reaction (PCR) products for integration into the yeast genome, an overnight culture was prepared by

inoculating one single colony of yeast in 3 ml YPD and incubated at an appropriate temperature. The next day, the overnight culture was diluted to OD_{600} 0.1 in 10 ml YPD medium per transformation. When the culture reached OD_{600} 0.4 to 0.8, the transformation was started. For this purpose, the cells were spun down for 3 min at 900 x g at RT and the supernatant was discarded. The cells were resuspended in 5 ml LiAc Mix and spun down for 3 min at 900 x g and RT. After discarding the supernatant, the cells were resuspended in 100 µl LiAc Mix (supplemented with 7 % (v/v) DMSO for storing of competent cells at -80 °C) per 10 ml culture volume. The competent cells were either used directly for transformation or stored at -80 °C. If competent cells from -80 °C were used in a transformation, they were thawed on ice before starting the transformation.

For transforming the cells, 100 µl cell suspension were mixed with 700 µl PEG mix, 10 µl yeast maker carrier DNA and 200 ng to 500 ng of DNA (plasmid or PCR product). For each transformation, a 'no DNA' control was performed. The transformation reactions were incubated for 30 min spinning on a wheel at RT, followed by a heat shock at 42 °C (37 °C for heat sensitive strains) for 15 min. The cells were spun down for 1 min at 900 x g and RT. The supernatant was discarded. The cells were resuspended in 300 µl YPD medium and incubated for 30 min at 30 °C (or appropriate temperature for heat sensitive strains). Plasmid transformations were directly plated on selective plates and incubated for 3 d at 30 °C (or appropriate temperature for temperature-sensitive strains). Transformations with PCR products for integration were plated on YPD agar, incubated overnight at 30 °C (or appropriate temperature for temperature-sensitive strains) and replica plated on selective agar, followed by incubation for 3 d at 30 °C (or appropriate temperature for temperature-sensitive strains).

2.2.4 Yeast strain generation

For tagging of a specific gene with an AID*-tag a plasmid carrying the respective tag and a selection marker was used as a template (Morawska and Ulrich, 2013). Oligonucleotides were designed for amplifying the tag and marker sequence by PCR and adding 50 bp homologous arms to the PCR product. The PCR product was transformed into yeast according to 2.2.3. Some AID* strains were taken from a genome-wide library of AID* degron strains, created by my colleague Eduardo Gameiro (Gameiro *et al.*, 2025).

Yeast knock out strains were taken from the yeast knock out collections (Wach *et al.*, 1994; Winzeler *et al.*, 1999; Giaever *et al.*, 2002).

2.2.5 Bacterial transformation

For transforming *E.coli* cells, commercially available competent DH5α cells were used. The cells were thawed on ice and 100 ng plasmid DNA in 0.5 µl ddH_2O were added. The cell suspension was carefully mixed and incubated for 30 min on ice. The sample was heat shocked for 1 min at 42 °C, followed by 1 min on ice. 300 ml LB (Luria broth) medium were added and the cells were incubated for 30 min at 37 °C. The bacteria were sowed on LB-Amp and incubated overnight at 37 °C.

2.2.6 Cell cycle arrest and release

In this study, cells were arrested in G1-phase of the cell cycle. An arrest in S- or G2/M-phase is possible as well. For arresting cells in G1, the used strains had to be carrying the MATa mating type, as they were arrested using the mating pheromone alpha-factor that is produced by MATalpha cells. 2.4 µM alpha-factor were added to exponentially growing yeast cultures. After 1.5 h to 2 h, the cells were arrested in G1, which was controlled under the microscope. Either the experiment was carried out in G1 or the alpha-factor was washed out for releasing them into S-phase. Before releasing the cells, the G1-arrested sample was taken, as well as a flow cytometry control. For the release, the cells were spun down for 3 min at 900 x g and RT and the supernatant was discarded. The cells were washed three times in one culture volume sterile ddH_2O and spun down again like before. The cells were resuspended in the same volume of YPD or suitable drop out medium (pre-warmed to 25 °C) as the initial culture volume. The release was performed at 25 °C in the water bath shaker. Samples were taken every 15 min until 105 min. For exact the time points, the samples were mixed with 1/100 sample volume of 10 % NaN_3. From each sample, a flow cytometry sample was taken to control the cell cycle phase. Depending on the question asked, the samples were used for example for Western blot or R-ChIP.

2.2.7 Western blot

2.2.7.1 Protein extraction

Protein extraction was carried out by Trichloroacetic acid (TCA) extraction. First, 2 OD_{600} units pelleted yeast cells (either freshly collected or stored at -20 °C) were resuspended in

140 µl solution 1 and incubated for 10 min on ice. 140 µl solution 2 were added and the samples were vortexed for 3 s. After incubating again for 10 min on ice, the samples were spun down at 18000 x g and 4 °C for 2 min. The supernatant was removed and the pellet was washed in 1 ml acetone. The samples were spun down at 18000 x g and 4 °C for 2 min. 100 µl (50 µl / 1 OD_{600} of cells) urea buffer was added to the samples, followed by incubation at 95 °C (70 °C if phosphorylated proteins were to be detected) and 1500 rpm for 3 min on a thermomixer. The samples were stored at -20 °C.

2.2.7.2 SDS-PAGE and transfer

For SDS-PAGE (SDS polyacrylamide gel electrophoresis), precast acrylamide gels from the BioRad Mini-PROTEAN™ TGX Stain-Free™ system were used. The gel percentage was chosen depending on the application and the detected proteins. The gels were placed in a BioRad Mini-PROTEAN Tetra Vertical Electrophoresis Cell and the chamber was filled with 1x SDS running buffer. The prepared samples (see 2.2.7.1 for standard protein extraction and 2.2.17 for fractionation assays) were loaded onto the gel. In general, 5 µl of protein extraction samples (1 OD_{600} cells / 100 µl urea buffer) were loaded next to 3.5 µl NEB broad range molecular weight standard. For lowly expressed proteins, the loaded volume was increased and/or the protein concentration was increased by using 50 µl urea buffer per 1 OD_{600} of cells. The chamber was connected to a PowerPac™ Power Supply. The gel was run at 200 V until the blue front from the urea buffer reached the end of the gel. Gels for quantification of Rnh1-HA or studying Rad53 phosphorylation were run at 100 V for 105 min.

For protein transfer, the BioRad Trans-Blot Turbo Transfer System apparatus was used. The filter paper and membrane (from BioRad Trans-Blot Turbo RTA Midi 0.2 µm LF PVDF Transfer kit) were presoaked in 1x transfer buffer. In a transfer cassette the transfer sandwich was stacked, starting with a filter paper, followed by the membrane and the gel, ending with a second filter paper. The transfer was performed with the pre-saved program from BioRad for mini gels and transfer of high molecular weight proteins (1 gel: 10 min at 1.3 A and up to 25 V; 2 gels: 10 min at 2.5 A and up to 25 V). After the transfer the membrane was incubated in ponceau solution for 5 min, followed by rinsing with VE water twice. The ponceau stained membrane was imaged using the ChemiDoc and it was proceeded like described under 2.2.7.3 Immunoblot.

2.2.7.3 Immunoblot

The membrane prepared under 2.2.7.2 was blocked in 5 % skim milk in PBS-T for 1 h at RT. The blocking solution was discarded and the primary antibody in 5 % skim milk in PBS-T or 3 % bovine serum albumin (BSA) in PBS-T was added and incubated either for 1 h at RT or overnight at 4 °C. The antibody concentrations were specific to the used antibody and can be found under 2.1.7. In case Rnh1-HA and Tubulin were detected using the Li-Cor system, both primary antibodies were added at the same time. After incubation of the primary antibody, the membrane was washed three times for 15 min in PBS-T at RT. The antibody incubation for the secondary antibody was performed. For this, the secondary antibody was diluted in 5 % skim milk in PBS-T and the blot was incubated for 1 h at RT. The membrane was washed three times for 15 min in PBS-T at RT, followed by one wash for 15 min in PBS and detection. The detection was either carried out with the Chemidoc Touch or using the Li-COR machine. When using the ChemiDoc, The membrane was placed in the machine and Supersignal West Pico Plus was added equally over the blot until it was fully covered. The membrane was imaged in the 'Calorimetric' mode under 'Auto-optimal' settings and in the 'small' zoom setting, followed by imaging in the 'Chemiluminescence' mode, detecting different time points in order to maintain longer and shorter exposure data. When using the Li-Cor, the blot was put into the machine and the image was acquired in the 700 nm and/or 800 nm channel (depending on used secondary antibodies) for 2 min each. Quantification of blots acquired with the Li-COR imager was performed using the Image Studio software. For analysis of ChemiDoc blots the Image Lab software was used.

2.2.8 Flow cytometry

Flow cytometry was used for determining the cell cycle profile of yeast cell cultures dependent on the DNA content of the cells. For this purpose, 1 ml exponentially cycling cells were spun down at 900 x g at RT. The cells were washed in 1 ml ddH_2O and spun down as before. The cells were resuspended in 70 % EtOH and stored at 4 °C until further processing.

The samples were spun at 16200 x g at RT for 5 min and the supernatant was discarded. The pellet was resuspended in 1 ml 50 mM Tris-HCl (pH 7.4) and the centrifugation was repeated. In case the cells did not precipitate well the centrifugation was repeated. The cells were resuspended in 500 µl 0.25 mg/ml RNase A and incubated at 37 °C for 2 h to 3 h

or overnight. 25 µl 20 mg/ml Proteinase K solution were added and the samples were incubated for 1 h to 2 h at 50 °C. The samples were transferred to FACS tubes and sonicated using a Branson Sonifier (10 s, constant mode, 10 % power). 500 µl 4 µM Sytox green in 50 mM Tris-HCl (pH 7.4) were added and the samples were measured using the BD FACS Fortessa, counting 20000 cells per sample. The analysis was carried out in the FlowJo software. The measured cells were gated into the main population in FSC-A vs. SSC-A. From there gating was performed in the SYTOX Green A vs. W channel for doublet exclusion. DNA content of the remaining population was blotted in a histogram of the SYTOX Green A channel (ex 488 nm, 530/30BP).

2.2.9 RNA extraction

For RNA extraction, between 10 ml and 20 ml exponentially growing cells were collected and spun down for 3 min at 900 x g at RT. The pellet was resuspended in 1 ml ddH_20 and transferred into a 1.5 ml centrifugation tube. The cells were spun down again for 3 min at 900 x g at RT and the supernatant was removed completely with the vacuum pump. The cells were stored at -80 °C until the RNA extraction was performed.

For the RNA extraction, phenol at pH 5.3 had to be prepared. For this purpose, crystalline phenol was given into a 50 ml centrifugation tube and melted in hot water. The same volume of AE-buffer pH 5.3 was added and the mixture was inverted five times. After separation of the phases, the upper, aqueous phase was discarded. This process was repeated two times.

Cell pellets were thawed on ice and resuspended in 400 µl AE buffer pH 5.3. After addition of 20 µl 20 % SDS, the samples were vortexed. 500 µl of the prepared phenol was added and the samples were again vortexed. After 5 min incubation at 65 °C and 5 min incubation on ice, the samples were spun down for 2 min at 20800 x g and 4 °C. The aqueous phase was transferred to a new tube and 500 µl Phenol : Chloroform : Isoamylalcohol (25 : 24 : 1) were added. The samples were inverted 5 times and incubated for 5 min at RT, followed by centrifugation for 2 min at 20800 x g and 4 °C. The aqueous phase was transferred to a new tube and 40 µl 3 M Sodium acetate and 1 ml ice cold 100 % EtOH were added. The samples were inverted 5 times and incubated on ice for 15 min, followed by centrifugation for 2 min at 20800 x g and 4 °C. The pellet was washed in 1 ml 80 % EtOH and spun down for 2 min at 20800 x g and 4 °C. The pellet was dried for 5 min and resuspended in 100 µl RDD buffer

containing 11 Kunitz units of DNase I. The samples were incubated at 37 °C and 350 rpm for 30 min. The RNA concentration was measured using the Nano Drop. In case the RNA was used for RNA sequencing (RNAseq), the quality of the RNA was tested using the Tape station (see 2.2.10). RNA samples were stored at –80 °C.

2.2.10 RNA quality control using the TapeStation

For analysis of RNA quality prior to RNA sequencing, the TapeStation was used in the high sensitivity RNA analysis program. The RNA was diluted to a concentration between 1 ng/ml and 25 ng/µl in RNase free water. 2 µl of the RNA dilution were mixed with 2 µl RNA high sensitivity sample buffer in Agilent optical tubes. The samples were incubated for 3 min at 72 °C, followed by 2 min on ice. The samples were spun down in a table top PCR tube centrifuge for 1 min and loaded into the TapeStation. The RNA high sensitivity tape was placed in the tape holder and the run was started. In order to have a good quality of RNA, the threshold for the RIN^e value calculated by the software is at least 9.5.

2.2.11 Measurement of transcript levels

2.2.11.1 Reverse transcription (RT)

In order to measure transcript levels, the RNA has to be reverse transcribed into cDNA. In this project, the reverse transcription was carried out using the reverse transcriptase Superscript III. 1 µg RNA was pre-incubated with 1 µl NTPs (Invitrogen, 10 mM each) and 2 µl random primers (Invitrogen, 0.2 m/µl) in 13 µl ddH_2O for 5 min at 65 °C. 7 µl of a master mix containing 4 µl 5x First Strand buffer, 1 µl 0.1 M DTT, 1 µl RNaseOut and 1 µl Superscript III per sample was added to the samples. The samples were incubated for 5 min at 25 °C, followed by 1 h at 50 °C and 15 min at 75 °C. The cDNA was stored at -20 °C.

2.2.11.2 qRT PCR

For qRT PCR (quantitative reverse transcription PCR), the cDNA from 2.2.11.1 was used. The cDNA was diluted to 50 µl. As a no RT control, also 1 µg untreated RNA was diluted in 50 µl ddH_2O. The PCR was carried out in 384 well plates using the CFX Real-Time PCR cycler with 384 well add-in from BioRad. The reaction volume was 10 µl, consisting of 4 µl cDNA or non-RT RNA, 0.9 µl DPEC treated H_2O, 0.05 µl of each primer (100 µM stock) and 5 µl Eva green Master Mix. The PCR plate was sealed using Microseal® 'B' PCR Plate Sealing Film and the spun down shortly. The PCR program was the following: Initial denaturation for 10 min

at 95°C, followed by 40 cycles of 15 s at 95°C and 1 min at 60 °C. In the end melting curves were measured in the range from 65.0 °C until 96.5 °C in 0.5 °C steps.

The qPCR results were analyzed using the Bio-Rad RFX Manager software. The c_q determination method was set to 'regression' and the data was exported. The further analysis was carried out in Excel. The mean of the technical replicates was calculated and values for the house keeping gene actin were subtracted. The following formula was used for the calculation:

$$Transcript\ level\ normalized\ to\ actin = 2^{-(c_{q,transcript\ of\ interest} - c_{q,actin})}$$

2.2.11.3 ddPCR

Digital droplet PCR (ddPCR) is a method for quantification of absolute transcript levels. The levels can be calculated as transcripts per cell or transcripts per sample. In order to get this number, yeast cultures can not be measured by OD_{600} measurement, but have to be counted. For this purpose, exponentially growing yeast cells were counted using the Cellometer X1 (Nexcelom). As the device sometimes counts debris or clumps of multiple cells as one cell, the image based count was adjusted manually. From all samples 10 ml cell culture were collected by spinning the samples for 3 min at 600 x g at RT and the dry pellets were stored at -80 °C until the RNA was extracted. The RNA was extracted following the protocol described under 2.2.9 with the following deviation. Due to the quantitative approach of ddPCR, the volumes taken from the aqueous phase had to be precise in order to calculate transcripts per cell in the end. After the centrifugation with phenol, 370 µl of the aqueous phase were taken and after the phenol : chloroform : isoamlyalcohol step 300 µl of the aqueous phase were taken. The extracted RNA was stored at -80 °C until reverse transcription. The RT followed the protocol described under 2.2.11.1. For reverse transcription, 2 µl of the RNA were used, irrespective of the RNA concentration. The cDNA was diluted to 100 µl and stored at -20 °C until the ddPCR was carried out.

For ddPCR, each sample consisted of 1 µl cDNA in 12.5 µl DPEC treated water with 500 nM of each primer for quantifications of *RNH1*, *RNH201*, *RNH202* and *RNH203*. For ACT1 transcript quantification the cDNA was prediluted 1:4 before pipetting 1 µl of this dilution. The samples were supplemented with 12.5 µl QX200™ ddPCR™ EvaGreen Supermix prior to droplet generation. For droplet generation, 20 µl of the sample and 70 µl droplet generator oil for EvaGreen were loaded into a DG8™ cartridge, covered by a DG8™ gasket

and the droplets were generated using the QX200™ droplet generator machine. 40 µl of the generated droplet were transferred into a 96 well ddPCR plate (BioRad) and the plate was sealed using the PX1 PCR plate sealer and PCR plate heat seal foil. The PCR was carried out in a C1000 Touch™ Thermal Cycler with 96–Deep Well Reaction Module using the following program: 5 min at 95 °C, followed by 40 cycles of 30 s at 95 °C and 1 min at 60 °C. The plate was cooled down to 4 °C for 5 min and reheated to 95 °C for 5 min prior to storage at 4 °C until droplet read.

For the droplet read, the PCR plate was moved into the QX200™ droplet reader and the droplets were analyzed. The Quantasoft™ analysis pro software gives out transcripts per sample which can be used for calculating the transcripts per cell considering the cell count from the beginning.

2.2.12 RNAseq

For RNA sequencing (RNAseq), 20 ml exponentially growing cells were collected by centrifugation for 3 min at 600 x g. The cells were transferred into a 1.5 ml centrifugation tubes, spun down again for 3 min at 900 x g and the dry pellets were stored at -80 °C. Additionally, two times 1 ml of the culture were collected for Western blot control for testing the expression of overexpressed proteins (see 2.2.7; only if applicable) and for flow cytometry control (see 2.2.8). The RNA was extracted and DNase I digested like described under 2.2.9. The extracted RNA was quality checked using the TapeStation (see 2.2.10). After passing all quality controls the samples were handed into the IMB genomics core facility. There the samples were treated as follows under 2.2.12.1 and 2.2.12.2, dependent on the library preparation method. The bioinformatics analysis was performed by Maya Wilkins.

2.2.12.1 Total RNAseq with rRNA depletion

rRNA depletion was performed with a starting amount of 1500 ng using the riboPool kit from siTOOLs following riboPoolKitManual_v1-4 (December 2021). The RNA clean-up was performed with a ratio of 1.8x of RNA Clean XP beads to RNA volume. Library preparation was performed with Illumina's TruSeq stranded Total RNA LT Sample Prep Kit following TruSeq Stranded total RNA Reference Guide (Oct.2017) (Document # 1000000040499v00) starting at the Fragmentation step. Libraries were amplified in 9 PCR cycles. Followed by profiling in a High Sensitivity DNA assay on a 2100 Bioanalyzer (Agilent technologies) and

quantified using the Qubit dsDNA HS Assay Kit, in a Qubit 2.0 Fluorometer (Life technologies). All samples were pooled together in equimolar ratio and sequenced on a NextSeq 500 Midoutput FC, SR for 1x 75 cycles plus 8 + 8 bp cycles for the dual index read.

2.2.12.2 Small RNAseq

T4 PNK treatment (NEB) was performed for all samples followed by a purification step using the RNeasy MinElute Cleanup protocol (QIAGEN). Next generation sequencing library prep was performed with NEXTflex Small RNA-Seq Kit V3 following Step A to Step G of Bioo Scientific`s standard protocol (V19.01) using the NEXTFlex 3' SR Adaptor and 5' SR Adaptor (5'rApp/NNNNTGGAATTCTCGGGTGCCAAGG/3ddC/ and 5'GUUCAGAGUUCUACAGUCCGA-CGAUCNNNN, respectively). Step A (NEXTflex 3` 4N Adenylated Adapter Ligation) was performed overnight at 20°C and for step F (Bead Cleanup) the modified protocol was used to retain tRNAs and snoRNAs. Libraries were prepared with a starting amount of 350 ng and amplified in 15 PCR cycles. Amplified libraries were purified by running an 8% TBE gel and size-selected for 196 – 328 nt corresponding to an insert size of 70 – 200 nt size range. Libraries were profiled in a High Sensitivity DNA on a 2100 Bioanalyzer (Agilent technologies) and quantified using the Qubit dsDNA HS Assay Kit, in a Qubit 2.0 Fluorometer (Life technologies). All samples were pooled in equimolar ratio and sequenced on 1 NextSeq 500/550 High output Flowcell, SR 1x 85 cycles plus 6 cycles for the index read.

2.2.13 3'RACE

For 3' rapid amplification of cDNA-ends (3'RACE), auxin-inducible degron (AID*) strains were used. The cultures were grown to OD_{600} 0.4 and 10 ml of the culture were collected and stopped with 0.01 % NaN_3. The cells were spun down for 3 min at 600 x g and the dry pellets were stored at -80 °C. To the remaining cultures, either 1 mM indole-3-acetic acid (IAA; for degrons in combination with the AFB2 F-box) or 1µM 5-Phenyl-1H-indole-3-acetic acid (5-Ph-IAA; for degrons in combination with osTIR1(F74G) F-box) were added and samples were collected in the same way as described before after 2.5 h and 5 h.

RNA extraction of the samples was carried out like described under 2.2.9. The 3'RACE procedure is described in Figure 12. The extracted and DNase I treated RNA was reverse transcribed like described under 2.2.11.1 using a 3'RACE specific primer (oCW128; poly-T primer carrying an adaptor sequence). The resulting cDNA was used in a PCR with a gene specific primer together with the reverse adaptor primer (oCW129). The PCR reaction mix

contained 1 µl cDNA, 9 µl ddH2O, 1.25 µl of each primer (10 µM) and 12.5 µl 2x Q5 MM. The PCR program was the following: 30 s at 98 °C, followed by 34 cycles of 5 s at 98 °C, 15 s at 66 °C and 20 s at 72 °C. The final elongation was carried out for 2 min at 72 °C. The samples were supplemented with 6 µl orange loading dye and 5 µl of each sample was loaded onto a 2 % agarose gel and run at 100 V for 1 h.

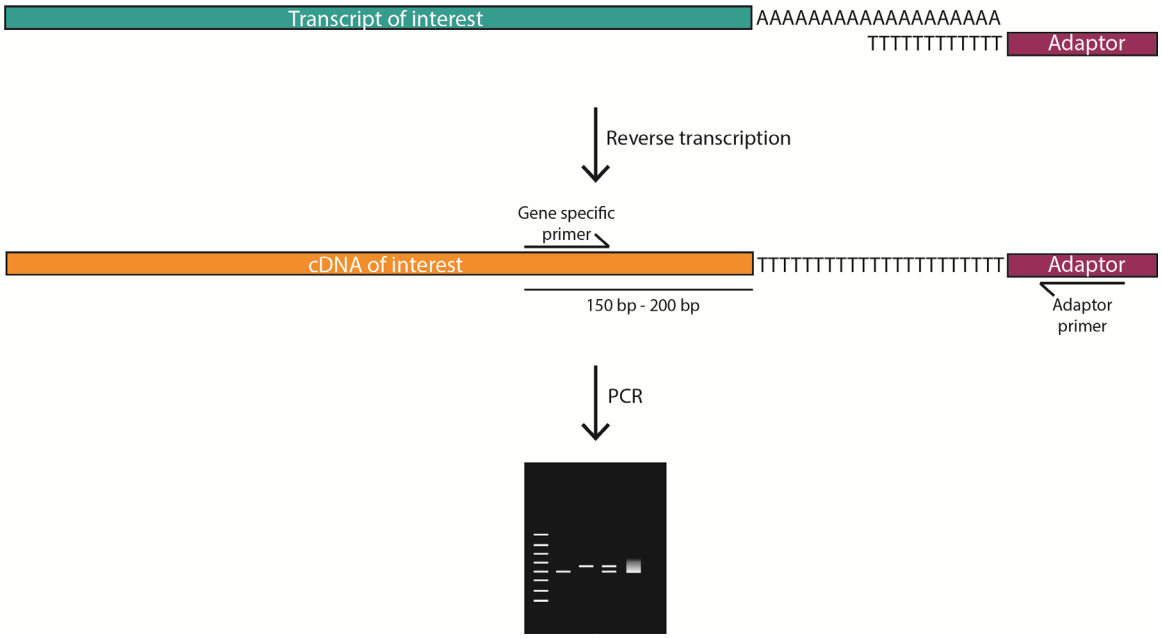

Figure 12 - Schematic outline of 3'RACE experiments. Poly-A tailed RNA is reversed transcribed using a poly-T primer that carries an adaptor sequence. The resulting cDNA is used for a PCR with a gene specific primer and the reverse adaptor primer sequence. The resulting PCR products were analyzed using agarose gel electrophoresis.

2.2.14 Chromatin immunoprecipitation

Chromatin immunoprecipitation (ChIP) experiments were in general conducted like described in our published method for R-ChIP (Wagner and Luke, 2022). R-ChIP is a ChIP, in which R-loop bound, HA-tagged, catalytic inactive RNase H1 is targeted by an anti-HA antibody. In case a DNA:RNA immunoprecipitation (DRIP) or ChIP for the elongation form of RNA polymerase II was carried out, the protocol was only changed by using either the S9.6 antibody or anti-pS2-RNAPII, respectively. These methods do not require overexpression of catalytic inactive RNase H1.

In brief, 150 ml exponentially growing cell cultures (for R-ChIP overexpressing RNase H1 or catalytic inactive RNase H1) were brought to the same OD_{600} value for each sample and replicate. For crosslinking, 4.9 ml 37 % formaldehyde (0.84 % final) were added to each culture. The crosslinking reaction was carried out for 10 min (15 min for RNA polymerase II

ChIP) at RT with shaking the flasks from time to time. The crosslinking was quenched by adding 7.5 ml 2.5 M Glycine for 5 min at RT with shaking the flasks from time to time. The cultures were moved into an ice bath for at least 5 min prior to centrifugation at 4 °C and 3000 x g for 3 min. The cell pellets were washed twice in 20 ml ice cold 1x PBS. The cell pellets were transferred to 1.5 ml centrifugation tubes and spun down again at 4 °C and 3000 x g for 3 min. All supernatant was removed and the cell pellets were stored at -80 °C until further processing.

All following steps until the elution from the beads were carried out on ice. 10 ml FA lysis buffer minus SOD was supplemented with one protease inhibitor tablet and for each sample 5 ml FA lysis buffer plus SOD was supplemented with 0.5 protease inhibitor tablet. The thawed samples was resuspended in 200 µl FA lysis buffer minus SOD with protease inhibitor and transferred to a lysing matrix C tube. The cell lysis was carried out using the FastPrep machine at the speed of 6 m/s for 30 s twice, placing the samples on ice in between for 1 min. For recovery, 800 µl of the FA lysis buffer plus SOD with protease inhibitor were added, the samples were vortexed briefly and transferred to a fresh 2 ml centrifugation tube. The samples were centrifuged at 17000 x g and 4°C for 7 min. The supernatant was discarded and the pellet was resuspended in 750 µl FA lysis buffer plus SOD with protease inhibitor. 20 µl of 20 % SDS was added, followed by another 750 µl FA lysis buffer plus SOD with protease inhibitor. The samples were transferred into 15 ml sonication tubes containing 0.8 g to 1.0 g sonication beads. The sonication was carried out in two times 10 cycles (30 s on, 30 s off) with a 15 min break on ice in between.

In the meantime, the magnetic beads were prepared. Per samples, 200 µl Dynabeads™ Protein G were filled into a 15 ml centrifugation tube and the filling level was marked. 10 ml 1x PBS were added and the tube was placed into a magnetic rack. 6 ml of the supernatant were removed and 5 % molecular biology grade BSA (final, w/v) were added. The beads were incubated for 1 h on a rotating wheel at 4 °C. The tube was again placed in the magnetic rack and all supernatant was removed. The beads were washed in 10 ml 1x PBS, followed by a wash in 10 ml FA lysis buffer plus SOD. The supernatant was removed until the marked initial filling level.

During the incubation of the beads, the sonicated samples were recovered into fresh 2 ml centrifugation tubes and centrifuged at 17000 x g and 4 °C for 15 min. The supernatant was collected and is called ChIP extract. The protein concentration of the ChIP extract was

measured using a Bradford assay. The samples were diluted to 1 mg/ml in 2.2 ml FA lysis buffer plus SOD with protease inhibitor. The samples were split in four fresh tubes with the following volumes: 1 ml for immunoprecipitation, 1 ml as immunoprecipitation negative control (no antibody), 50 µl as input sample for later calculation of the percentage of sample immunoprecipitated and 100 µl for sonication control.

The input samples was stored at -20 °C until further processing. The sonication control samples were mixed with 100 ml Elution buffer B, supplemented with 7.5 µl Proteinase K (20 mg/ml) and incubated overnight shaking at 450 rpm and 65 °C. The samples were EtOH precipitated by adding 1 ml 100 % EtOH and incubating 20 min at -80 °C. The samples were centrifuged for 15 min 20000 x g at 4 °C. The supernatant was removed and the pellets were air dried. The samples were resuspended in 20 µl ddH_2O and were supplemented with 1 µl RNase A (10 mg/ml). After incubating for 30 min at 37 °C, the samples were supplemented with loading dye and analyzed on a 1.5 % agarose gel (run 35 min at 100 V). Optimal sonication yielded in fragment sizes between 100 bp and 500 bp.

The immunoprecipitation (IP) samples were precleared by adding 30 µl of the prepared magnetic beads and incubation for 1 h on a rotating wheel at 4 °C. The samples were placed in a magnetic rack and the supernatant was transferred to a fresh tube. For the negative control samples, no antibody was added, while antibody was added (10 µl Anti-HA 3F10 for R-ChIP, 4 µl S9.6 for DRIP or 5 µl of Anti-pS2-RNAPII for the elongating form of RNA polymerase II) to the immunoprecipitation samples. The samples were incubated for 30 min on a rotating wheel at 4 °C. 50 µl of the prepared magnetic beads were added and the samples were incubated overnight on a rotating wheel at 4 °C.

The IP samples were washed in four steps. Each step was carried out in the same way, but with different buffers (increasing stringency). The samples were placed on a magnetic rack and the supernatant was removed. 1 ml of the buffer for the following step were added and the samples were incubated for 5 min at 4 °C. The order of the buffers was: first FA cell lysis buffer plus SOD, second FA 500 / lysis buffer, third Buffer III and forth 1x TE buffer.

After the last wash, the magnetic beads were resuspended in 100 µl Elution buffer B immediately. At this point, the input samples were thawed and supplemented with 150 µl Elution buffer B. For the elution, the input samples and the IP samples were treated the same way. All samples were incubated for 8 min at 65 °C and 850 rpm on a heat block. The IP samples were placed into a magnetic rack and the supernatant was transferred to a fresh

tube. 100 µl of fresh Elution buffer B were added and the elution was repeated. After pooling the eluents, 7.5 µl Proteinase K (20 mg/ml) were added to the IP and input samples. The samples were incubated overnight at 65 °C, shaking at 450 rpm on a heat block.

The samples were purified using the Qiagen PCR purification kit, eluting the DNA in 50 µl DPEC treated water. The quantitative real time PCR was prepared in a 384 well PCR plate. The reaction mix per well contained 1 µl DNA, 2 µl DPEC treated water, 1 µl of each primer (5 µM) and 5 µl Eva green qPCR Master mix. The RT-qPCR was carried out under the following conditions: 10 min at 95 °C, followed by 40 cycles of 15 s at 95 °C and 1 min at 60 °C. In the end a melting curve was performed from 65.0 °C until 96.5 °C in 0.5 °C steps.

The analysis of the data was carried out using the Bio-Rad CFX Manager software. The data was imported, the C_q determination method was set to 'regression' and the data was exported to Excel. The mean C_q of the technical replicates was calculated and the C_q value of the input sample was corrected to account for the 1:20 dilution compared to the IP samples:

$$log_2(20) = 4.322$$

$$C_q(corr.input) = C_q(input) - 4.322$$

The percent input of the IP samples was calculated:

$$\Delta C_q = C_q(corr.input) - C_q(sample \pm antibody)$$

$$Percent\ input = 100 * 2^{\Delta C_q}$$

2.2.15 Spotting assay

For conducting a spotting assay, suitable agar plates were prepared the day before the cells were spotted. Overnight cultures of the strains to be spotted were prepared in 3 ml of suitable liquid medium.

The OD_{600} of the overnight cultures was measured. In a 96 well plate, the overnight cultures were diluted to OD_{600} 0.5 200 µl dilutions in sterile ddH_2O, followed by dilution in four serial steps with a factor of 1:10. The yeast dilutions were spotted onto the prepared agar plated using a replica plater for either 96 wells or 48 wells. After drying the plates next to a Bunsen burner flame, the plates were incubated at 30 °C if not indicated differently. Images of the plates were taken after 24 h, 48 h and 72 h using the ChemiDoc (Colorimetric modus, 0.3 s imaging time and largest possible imaging frame). The images were edited in the Image Lab

software, where a frame for cutting the images was kept at the same pixel size and the brightness and contrast were adjusted using the 'auto adjust' function.

2.2.16 Cycloheximide chase assay

In order to measure protein stability, Cycloheximide (CHX) chase assays were performed. For this purpose, cells were grown to exponential phase and depending on the experimental setup pretreated with different substances. At the beginning of the CHX chase assay, an untreated sample was taken as 0 min time point. The cell cultures were either treated with 200 µg/ml CHX or stayed untreated. Samples were collected every 15 min by adding the collected volume to a sufficient amount of 10 % NaAz in order to reach 0.01 % NaAz (end concentration) on ice. The volume was corrected in order to reach 2 OD_{600} units. The samples were spun down for 3 min at 600 x g at RT and the supernatant was discarded. The samples were transferred to micro centrifugation tubes and stored at -20 °C until further processing. The protein stability was determined using by Western blotting (2.2.7).

2.2.17 Chromatin binding assay

At least 12 OD of exponentially cycling cells were collected and spun down at 600 x g at RT. The supernatant was discarded, the pellets were resuspended in 1 ml ddH_2O and transferred to fresh micro centrifugation tubes. The samples were again spun down at 900 x g at RT and the dry pellets were stored at -20 °C until further processing. The pellets were thawed on ice and resuspended in 1 ml spheroplasting buffer. The optical density of the suspension was measured. 12 OD units were diluted in 1 ml spheroplasting buffer. 5 µl Zymolyase T20 and 1 µl 1 M DTT were added and the samples were incubated at 30 °C for 40 min. The cells were spun down at 400 xg for 2 min and the supernatant was removed. The pelleted cells were resuspended in 300 µl extraction buffer with protease inhibitor and PosphoStop and split into three tubes containing 50 µl for the whole cell extract , 50 µl for the soluble fraction and 200 µl for the chromatin bound fraction.

The different fractions were treated in different ways:

- Whole cell extract: 1.25 µl 10 % Triton-100 were added, the samples were quickly vortexed and incubated for 5 min on ice. 1 µl SM nuclease was added and the samples were incubated for 15 min on ice. 20 µl urea buffer were added and the samples were boiled at 75 °C for 5 min.

- Soluble fraction: 1.25 µl 10 % Triton-100 were added, the samples were quickly vortexed and incubated for 5 min on ice. The samples were spun for 10 min at 20000 x g and 4 °C. 50 µl of the supernatant were transferred to a fresh tube, 20 µl urea buffer were added and the samples were boiled at 75 °C for 5 min.
- Chromatin bound fraction: 5 µl 10 % Triton-100 were added, the samples were quickly vortexed and incubated for 5 min on ice. 1 ml 30 % ice cold sucrose was added into fresh tubes and the samples were layered on top. The samples were spun for 10 min at 20000 x g and 4 °C. The supernatant was removed and the pellets were resuspended in 200 µl extraction buffer supplemented with PhosphStop and proteinase inhibitor and 5 µl 10 % Triton-100. The sucrose step was repeated. The supernatant was removed and the pellet was resuspended in 50 µl extraction buffer supplemented with PhosphStop and proteinase inhibitor and 1.25 µl 10 % Triton-100. 1 µl SM nuclease was added and the samples were incubated on ice for 15 min. 20 µl urea buffer were added and the samples were boiled at 75 °C for 5 min.

The samples were loaded to a 15 well 4 to 15 % gradient polyacrylamide gel (4 µl for whole and soluble, 6.8 for chromatin fraction) and run at 140 V for 51 min. The following steps were performed according to the Western blot protocol (2.2.7). As loading control for the chromatin fraction an antibody against histone H3 was used, while for the soluble fraction anti-Pgk1 was used.

2.2.18 Chromatin spreads for measurement of RNA:DNA hybrids

This method was originally published by the D'Amours lab (Roy *et al.*, 2024). Exponentially growing cells from a 15 ml culture were spun down at 3000 x g. The cells were resuspended in 1 ml ZK buffer and 40 µl 1 M DTT were added. The cells were incubated at RT for 2 min with gentle shaking. The cells were spun down again and resuspended in 1 ml ZK buffer, supplemented with 25 µl zymolyase T20. The samples were incubated for 45 min at 30 °C, shaking at 100 rpm. The cells were spun down at 4 °C at 17000 x g and resuspended in 2.5 ml cold MES buffer for washing. The centrifugation was repeated and the cells were gently resuspended in 300 µl cold MES buffer.

The slides were prepared by first dipping in ddH_2O, followed by dipping them twice in 70 % EtOH. Between each wash the slides were dried using a Kim wipe. For spreading, 20 µl of cells suspension were spotted on a slide. 40 µl PFA solution (PFA solution has to be

prepared freshly on the same day) were added and the slide was gently swirled for mixing. 80 µl 1 % NP40 solution was added and again gently swirled for mixing. The slides were incubated for 2 min, followed by addition of another 80 µl PFA solution. For spreading, a clean P1000 pipet tip was passed over the slide lengthwise for spreading the DNA without touching the slide, only the liquid. A schematic representation of the protocol can be found in Figure 13. The slides were covered and dried for 24 h under the fume hood. The slides were directly immuno stained or stored at -20 °C until further processing.

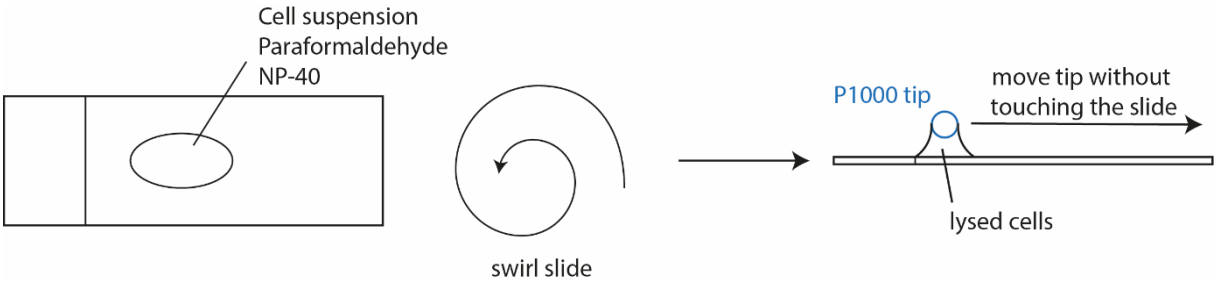

Figure 13 - Schematic description of chromatin spreading.

Prior to immuno staining, the sucrose coating was removed by submerging the slides for 1 min in 1:500 Kodak photoflo, followed by 5 min in 1x TBS. The slides were drained by holding them vertically onto a paper tissue. The samples were blocked by adding 350 µl 1xTBS + 5 % BSA and incubated for 15 min in a wet chamber at RT. The blocking solution was drained like before and 80 µl primary antibody (1:100 S9.6 in 1xTBS + 5 % BSA) were added. The samples were covered using a cover slip and incubated overnight at 4 °C.

The slides were washed three times in 1x TBS for 10 min with slow shaking. All following steps were carried out in the dark. The liquid from the slides was drained like described before and 80 µl secondary antibody (1:666 Cy3 Jackson Immuno in TBS + 5 % BSA) were added. For incubation, a cover slip was added and the samples were incubated for 2 h at 4 °C. The slides were washed twice in 1x TBS for 10 min. After drying completely under the fume hood 40 µl Vectashield containing 5 µg/ml DAPI were added onto the samples. A coverslip was put on and sealed with nail polish. The samples were either imaged directly or stored at 4 °C. For imaging, the Echo Revolve microscope was used. Z-stacks with 0.3 µm were taken in the DAPI channel (Exposure time: 5 ms, 40 % light intensity), TxRed channel (Exposure time: 55 ms, 100 % light intensity) and in the transmitted light channel (Exposure time: 5 ms, 100 % light intensity). The images were analyzed using Fiji. First, the plane in the z-stack with the best DAPI resolution was chosen. In this image, the threshold was

adjusted to aim for only DAPI stained regions. The regions of interest (ROI) were added to the ROI manager *via* the function 'analyze particles' and like this the S9.6 foci within the DAPI region could be counted manually in the TxRed channel.

3. Results

Little is known about the regulation of endogenous RNase H1 (also abbreviated Rnh1 in budding yeast). In this project, I found that Rnh1 is upregulated upon Sen1 loss. In this situation, Rnh1 becomes essential for preventing transcription-replication conflicts (TRCs)

3.1 Catalytic inactive *rnh1(D193N)* is toxic when RNA:DNA hybrids accumulate

To learn about RNase H1 regulation, the effects of increased Rnh1 levels on cell viability was studied. For this purpose, an inducible system for overexpression was used. The galactose inducible system was introduced using a high copy number plasmid that led to a high expression of either wild type *RNH1* or the catalytic inactive allele *rnh1(D193N)* (Figure 14 A). In a wild type (wt) context, overexpression of both, *RNH1* and *rnh1(D193N)* has a slight effect on viability, while a short-term overexpression of 5 h has no effect on the cell cycle profile (Figure 14 B). Challenging the cells by exposure to the DNA damage accumulating agents MMS and HU, enhances this effect and the cells grow sick (Figure 14 B).

Rnh1 is important for the resolution of RNA:DNA hybrids, so the overexpression was also performed in the RNA:DNA hybrid accumulating backgrounds *sen1-1, rnh1 rnh201, top1* and *mft1* (Figure 14 C). While overexpression of wild type *RNH1* has no effect on the viability and cell cycle distribution in these backgrounds, the catalytic inactive allele leads to a strong reduction in viability in all four backgrounds and accumulation of cells in G2/M-phase. In summary, high levels of RNase H1 do not have negative impacts on the cells, while high levels of the inactive protein are harmful if RNA:DNA hybrids are pre-accumulated.

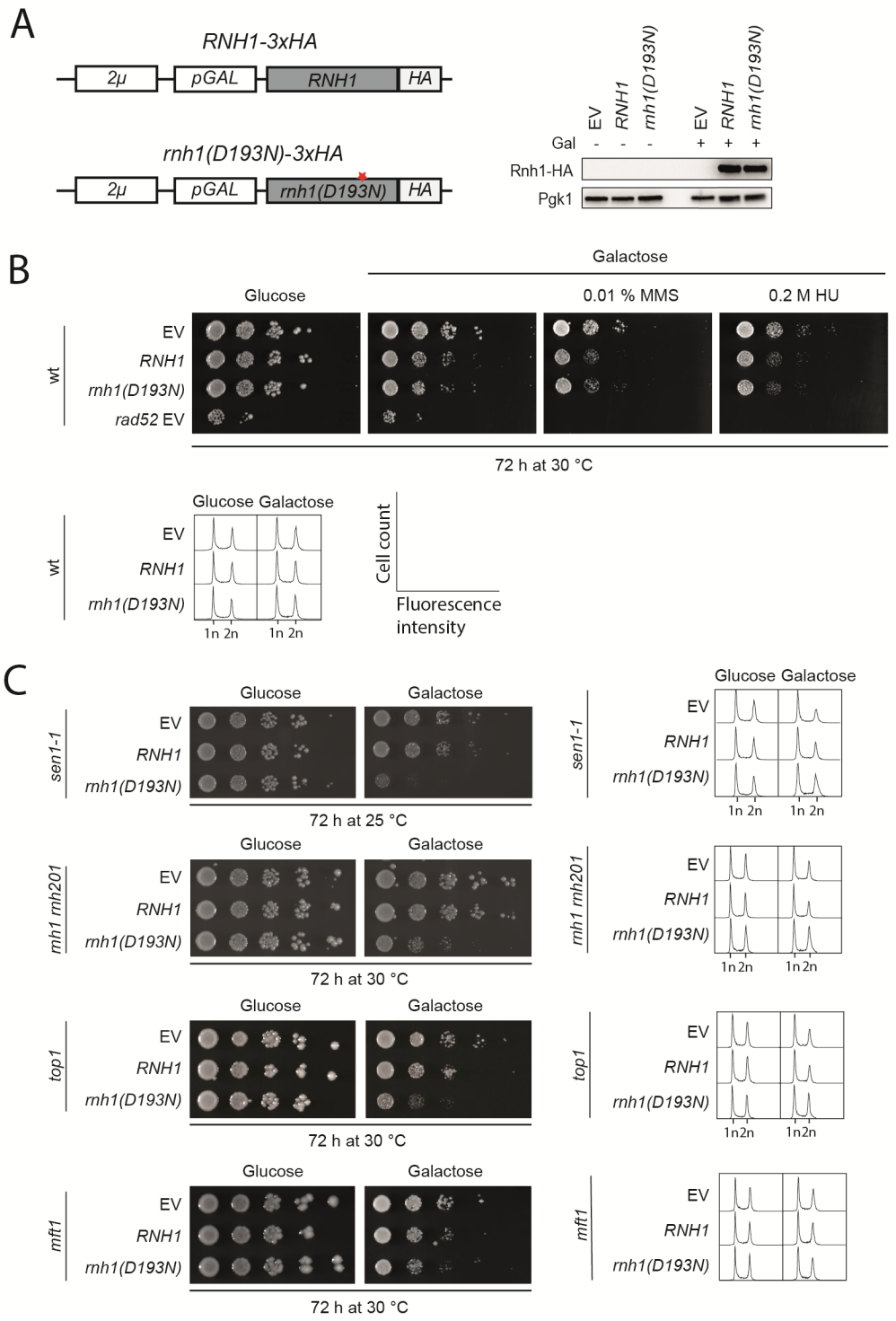

Figure 14 - Overexpression of catalytic inactive RNase H1 is toxic in the presence of high RNA:DNA hybrid levels. ***(A)*** *Schematic illustration of the allele for overexpression of RNase H1 and the catalytic inactive version RNase H1 (D193N; red star indicates mutation) and a test expression of both galactose inducible proteins.* ***(B)*** *and* ***(C)*** *Tenfold serial dilutions of the indicated budding yeast strains were spotted on SC-Leu agar plates containing either glucose or galactose (B: additional plates containing galactose and 0.01 % MMS or 0.2 M HU were added) and incubated for 72 h at 25 °C or 30 °C. Additionally, the same strains were grown in liquid SC-Leu medium containing 2 % raffinose which was supplemented with either 2 % glucose or 2 % galactose for 5 h. The DNA content was analyzed using flow cytometry for determining the cell cycle distribution of the cultures. EV: empty vector, MMS: methyl methanesulfonate, HU: hydroxyurea.*

3.2 RNase H1 resolves a sub-population of RNA:DNA hybrids

As described above, the overexpression of active RNase H1 does not influence the viability of either wild type or *rnh1 rnh201* cells. To study if the overexpressed enzyme and its catalytic inactive version are binding to the chromatin at known R-loop loci (Chan *et al.*, 2014; El Hage *et al.*, 2014; San Martin-Alonso *et al.*, 2021) an RNase H1 ChIP (Chromatin immune precipitation) experiment was performed. From the same samples a DRIP (DNA:RNA immune precipitation) experiment was performed for studying the effect of overexpression on RNA:DNA hybrid levels. Comparing the binding of overexpressed Rnh1-HA (Rnh1-3xHA, abbreviated at Rnh1-HA from here on) in wt and *rnh1 rnh201* cells, no difference is detectable (Figure 15 A and B). On the contrary, the catalytic inactive allele D193N shows an increased binding in the *rnh1 rnh201* background (Figure 15 A). In wt, Rnh1 and *rnh1(D193N)* show a similar binding behavior at the *GCN4* and *PDC1* loci, while *rnh1(D193N)* binds stronger to *SUF2* and 5s rDNA (Figure 15 A). These results are validated by the low background signal in the control IP without antibody (Figure 15 B). In summary, the amount of Rnh1 binding is not influenced by the levels of RNA:DNA hybrids, most likely due to the transient binding during RNA:DNA hybrid degradation. This is different for the catalytic inactive version which increases its binding in the presence of accumulated RNA:DNA hybrids. This effect is due to the fact that it does not degrade the RNA:DNA hybrid but stays bound.

In the DRIP experiment (DNA:RNA immune precipitation), the RNA:DNA hybrid resolution capability of RNase H1 was tested at the same loci as in the RNase H1 ChIP (Figure 15 C and D). In wt, *RNH1* overexpression does not decrease the RNA:DNA hybrid levels compared to the empty vector control (EV), while in *rnh1 rnh201* cells a strong hybrid reduction is detectable at the *SUF2* locus, while the levels stay constant for *GCN4*, *PDC1* and 5s rDNA loci. Overexpression of *rnh1(D193N)* on the other side leads to an increase in hybrid levels at the *SUF2* and 5s rDNA loci in wt cells, while *GCN4* and *PDC1* stay at control levels. In *rnh1 rnh201* cells overexpressed *rnh1(D193N)* at all loci leads to an increase in hybrids. In summary, overexpression of *RNH1* keeps R-loop levels at or below wild type levels. Nonetheless, the protein does not change its binding behavior even in backgrounds with high hybrid levels. This is most likely due to the transient binding of RNase H1. On the other hand, *rnh1(D193N)* overexpression leads to an R-loop stabilization at some loci in wt

and all loci in *rnh1 rnh201* cells. As the enzyme is catalytic inactive, it binds RNA:DNA hybrids and stabilizes them, leading to higher hybrid levels.

From these results it seems that RNase H1 can bind to all RNA:DNA hybrids, but only degrades a subset of them. The Koshland lab published the same observation (Zimmer and Koshland, 2016). Opening the question, how RNase H1 discriminates between RNA:DNA hybrids that it degrades and those it is not degrading. Furthermore, together with the spotting results from Figure 14 where catalytic inactive RNase H1 is toxic when overexpressed appears, that Rnh1 degrades RNA:DNA hybrids mainly if hybrid levels are dysregulated, here induced by confirmed RNA:DNA hybrid accumulating genetic backgrounds.

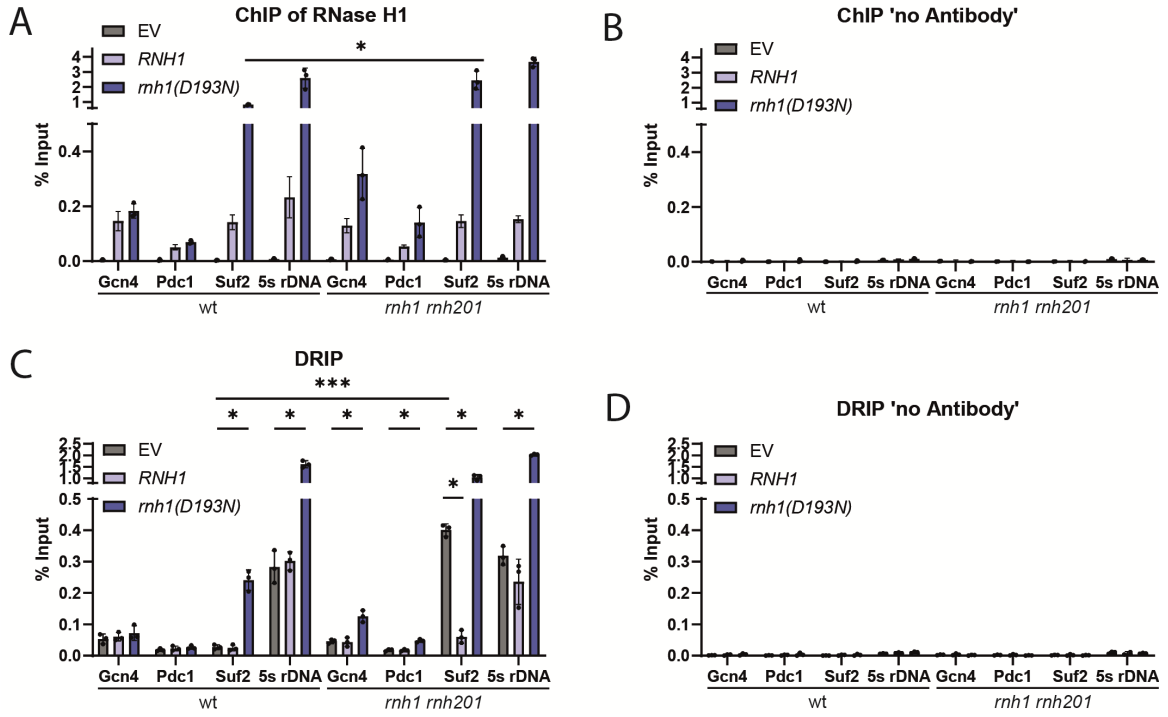

Figure 15 - RNase H1 does not degrade all RNA:DNA hybrids equally. ***(A)*** *RNase H1 ChIP for determining the binding of RNase H1-HA and RNase H1 D193N-HA to chromatin, pulling down the HA-tag, after overexpression for 8 h. Unpaired t-test (*: p<0.05)* ***(B)*** *Background control of (A) without antibody* ***(C)*** *DRIP from the same samples used for (A) and (B) for capturing RNA:DNA hybrid levels. Unpaired t-test (*: p<0.05, ***: p<0.001)* ***(D)*** *Background control of (C) without antibody.*

3.3 RNase H1 overexpression does not influence the transcriptome

RNA:DNA hybrids are regulators of transcription (Costantino and Koshland, 2015; Grunseich *et al.*, 2018). Overexpression of RNase H1 is a broadly used tool to reduce RNA:DNA hybrids genome-wide, while the overexpression of the catalytic inactive version is used as a probe for R-loop detection (Chédin *et al.*, 2021; Mukhopadhyay *et al.*, 2024), even if it influences RNA:DNA hybrid levels (Figure 15). For studying the effect of RNase H1 mediated increases and decreases of RNA:DNA hybrids, total RNA sequencing (RNAseq) was performed. In a wild type background, overexpression of RNase H1 does not change the transcriptome (Figure 16 A), while in Figure 16 B overexpression of the catalytic inactive version upregulates two genes, *GND2* (6-phosphogluconate dehydrogenase) and *HSP26* (Heat shock protein 26).

The *rnh1 rnh201* double mutant is known for accumulated RNA:DNA hybrids due to the inhibited degradation of RNA:DNA hybrids. Lowering the levels by RNH1 overexpression leads to an upregulation of *GND2* and overexpression of the catalytic inactive allele *rnh1(D193N)* has no impact on the transcriptome (Figure 16 C and D). In total, changing RNA:DNA hybrid levels by overexpression of RNase H1 or its catalytic inactive counterpart has little effect on the transcriptome in *S. cerevisiae* , arguing, that the hybrids regulated by RNase H1 are not regulatory RNA:DNA hybrids. It has to be considered, that small RNAs (smaller than 70 nt) and ribosomal RNAs were excluded in the analysis due to technical reasons. This is why changes in their expression cannot be excluded.

In contrast to overexpression, the deletion of *RNH1* lead to downregulation of five mitochondrial transcripts which could be caused by problems in replication of the mtDNA (Holt, 2019). Additionally, *RRN3* (transcription factor important for RNA polymerase I recruitment to rDNA), *BDH2* (alcohol dehydrogenase) and *HSP12* (heat shock protein involved in maintaining membrane organization) were upregulated. These are minor changes enforcing the argument, that RNase H1 is not targeting regulatory RNA:DNA hybrids.

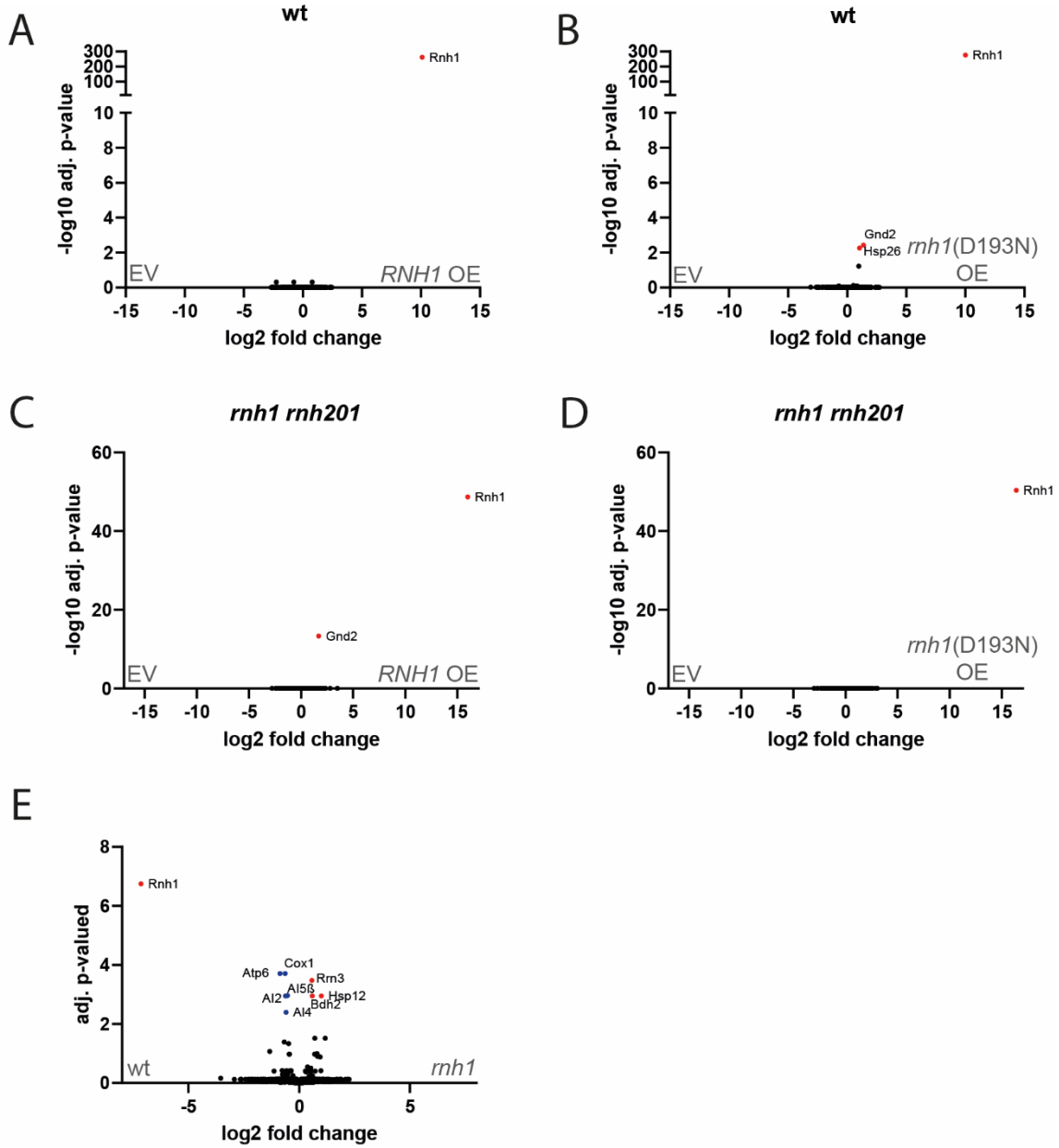

Figure 16 – RNase H1 levels have a minor influence on the transcriptome. ***(A)*** *Total RNA sequencing of wild type cells overexpressing RNH1 vs. EV control. Threshold for significance: p<0.01.* ***(B)*** *Total RNA sequencing of wild type cells overexpressing rnh1(D193N) vs. EV control. Threshold for significance: p<0.01.* ***(C)*** *Total RNA sequencing of rnh1 rnh201 cells overexpressing RNH1 vs. EV control. Threshold for significance: p<0.01.* ***(D)*** *Total RNA sequencing of rnh1 rnh201 cells overexpressing rnh1(D193N) vs. EV control. Threshold for significance: p<0.01.* ***(A-D)*** *Overexpression was carried out for 5 h at 30 °C in SC-Leu + 2 % raffinose + 2 % galactose medium. EV: empty vector* ***(E)*** *Total RNA sequencing or rnh1 vs wild type cells. Blue dots indicate significant down regulated genes from mtDNA, red dots indicate significant upregulated genes from genomic DNA. The cells were grown from OD 0.1 to OD 0.6 in YPD at 30 °C. wt: wild type. Threshold for significance: p<0.01.*

3.4 RNase H1 becomes essential if Sen1 helicase is dysfunctional

For understanding RNase H1 regulation, it is important to understand genetic interactions it is involved in. Here different mutants were chosen that are known to increase RNA:DNA hybrid levels. Rnh201 is the catalytic subunit of RNase H2 which is, as Rnh1, an important RNA:DNA hybrid endonuclease. In addition to its RNA:DNA hybrid resolution capability, it can excise single incorporated ribonucleotides. Deletions of *RNH201* and *RNH1* do not show a genetic interaction in unchallenged conditions (Figure 17 A). From the literature we know that *rnh1 rnh201* is sensitive to genotoxic drugs like MMS (Lockhart *et al.*, 2019; Heuzé *et al.*, 2023). Topoisomerase 1 (Top1) prevents RNA:DNA hybrids by relieving topological stress (Promonet *et al.*, 2020). No genetic interaction between deletions of *TOP1* and *RNH1* could be detected (Figure 17 A). The THO complex is important for transcription elongation and known to prevent high RNA:DNA hybrid levels (San Martin-Alonso *et al.*, 2021). Here, the complex member *MFT1* was deleted. *mft1* shows no genetic interaction with *rnh1* (Figure 17 A). Sen1 helicase has multiple roles in transcription termination, during transcription-replication conflicts and is known to be an RNA:DNA hybrid helicase (Aiello *et al.*, 2022; Xie, Libri and Porrua, 2023). Here, the temperature-sensitive loss of function allele *sen1-1* was used. At the semi-permissive temperature 28 °C *sen1-1* alone is sick, but in combination with *RNH1* deletion, the cells are growing very little (Figure 17 A). This synthetic lethality argues that RNase H1 is essential in the *sen1-1* context.

Repeating the experiment using the catalytic inactive allele *rnh1(D193N)* does not influence the viability of a double mutant *sen1-1 rnh1(D193N)* (Figure 17 B). As a control, genetic interactions of the *sen1-1* mutant with the other RNA:DNA hybrid accumulating mutants were studied (Figure 17 C). *sen1-1* shows no genetic interaction with deletions of *RNH201* and *TOP1* (Figure 17 C). Combining *sen1-1* with *MFT1* deletion is synthetic lethal at 30 °C (Figure 17 C). Sen1 mutants and mutants of the THO complex are known for high RNA:DNA hybrid levels (San Martin-Alonso *et al.*, 2021). Most likely the combination of both leads to a lethal hybrid concentration. In conclusion, RNase H1 becomes essential in a *sen1-1* mutant, indicating that Sen1 might be important for RNase H1 regulation.

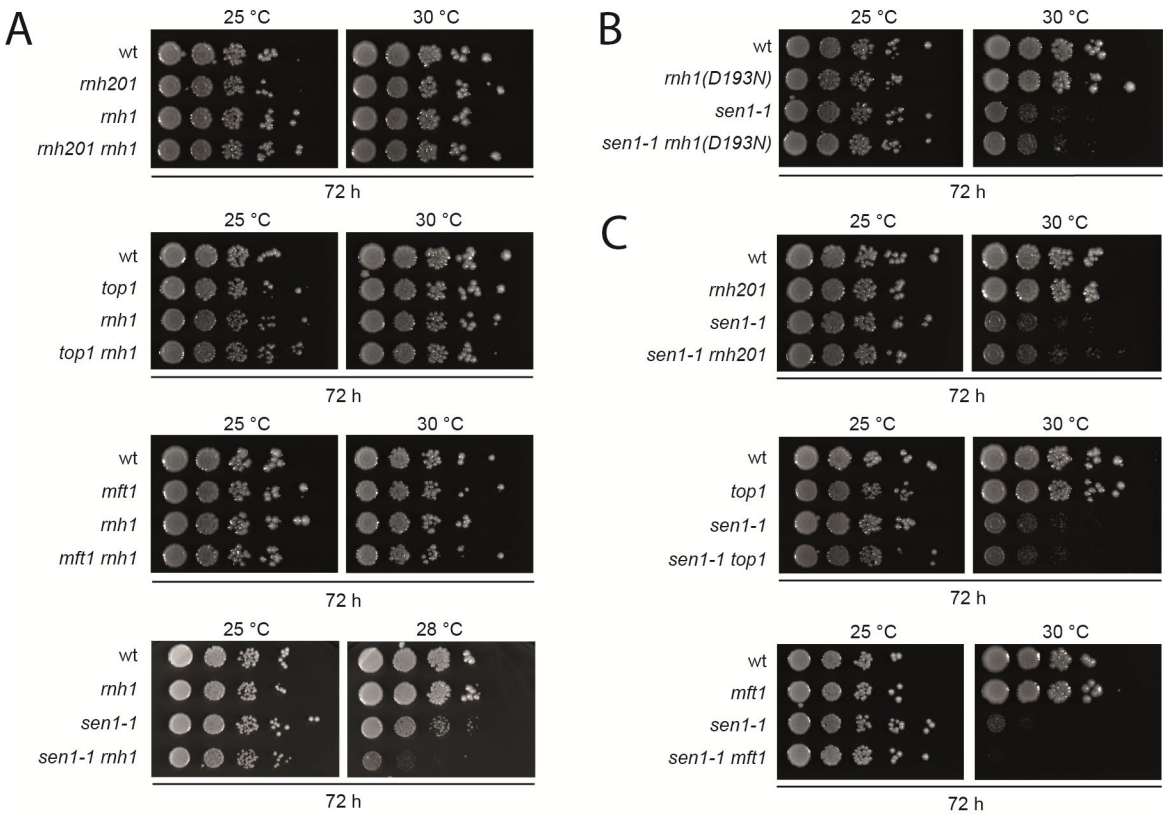

Figure 17 – RNase H1 is essential in the loss of function mutant sen1-1. ***(A), (B)*** *and* ***(C)*** *Tenfold serial dilutions of the indicated budding yeast strains were spotted on YPD agar plates containing and were incubated for 72 h at 25 °C and 28 °C or 30 °C.*

3.5 RNase H1 is upregulated in the absence of Sen1 helicase

RNase H1 is essential if Sen1 is dysfunctional (Figure 17), which indicates that there may be cross-talk between Sen1 and RNase H1 in terms of regulation and activity. To test this hypothesis, Rnh1 levels were studied after auxin induced degradation of Sen1-AID*. All proteins carrying an auxin inducible degron tag were additionally 9xMYC-tagged for detection. Figure 18 A explains the experimental setup. Cells were inoculated to OD 0.1. After reaching OD 0.4 they were supplemented with auxin. Samples were taken every 30 min for 5 h. In Figure 18 B and C an auxin inducible Sen1-AID* degron was used. Sen1-AID* was depleted for 5 h and Rnh1-HA levels were quantified from a Western blot. After 1.5 h Rnh1 was significantly upregulated. This upregulation increased during the 5 h of depletion leading to six times higher RNase H1 levels.

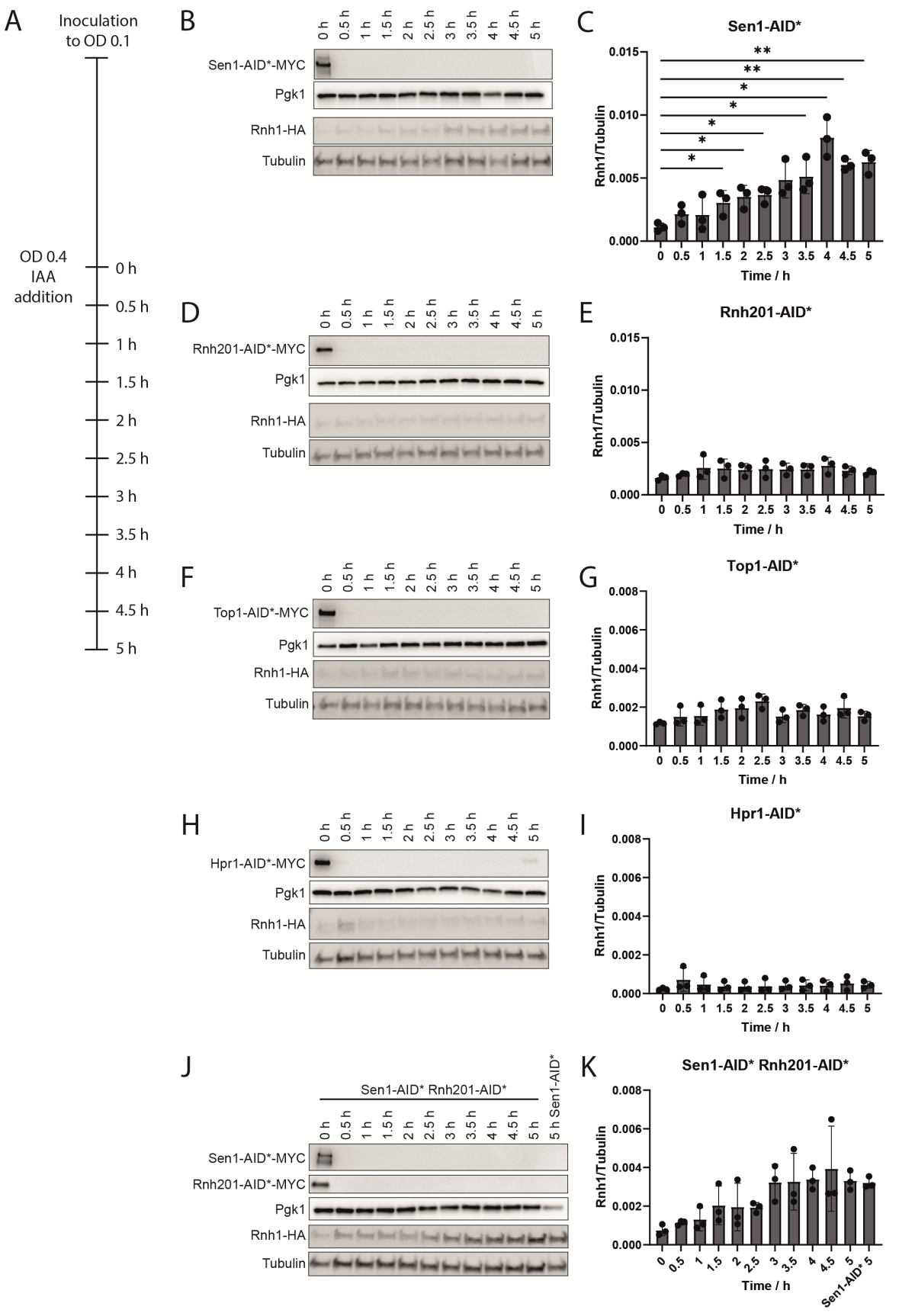

Figure 18 - RNase H1 is upregulated in the absence of Sen1. ***(A)*** *Time line for growing samples in B to K* ***(B)*** *Representative Western blot analysis of endogenous Rnh1-HA levels over a time course of 5 h after depleting Sen1-AID*.* ***(C)*** *Quantification of the representative Western blot in (B) and two*

more biological replicates. Unpaired t-test (: p<0.05; **: p<0.01).* ***(D)*** *Representative Western blot analysis of endogenous Rnh1-HA levels over a time course of 5 h after depleting Rnh201-AID*.* ***(E)*** *Quantification of the representative Western blot in (D) and two more biological replicates.* ***(F)*** *Representative Western blot analysis of endogenous Rnh1-HA levels over a time course of 5 h after depleting Top1-AID*.* ***(G)*** *Quantification of the representative Western blot in (F) and two more biological replicates* ***(H)*** *Representative Western blot analysis of endogenous Rnh1-HA levels over a time course of 5 h after depleting Hpr1-AID*.* ***(I)*** *Quantification of the representative Western blot in (H) and two more biological replicates.* ***(J)*** *Representative Western blot analysis of endogenous Rnh1-HA levels over a time course of 5 h after depleting Sen1-AID* Rnh201-AID*.* ***(K)*** *Quantification of the representative Western blot in (J) and two more biological replicates. IAA: 3-Indoleacetic acid (auxin)*

Like in the spotting assays above (Figure 17), also other factors that are important for RNA:DNA regulation (Rnh201-AID*, Top1-AID*, Hpr1-AID*) were depleted and Rnh1 levels were measured (Figure 18 D-I). None of them led to an upregulation in RNase H1 protein levels.

It is published, that the triple mutant *sen1-1 rnh1 rnh201* is inviable, even at permissive temperatures, as is the triple mutant *rnh1 rnh201* Sen1-AID* after Sen1 depletion (Costantino and Koshland, 2018; Lockhart *et al.*, 2019). This genetic interaction could indicate that the importance of RNase H1 is higher in a Sen1-AID* Rnh201-AID* strain after degrading both enzymes, leading to even higher Rnh1 levels than in the Sen1-AID* strain. This is not the case (Figure 18 J and K). After 5 h of depletion, the double degron Sen1-AID* Rnh201-AID* has the same Rnh1 levels as the single Sen1-AID* degron. There are two possible explanations for this. First, Rnh1 is targeting different RNA:DNA hybrids than Rnh201 and does not account for RNA:DNA hybrids accumulating due to Rnh201-AID* depletion in the double degron. Second, and more likely, 5 h of depletion might not be enough to show a difference between Sen1-AID* and Sen1-AID* Rnh201-AID* as the maximal speed of Rnh1 biosynthesis is reached. In summary, RNase H1 expression levels are strongly coupled to Sen1 presence and activity in *S. cerevisiae*.

3.6 Sen1 levels rise after *RNH1* deletion

RNase H1 is upregulated upon Sen1-AID* depletion (Figure 18) and becomes essential in the *sen1-1* background (Figure 17). Due to this strong genetic interactions, it is possible that a Sen1 levels as well are regulated in an Rnh1-dependent manner. For studying this, Sen1 protein levels were measured in an *RNH1* deletion (Figure 19). A clear upregulation of Sen1-MYC was detected. This results indicates that both, Rnh1 and Sen1 act on the same

substrate. In case one of them is not present, the other is upregulated in order to prevent a more extreme RNA:DNA hybrid accumulation and DNA damage in the consequence.

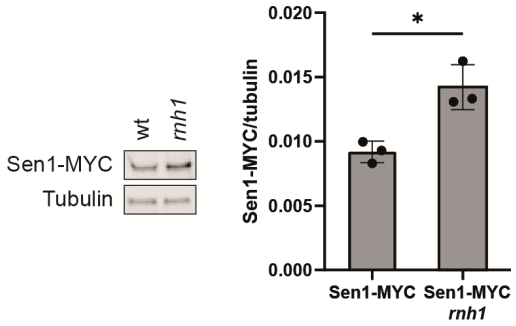

Figure 19 – Sen1 levels are increased in a RNH1 deletion. Protein levels of Sen1-MYC were measured by western blot in exponentially growing cells in a wild type background or RNH1 deletion. The experiment was carried out by Matteo Longaretti. Unpaired t-test (: p<0.05). wt: wild type.*

3.7 RNase H2 is not upregulated upon Sen1-AID* depletion

Both RNase H1 and RNase H2 are degrading RNA:DNA hybrids and R-loops (Cerritelli and Crouch, 2009; Niehrs and Luke, 2020). Both enzymes target the same structure and it might be, that due to this, both enzymes are upregulated upon Sen1-AID* depletion. This is why protein levels of the RNase H2 subunits Rnh201 and Rnh202 were tested (Figure 20). The third subunit Rnh203 was not detectable and could not be quantified. Exponential cell cultures were supplemented with auxin and samples were collected every hour over a time course of 5 h (Figure 20 A). In contrast to the Rnh1 effect, Rnh201 levels were decreasing after depletion of Sen1-AID* (Figure 20 B), while Rnh202 levels stay constant (Figure 20 C). These results, together with the genetic interactions where *sen1-1* grows sick if *RNH1* is deleted, but has no additivity with deletion of *RNH201* (Figure 17) argue, that specifically RNase H1 is important in a Sen1 context while RNase H2 is not as important if Sen1 is lacking.

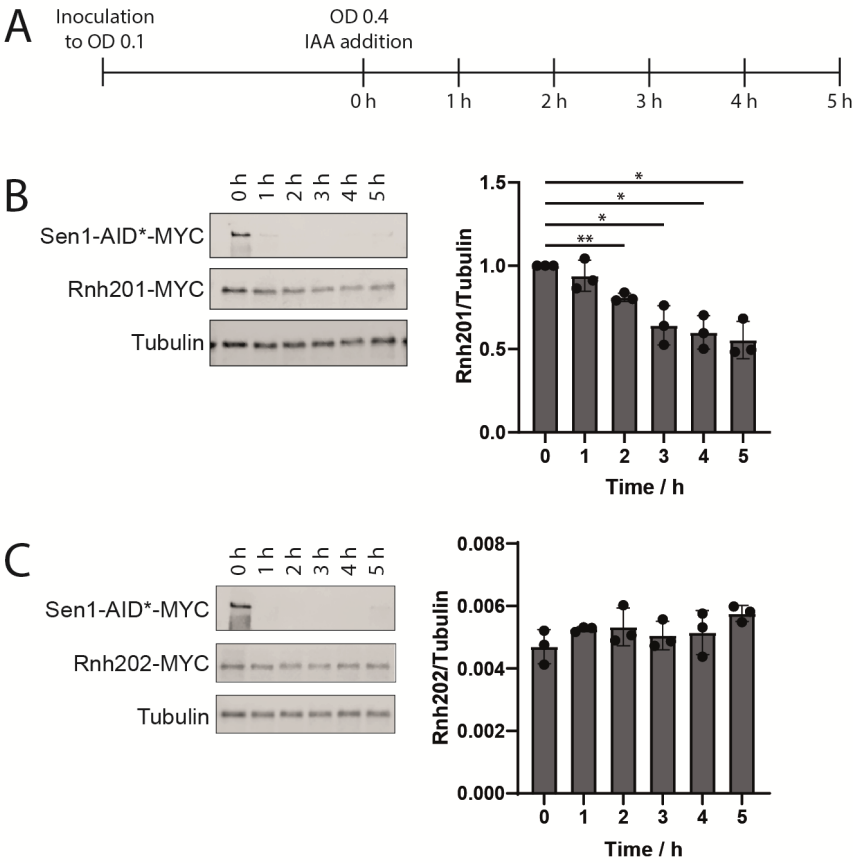

Figure 20 – RNase H2 is not upregulated in the absence of Sen1. ***(A)*** *Time line for growing samples in B and C* ***(B)*** *Western blot analysis of endogenous Rnh201-6xMYC levels over a time course of 5 h after depleting Sen1-AID*. Bar graph shows quantification of Western blot. Unpaired t-test (*: p<0.05; **: p<0.01).* ***(C)*** *Western blot analysis of endogenous Rnh202-3xMYC levels over a time course of 5 h after depleting Sen1-AID*. Bar graph shows quantification of Western blot. IAA: 3-Indoleacetic acid (auxin)*

3.8 RNase H1 upregulation is caused by Sen1 specific DNA damage

Sen1 is an essential gene (Giaever *et al.*, 2002). Depletion of the Sen1 degron causes the cells to die due to genotoxic stress (Mischo *et al.*, 2011). DNA damage can be caused due to different reasons. Examples are transcription-replication conflicts that arise in the absence of Sen1, chemical substances or defects during replication. To rule out that any DNA damage causes an upregulation of Rnh1, but the effect being Sen1 specific, Rnh1-HA cells were treated either with 150 mM HU or 0.02 % MMS, causing genotoxic stress (Figure 21 A). While the DNA damage response factors Rad53 and Rnr3 reacted to the treatment, Rnh1-HA levels were decreasing. This indicates that not any genotoxic stress causes Rnh1 upregulation, but Sen1 specific genotoxic stress does.

Another control that was performed is the depletion of Cdc20-AID* (Figure 21 B). *CDC20* is, like *SEN1*, an essential gene in budding yeast. Depletion of Cdc20-AID* causes the cells to die, due to its function as an activator of the anaphase-promoting complex, necessary for mitosis to occur (Hartwell *et al.*, 1973; Visintin, Prinz and Amon, 1997). Different than in Sen1-AID*, in the Cdc20-AID* strain after auxin addition RNase H1 is not upregulated (Figure 21 B), again indicating that the upregulation is a Sen1 specific effect.

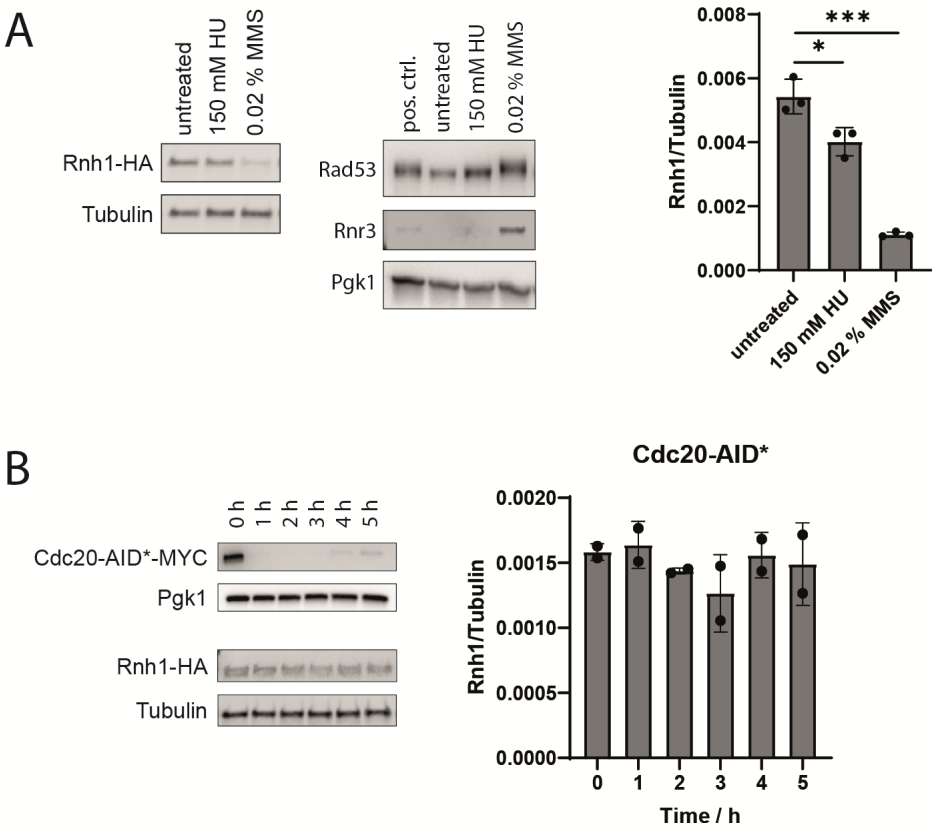

Figure 21 – RNase H1 upregulation in Sen1-AID is not due to cell death.* ***(A)*** *Western blot analysis of cells treated with 150 mM HU or 0.02 % MMS for 5 h at 30 °C. Bar graph shows quantification of Rnh1-HA Western blot over Tubulin Western blot. Unpaired t-test (*: p<0.05; **: p<0.01; ***: p<0.001).* ***(B)*** *Western blot analysis of Rnh1-HA levels in cells depleted for Cdc20-AID* over 5 h. MMS: methyl methanesulfonate, HU: hydroxyurea.*

3.9 Absence of Sen1 changes the transcript abundance of many genes

The upregulation of RNase H1 in a Sen1-AID* depletion context can be mediated by higher protein production or by stabilization of the protein. Here, transcription elongation and transcript levels of *RNH1* were measured to find out, if the upregulation is happening on a transcriptional level. First, levels of the elongating form of RNA polymerase II (RNAP II) were measured. The elongating form of RNAPII can be discriminated by phosphorylation of

Serine 2 (pS2), against which an antibody is available that is suitable for ChIP (Buratowski, 2009). This approach was chosen due to the high changes in transcript levels for all genes in the Sen1-AID* strain, caused by the transcription termination function of Sen1 (Aiello *et al.*, 2022; Xie, Libri and Porrua, 2023). Due to this global transcriptional upregulation, also housekeeping genes were dysregulated and the results were different depending on the chosen gene for nomalization in qRT PCR (data not shown), not allowing any conclusion. While for the genes of all the RNase H2 subunits and *ACT1* the ongoing transcription was increasing after 2.5 h and was even stronger after 5 h, Rnh1 first showed an increase after 2.5 h and stayed stable until 5 h (Figure 22 A). The high background levels in the 5 h condition of Rnh1 (Figure 22 B) make it hard to interpret this time point. In general, this experiment shows that the transcript upregulation is not specific to Rnh1, while the upregulation in protein levels is (Figure 18 and Figure 20).

As the ChIP of RNAP II did not give a definite answer, digital droplet PCR (ddPCR) was performed (Figure 22 C). This method allows the quantification of transcripts per cell. For the transcripts of *ACT1* and the three RNase H2 subunits the pattern stayed the same, showing a constant increase of each transcript over time. For the transcripts of *RNH1* an initial increase after 2.5 h could be detected, followed by a drop in transcript levels per cell. This pattern does not fit the constant increase in Rnh1 protein levels. From these experiments no clear conclusion can be taken whether Rnh1 protein levels are regulated on a transcriptional level or not.

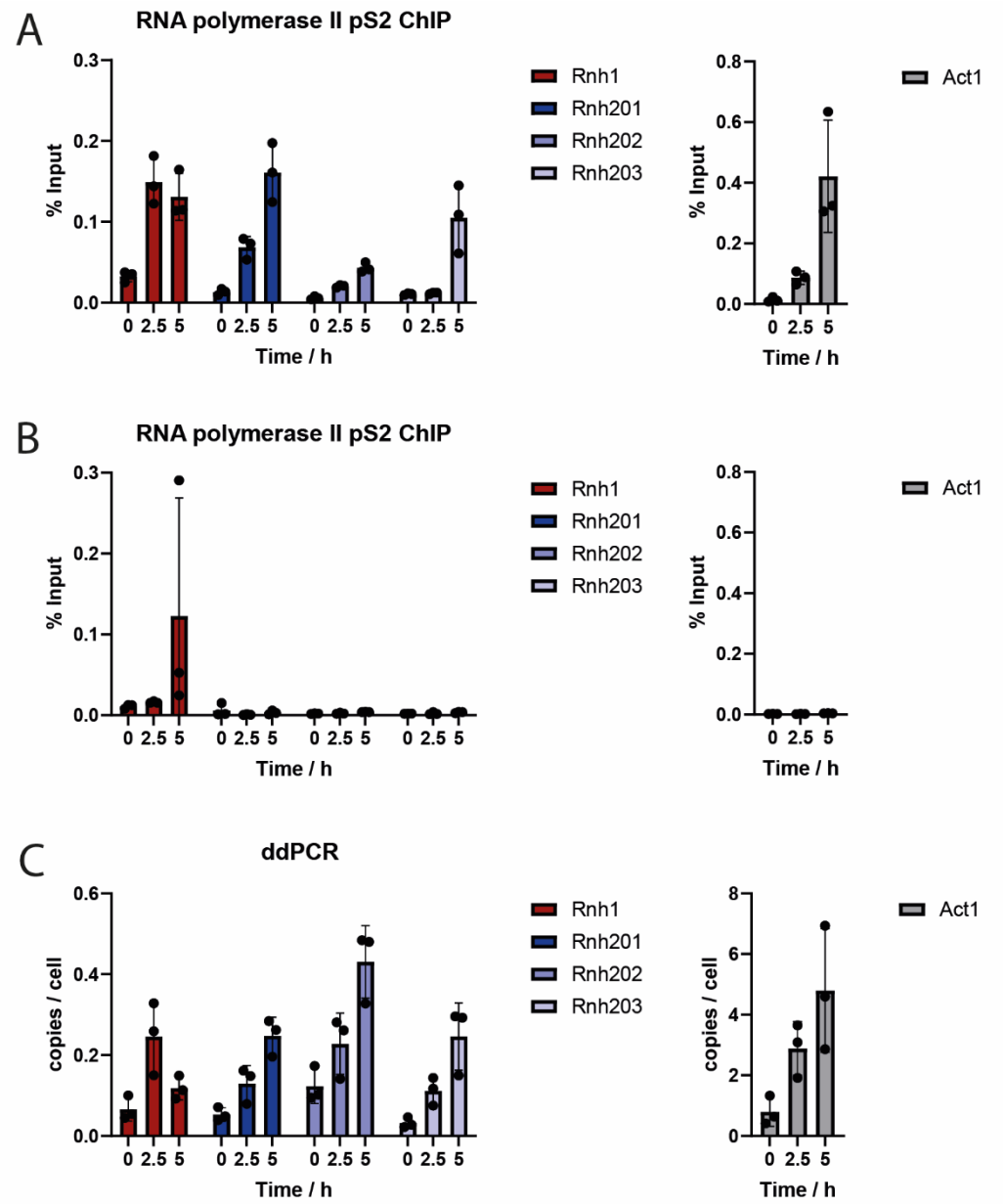

Figure 22 – Quantification of transcription and transcripts in Sen1-AID is not possible in a reliable way.* ***(A)*** *Quantification of ongoing transcription by ChIP of RNAPII pS2 before Sen1-AID* depletion and after 2.5 h and 5 h of auxin treatment (1 mM IAA). Transcription was quantified at the genes RNH1, RNH201, RNH202, RNH203 and ACT1.* ***(B)*** *Background control for (A), in which no antibody was added to the ChIP.* ***(C)*** *Digital droplet PCR for quantification of transcripts per cell before Sen1-AID* depletion and after 2.5 h and 5 h of auxin treatment. Transcripts were quantified at the genes RNH1, RNH201, RNH202, RNH203 and ACT1.*

3.10 RNase H1 upregulation is not caused by defective transcription termination

Sen1, together with Nrd1 and Nab3, acts in the NNS complex to terminate non-coding RNA polymerase II transcription. Even if the *RNH1* gene is a coding gene, possible effects caused

by the intact NNS caused by Sen1 depletion had to be ruled out. For this, first Nab3-AID* was depleted over 5 h and Rnh1-HA levels were measured (Figure 23 A). The depletion of Nab3-AID* leads to decreased levels of Rnh1-HA. The same happened for the depletion of Nrd1-AID*, where first Rnh1-HA levels increased, followed by a strong decrease close to the detection limit (Figure 23 B). Both, the effect in the Nrd1-AID* and the Nab3-AID* strain indicate that Rnh1 upregulation after Sen1-AID* depletion is not caused by defects of the NNS complex. Additionally, in both Nrd1-AID* and Nab3-AID* ddPCR analysis of total transcripts per cell after 2.5 h and 5 h of depletion was carried out (Figure 23 C and D). While the transcripts of the three RNase H2 subunits and *ACT1* showed a steady increase, *RNH1* transcription was upregulated after 2.5 h and went down again after 5 h in both, Nab3-AID* and Nrd1-AID* (Figure 23 C and D). To conclude, the depletion of Nrd1-AID* and Nab3-AID* showed the same pattern of *RNH1* transcript upregulation as the depletion of Sen1-AID* (Figure 22 C and Figure 23 C and D), leading to decreased Rnh1 protein levels. In summary, the same effect on the transcript levels in Nab3-AID*, Nrd1-AID*, and Sen1-AID* leads to the opposite effect on the protein levels in Nrd1-AID* and Nab3-AID* compared to Sen1-AID*. From this, it can be concluded, that Rnh1 protein upregulation is not caused by increased transcript levels.

Another possibility is that alternative transcripts that arise due to read-through transcription stabilize *RNH1* transcripts or enhance translation. For testing this, 3'RACE (3' rapid amplification of cDNA-ends) experiments were carried out in Sen1-AID*, Nrd1-AID* and Nab3-AID*. The known NNS complex target gene *SNR13* (Mischo *et al.*, 2011) was tested for read-through transcription as a positive control (Figure 23 E). While in wild type cells the addition of IAA alone led to an increased short range read-through (PCR product size increases from ~200 bp to ~300 bp), depletion of any of the NNS complex members led to a long read-through product that ends at about the length (~1400 bp) of the gene downstream of *SNR13*, *TRS31* which is a coding gene and due to this terminated NNS independent. In comparison, 3'RACE at the *RNH1* locus did not lead to significant read-through in the absence of the NNS complex. In summary, Rnh1 protein upregulation in Sen1-AID* is not caused by deficient NNS complex mediated transcription termination.

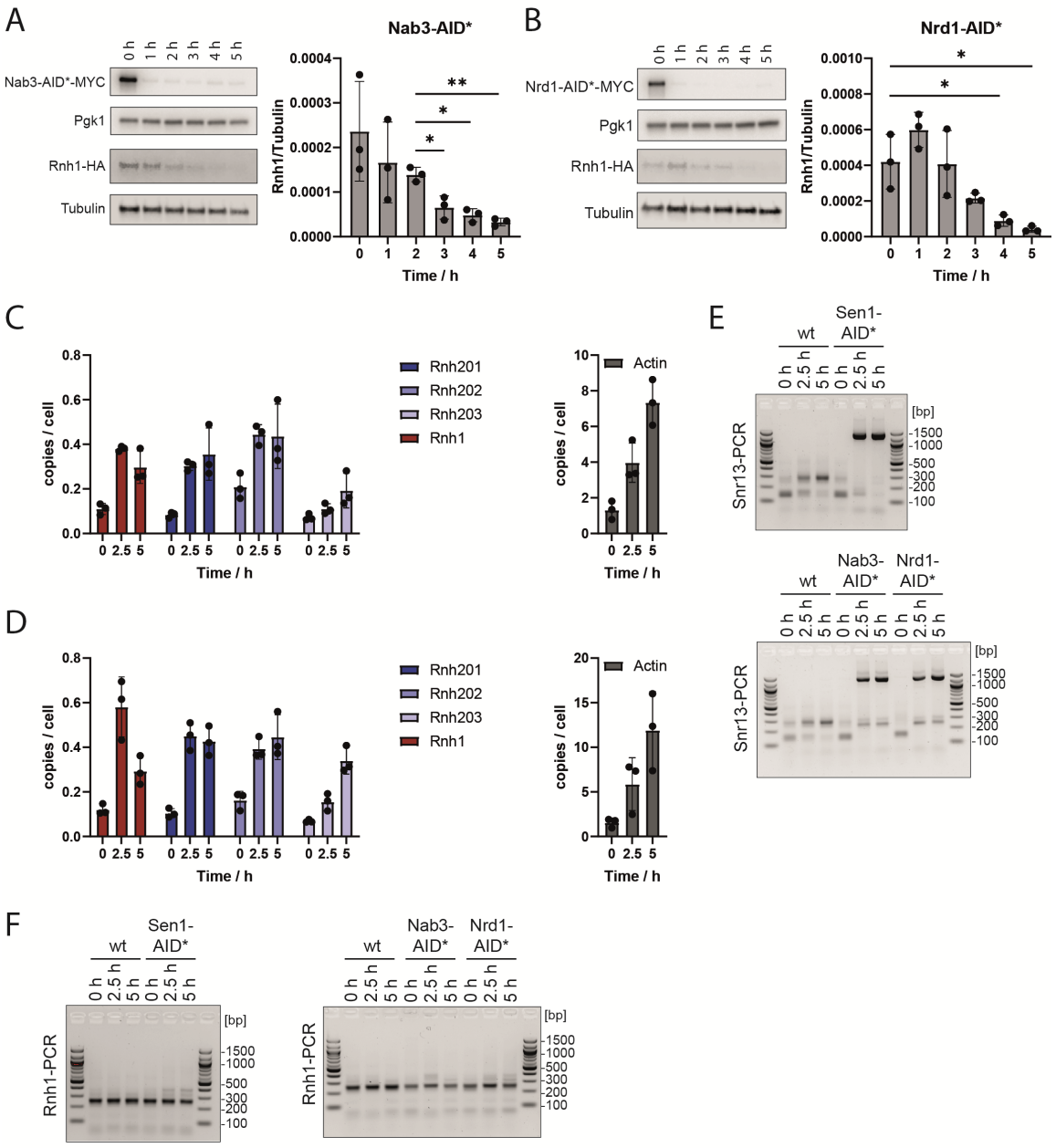

Figure 23 – Sen1's function in the NNS complex is not important for RNase H1 upregulation. Western blot analysis of endogenous Rnh1-HA levels over a time course of 5 h after depleting Nab3-AID. Bar graph shows quantification of Western blot. Unpaired t-test (*: p<0.05; **: p<0.01).* ***(B)*** *Western blot analysis of endogenous Rnh1-HA levels over a time course of 5 h after depleting Nrd1-AID*. Bar graph shows quantification of Western blot. Unpaired t-test (*: p<0.05).* ***(C)*** *Digital droplet PCR for quantification of transcripts per cell before Nab3-AID* depletion and after 2.5 h and 5 h of auxin treatment. Transcripts were quantified at the genes RNH1, RNH201, RNH202, RNH203 and ACT1.* ***(D)*** *Digital droplet PCR for quantification of transcripts per cell before Nrd1-AID* depletion and after 2.5 h and 5 h of auxin treatment. Transcripts were quantified at the genes RNH1, RNH201, RNH202, RNH203 and ACT1.* ***(E)*** *3'RACE analysis of read-through transcription at the SNR13 gene. The indicated strains were grown to exponential phase, supplemented with auxin and samples were collected after 2.5 h and 5 h of treatment.* ***(F)*** *3'RACE analysis of read-through transcription at the RNH1 gene. The indicated strains were grown to exponential phase, supplemented with auxin and samples were collected after 2.5 h and 5 h of treatment.*

3.11 Rnh1 protein is not stabilized in the absence of Sen1

Protein upregulation can be caused either by increased biosynthesis or by higher stability of the protein itself. For testing the protein stability, a cycloheximide (CHX) chase assay was performed. Cycloheximide blocks translation. Exploiting this fact the dynamics of protein degradation can be studied. In the case of Rnh1, depletion of Sen1 does not lead to a stabilization of the protein, the opposite is true and Rnh1 gets destabilized. This indicates that indeed more Rnh1 protein is synthesized in the cells.

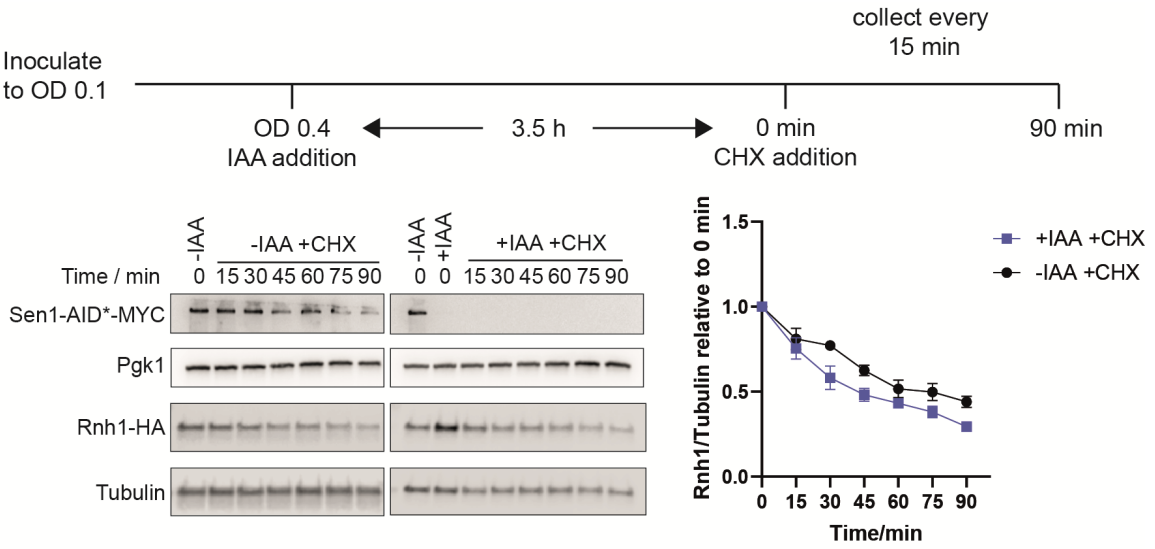

Figure 24 - RNase H1 stability is not increased upon Sen1 depletion. Cells were grown to OD 0.4, followed by incubation with or without IAA for 3.5 h. Cycloheximide (CHX) was added and samples were collected every 15 min for 1.5 h. Rnh1 is Rnh1-6xHA.

3.12 Upregulated RNase H1 associates with chromatin

RNase H1 is upregulated in the absence of Sen1. Such an upregulation does not automatically cause increased binding to chromatin. For testing, if the upregulated Rnh1 protein is binding to the chromatin, an chromatin enrichment assay was carried out. In this assay Rnh1 levels in the whole cell extract were compared to Rnh1 in the soluble fraction and to the chromatin bound protein (Figure 25 A). The fractionation assay showed that upon depletion of Sen1-AID* after 2.5 h and 5 h a similar increase of Rnh1-HA is detectable in the whole cell extract and the chromatin fraction. This assay evaluates chromatin binding genome-wide. The Aguilera lab published, that Sen1-AID depletion in S-phase leads to increased R-loop levels at the *GCN4*, *PDC1*, and *PDR5* loci (San Martin-Alonso *et al.*, 2021). If Rnh1 is upregulated to deplete RNA:DNA hybrids that arise due to Sen1 loss, it should be

found at these Sen1 specific loci. For studying this, a ChIP of endogenous catalytic inactive *rnh1(D193N)* was performed (Figure 25 B and C). Upon depletion of Sen1-AID*, an accumulation of *rnh1(D193N)* was detected at all loci, while the background control without antibody did not change. Furthermore, the Aguilera lab showed that also the depletion of Hpr1-AID leads to increased R-loop levels in G1- and S-phase (San Martin-Alonso *et al.*, 2021). Repeating the experiment with depletion of Hpr1-AID* instead of Sen1-AID* does not lead to an accumulation of *rnh1(D193N)* at the same loci above the levels detected in untreated cells (Figure 25 D and E). This indicates that Rnh1 indeed goes to Sen1 specific loci in case Sen1 cannot prevent the formation of RNA:DNA hybrids itself. This effect is specific to RNA:DNA hybrids formed in the absence of Sen1.

Rnh1 upregulation is not mediated by higher protein stability after Sen1-AID* depletion (Figure 24). Nonetheless, Rnh1 could be stabilized when bound to chromatin. We used truncation mutants carrying deletions of either hybrid binding domain one (HB1) or hybrid binding domain two (HB2) for studying the stabilizing effects of protein binding to the chromatin. For technical reasons 6 HA-tags were added to the enzymes (Figure 25 F). First, it was tested if the binding to known Rnh1 loci is impaired by the deletion of the single hybrid binding domains (Figure 25 G). For both tested loci, the binding capacity was reduced to under 10 % of the binding capacity of full length Rnh1. In a second step, the upregulation of the truncation mutants upon Sen1-AID* depletion was tested (Figure 25 H). The decreased binding capacity did not cause a reduced upregulation of the Rnh1 truncation mutants, indicating, that stabilization through hybrid binding is not causing the upregulation of Rnh1. In summary, upregulated Rnh1 binds to RNA:DNA hybrids throughout the genome, but is not stabilized by this binding.

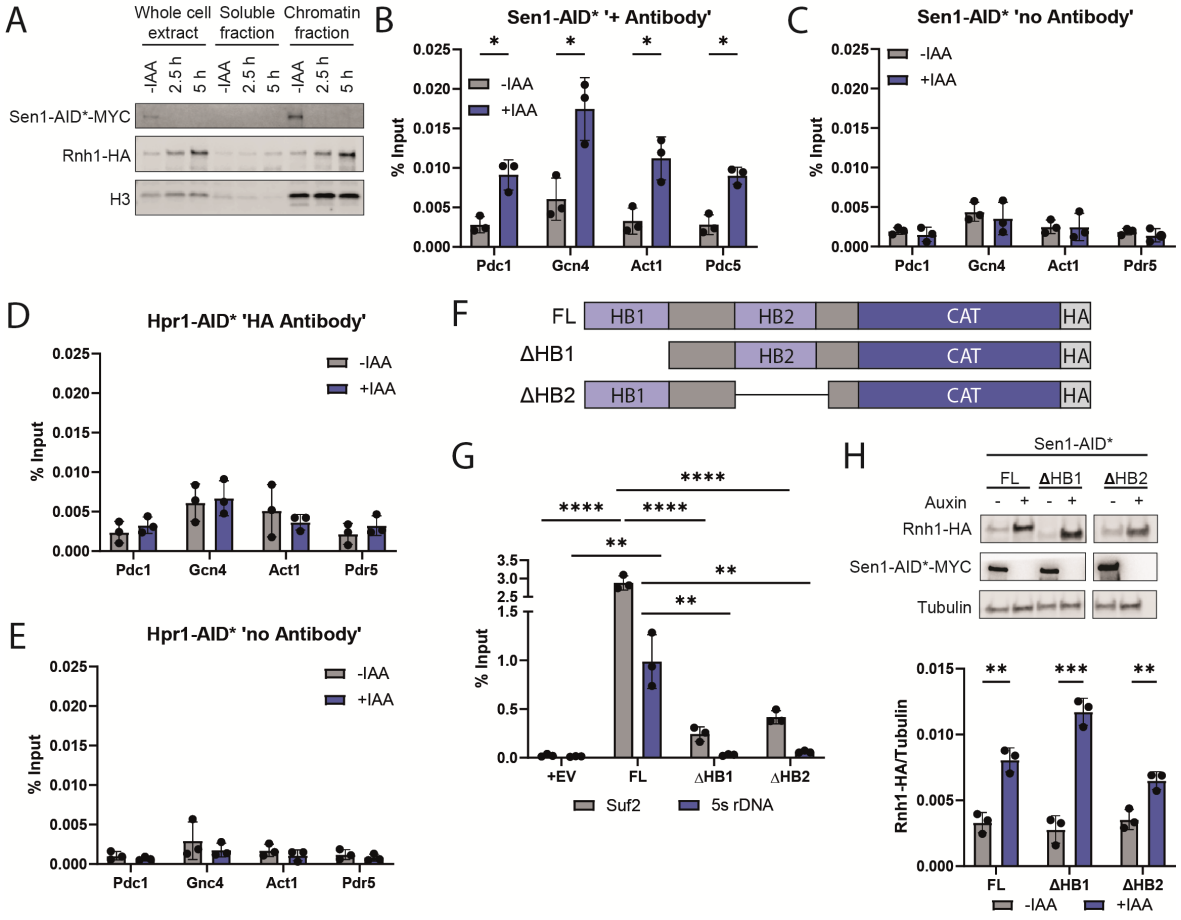

Figure 25 – Upregulated RNase H1 associates with the chromatin. Fractionation assay for analyzing if upregulated RNase H1 is bound to the chromatin. Exponential cells were treated for 2.5 h and 5 h with 1 mM IAA to deplete Sen1-AID.* ***(B)*** *ChIP analysis of endogenous rnh1(D193N) binding upon 5 h of Sen1-AID* depletion to genomic loci known for increased RNA:DNA hybrids in Sen1-AID and Hpr1-AID. Unpaired t-test (*: p<0.05).* ***(C)*** *Background control of (B).* ***(D)*** *ChIP analysis of endogenous rnh1(D193N) binding upon 5 h of Hpr1-AID* depletion to genomic loci known for increased RNA:DNA hybrids in Sen1-AID and Hpr1-AID.* ***(E)*** *Background control of (D).* ***(F)*** *Schematic representation of truncation mutants deleted for either hybrid binding domain 1 or 2 used in panels (G) and (H). FL: full length, HB: hybrid binding domain, CAT: catalytic domain, HA: HA-tag.* ***(G)*** *ChIP analysis of the binding capability of RNase H1 and its truncation mutants to RNA:DNA hybrid rich loci. Experiment performed by Fabio Bento. Unpaired t-test (**: p<0.01, ***: p<0.001; ****: p<0.0001).* ***(H)*** *Analysis of endogenous Rnh1 upregulation in Sen1-AID* depletion dependent on chromatin binding ability. Exponential cells were treated with 1 mM IAA for 5 h at 30 °C and protein levels were analyzed in a Western blot. Experiment performed by Matteo Longaretti. Unpaired t-test (**: p<0.01, ***: p<0.001).*

3.13 Sen1's function in RNAP III termination influences Rnh1 expression

Sen1 is involved in the transcription termination of all three RNA polymerases. The depletion of Sen1, therefore, can stabilize RNA:DNA hybrids formed co-transcriptionally during transcription from all three RNA polymerases. The upregulation of RNase H1 could be caused by this function of Sen1. For this reason, at the same time Sen1-AID* was

depleted, *rpa190-1* was inactivated (subunit of RNA polymerase I; temperature shift from 25 °C to 37 °C) and Rpb1-AID* (subunit of RNA polymerase II) or Rpo31-AID* (subunit of RNA polymerase III) were co-depleted with Sen1-AID*.

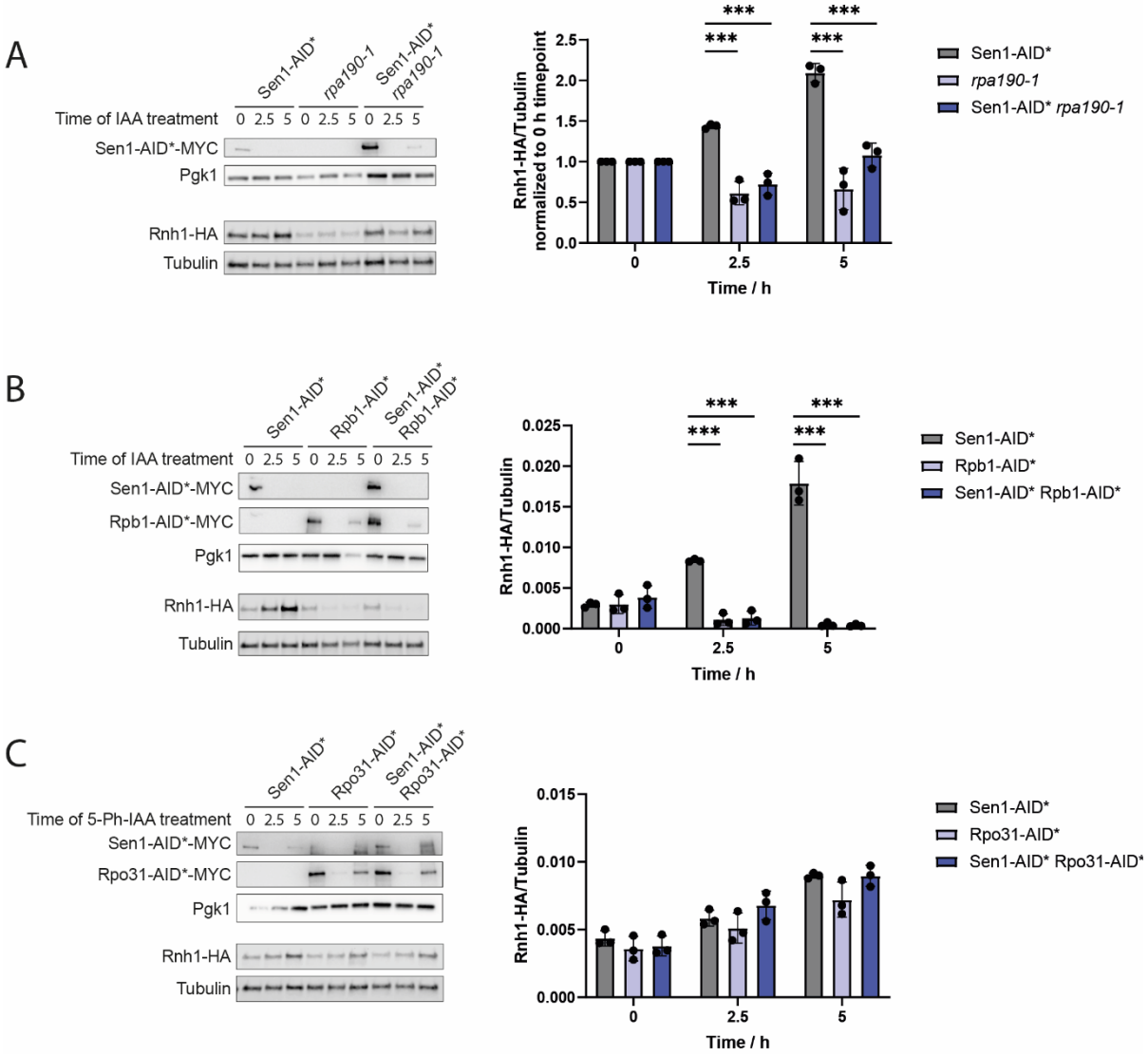

Figure 26 - Sen1's function in RNAP III termination influences Rnh1 expression. ***(A)*** *Western blot analysis of endogenous Rnh1-HA levels after depleting Sen1-AID* and or inactivating rpa190-1. 1mM IAA was added to exponentially growing cells and the temperature was shifted from 25 °C to 37 °C for 2.5 h and 5 h. Bar graph shows quantification of the representative Western blot on the left and two more biological replicates. Unpaired t-test (***: p<0.001).* ***(B)*** *Western blot analysis of endogenous Rnh1-HA levels after depleting Sen1-AID* and or Rpb1-AID* for 2.5 h and 5 h with 1 mM IAA. Bar graph shows quantification of the representative Western blot on the left and two more biological replicates. Unpaired t-test (***: p<0.001).* ***(C)*** *Western blot analysis of endogenous Rnh1-HA levels after depleting Sen1-AID* and or Rpo31-AID* for 2.5 h and 5 h with 1 µM 5-Ph-IAA. Bar graph shows quantification of the representative Western blot on the left and two more biological replicates.*

First, RNAP I was inactivated. For comparability, the samples were normalized to the 0 h time point due to the low Rnh1 levels the *rpa190-1* background carries from the beginning.

While the depletion of Sen1-AID* leads to increased Rnh1-HA levels as described before (Figure 18 B and C), the inactivation of *rpa190-1* leads to decreased Rnh1-HA levels. Combination of both alleles first leads to a decrease (2.5 h time point), followed by an increase of Rnh1-HA (5 h time point). The absence of functional RNA polymerase I leads to decreased rRNA levels and with this to problems in ribosome assembly, followed by decreased translation capability. This most likely is the reason why Rnh1 levels decrease in this mutant. Sen1 is important for releasing RNA polymerase I (RNAP I) and its nascent RNA from the DNA once transcription pauses (Xie *et al.*, 2022). If Rnh1 would get important at RNAP I in the absence of Sen1, the absence of rDNA transcription in *rpa190-1* cells at elevated temperatures would not lead to an Rnh1 upregulation. On top, if Sen1-AID* would be depleted in the *rpa190-1* mutant at elevated temperatures, this would abolish the upregulation of Rnh1 because Sen1 would not be needed for the termination in the first place. The result in the Sen1-AID* *rpa190-1* double mutant is not as clear as expected. First, the Rnh1 levels decrease, followed by an increase back to levels seen before the treatment. This is why from this experiment no clear conclusion can be drawn if Rnh1 backs up Sen1's function in RNAP I termination, even though the higher Rnh1 levels in the double mutant compared to *rpa190-1* indicate that the Sen1-AID* degradation effect still leads to an upregulation of RNase H1.

Sen1, together with Nrd1 and Nab3, is important for termination of non-coding RNAs that are transcribed by RNA polymerase II (reviewed by Xie, Libri and Porrua, 2023). Nonetheless, also protein coding genes are dysregulated after Sen1 depletion (Figure 22). Co-depletion of Sen1-AID* and the biggest subunit of RNAP II Rpb1-AID* should abolish Rnh1 upregulation in case Rnh1 backs up Sen1's function in the NNS complex. On the other hand, without functioning RNAP II, no mRNA of Rnh1 can be produced. In budding yeast, mRNA has an average half-life of 22 min (Chia and McLaughlin, 1979). This indicates that soon after RNAP II depletion, most translation has to stop due to a lack of mRNA. This effect is what leads to the result shown in Figure 26 B, where depletion of Rpb1-AID* diminishes Rnh1 levels after 2.5 h to around 30 % of the initial protein levels and about 15 % after 5 h of depletion. This is similar in the case of the co-depletion of Sen1-AID* and Rpb1-AID*, ending in only 10 % of the initial protein levels after 5 h. Due to this effect, it cannot be concluded if Sen1's function in RNAP II termination influences Rnh1 levels. Nonetheless, it

indicates that the regulation of Rnh1 has a transcription coupled component, even if no clear conclusion can be drawn from the transcript levels (Figure 22).

RNA polymerase III (RNAP III) can be terminated either in a protein independent way (when approaching T-tracts), or in a Sen1-dependent manner (Rivosecchi *et al.*, 2019; Xie *et al.*, 2022; Xie, Libri and Porrua, 2023). RNAP III transcribes tRNAs which are highly transcribed and RNA:DNA hybrids at tRNA genes were shown to be targets of RNase H1 (El Hage *et al.*, 2014, Figure 15). In case RNase H1 acts as a backup for Sen1's function at RNAP III, no upregulation of Rnh1 protein levels would be detectable after co-depletion of Sen1-AID* and Rpo31-AID*. Interestingly, the depletion of Rpo31-AID* alone is sufficient for upregulating Rnh1 (Figure 26 C). This could be caused by RNA:DNA hybrids that are formed while depleting actively transcribing Rpo31-AID*. As mentioned before, loci of RNAP III transcription are highly transcribed targets of Rnh1. This could lead to stress caused by RNA:DNA hybrids that triggers Rnh1 upregulation in a similar way as Sen1-AID* upregulation. Depleting both at once, Sen1-AID* and Rpo31-AID*, does not lead to an additive effect and Rnh1 levels reach the same values as in the Sen1-AID* cells. This indicates that Sen1 and Rnh1 target RNA:DNA hybrids that arise upon Rpo31-AID* depletion. Sen1, besides its transcription termination functions, travels with the replisome and prevents TRCs (Appanah *et al.*, 2020; Aiello *et al.*, 2022). The tRNA genes are hot spots of TRCs (Tran *et al.*, 2017). Likely, Rnh1 is important for preventing these TRCs at highly transcribed loci in the absence of Sen1 by depleting the RNA:DNA hybrid portion of the conflict.

3.14 RNase H1 upregulation after Sen1 loss depends on S-phase progression

Sen1 has multiple functions. For avoiding and resolving TRCs it is traveling with the replisome. If Rnh1 is upregulated due to replication coupled functions of Sen1, Sen1-AID* depletion outside of S-phase should abolish the upregulation. For this reason, cells were arrested in G1 prior to depleting Sen1-AID* and Rnh1 levels were compared to those in cycling cells. While in cycling cells Rnh1 protein levels increased after depleting Sen1, G1-arrested cells show lower Rnh1 levels than exponential cells without IAA and these levels were not sensitive to Sen1-AID* depletion (Figure 27 A and B). This indicates that for Rnh1 upregulation replication has to be actively ongoing.

As cells need to be replicating for RNase H1 to be upregulated, the question arose if a single S-phase is sufficient to upregulate RNase H1. To answer this question, cells were arrested in G1 for 1.5 h, prior to Sen1-AID* depletion. After 30 min of auxin treatment, alpha-factor was washed out and RNase H1 levels were studied over time (Figure 27 C and D). G1-arrested cells naturally have lower RNase H1 levels than cycling cells (Figure 27 A and B). Due to this fact, a drop between exponentially cycling cells and G1-arrested cells in Rnh1 protein levels can be detected. After washing out the alpha-factor, RNase H1 levels start rising again in both, IAA treated and untreated cells. After 2 h of release, a significant increase of RNase H1 levels after Sen1-AID* depletion can be detected compared to the cells with active Sen1-AID*. This indicates that a single S-phase progression is sufficient to increase RNase H1 levels. Looking at the cell cycle profiles (Figure 27 C), auxin untreated cells start reaching G2/M-phase after 60 min, while auxin treated cells only reach G2/M-phase after 90 min. This delay is in accordance with the results published by the Aguilera lab in which Sen1-AID depletion leads to slower S-phase progression (San Martin-Alonso *et al.*, 2021).

As RNase H1 is especially important during replication in cases Sen1 is missing, we wanted to find out, if it is sufficient to express RNase H1 only in S-phase. For this, a spotting assay was performed in which the temperature-sensitive loss of function mutant *sen1-1* was combined with cell cycle dependent *RNH1* alleles, which are either expressed in G1-, S-, or G2/M-phase (Figure 27 E). Against our expectations, restricting *RNH1* expression to S-phase lead to the same viability as *RNH1* deletion, while expression in G2/M-phase increased the viability. The rescue in G2/M indicates that Rnh1 is important to resolve TRCs at late replicating loci. Restricting Rnh1 expression to G1-phase reduced the viability of the cells further compared to *RNH1* deletion in a *sen1-1* background. This effect indicates, that in G1-phase *RNH1* expression has to be at lower levels, explaining the low levels in G1-arrested cells (Figure 27 A – D). The G1-allele is expressed under *pSIC1*, which cannot mimic endogenous Rnh1 levels due to gene specific regulatory mechanisms.

In summary, Rnh1 is upregulated during S-phase if Sen1 is lost. This helps prevent TRCs which usually are prevented by Sen1. Surprisingly, Rnh1 is most important in G2/M-phase in *sen1-1* cells. This indicates, that it is especially important at late replicating loci or where the replication fork is stalled. There, cells get check point arrested and Rnh1 comes into play for resolving the RNA:DNA hybrid portion of the TRC.

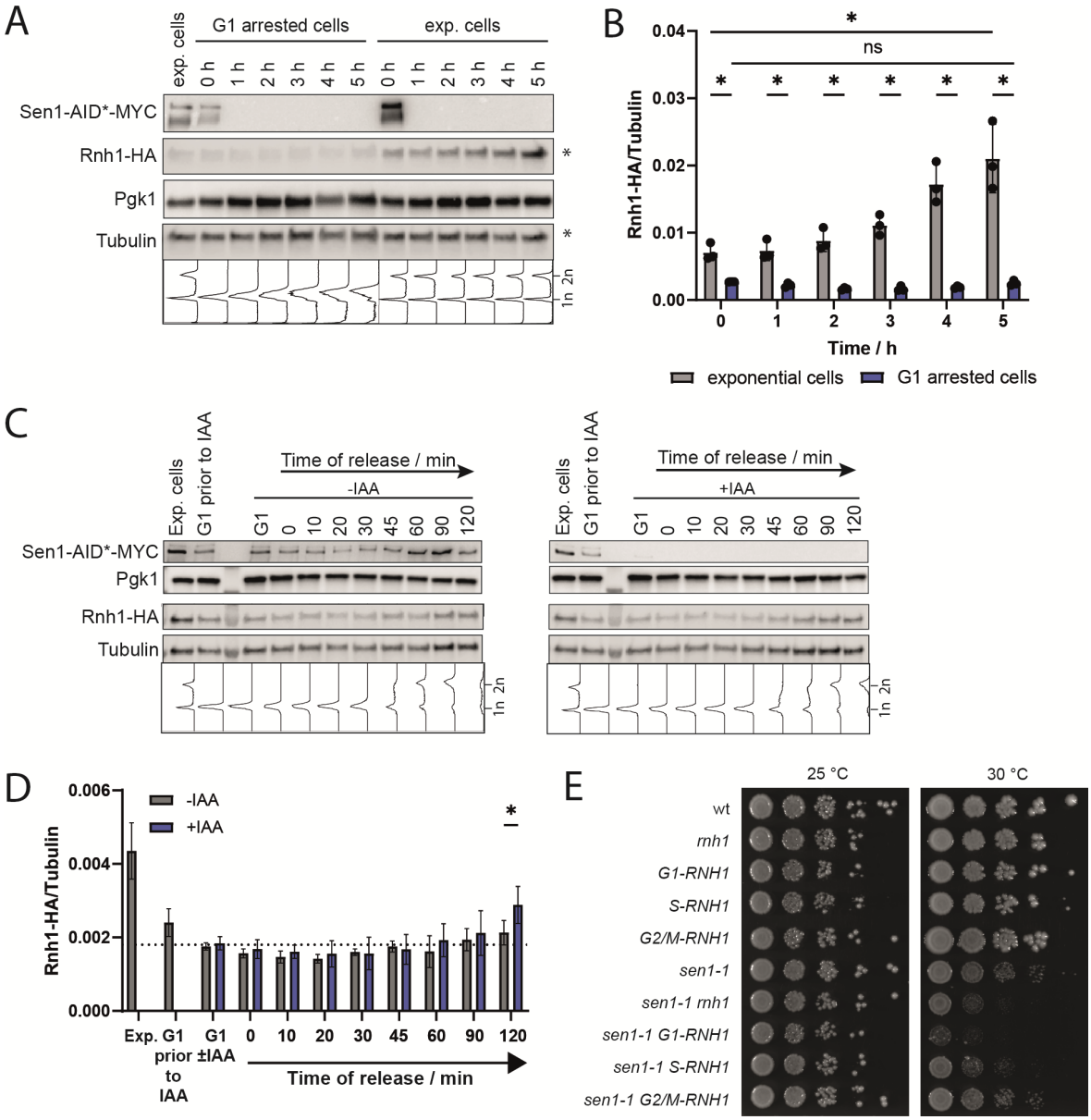

Figure 27 - RNase H1 upregulation upon Sen1-AID depletion requires the cells to go through replication.* ***(A)*** *Western blot comparing Rnh1-HA levels in G1-arrested cells with exponentially growing cells. bar1Δ cells were either arrested in G1 by incubation with 0.24 µM alpha-factor or kept in exponential phase. After 1.5 h of arrest, 1 mM IAA was added to both conditions. The cells were incubated for 5 h with collecting samples every hour. *: indicates loading that belongs to Rnh1-HA blot.* ***(B)*** *Quantification of (A). Unpaired t-test (*: p<0.05).* ***(C)*** *Western blot for measuring Rnh1-HA levels in cells that go through their first S-phase after G1-arrest with Sen1-AID* depletion. Cells were arrested for 90 min, 1 mM IAA was added for 30 min and the cells were released into S-phase at 25 °C.* ***(D)*** *Quantification of (C). Unpaired t-test (*: p<0.05).* ***(E)*** *Tenfold serial dilutions of the indicated budding yeast strains were spotted on YPD agar plates containing and were incubated for 72 h at 25 °C and 30 °C. All experiments from this Figure were performed by the Master student Sophia Sergi under my supervision.*

3.15 RNase H1 is required to maintain S-phase progression in Sen1-AID*

Rnh1 upregulation depends on S-phase coupled functions of Sen1. This opens the question, if the slowed down S-phase progression phenotype described by the Aguilera lab is further slowed down in the absence of Rnh1. We performed an experiment, in which we studied the S-phase progression of Sen1-AID* strains in the presence and absence of Rnh1 (Figure 28 A). Comparing the Sen1-AID* strain with and without the addition of IAA, the slowed down S-phase described by the Aguilera lab could be, again, replicated. Sen1-AID* *rnh1* without auxin showed no difference to Sen1-AID* without auxin, indicating, that the *RNH1* deletion has no impact on S-phase progression. This changed in the absence of Sen1-AID*. In this scenario, deleting *RNH1* on top of depleting Sen1 leads to an even more slowed down S-phase progression (best seen between 50 min and 70 min). This result indicates that Rnh1 is necessary in the absence of Sen1 due to Sen1's replication coupled functions. Sen1 travels with the replisome *via* its association with Ctf4 and Mrc1 and resolves transcription-replication conflicts (Appanah *et al.*, 2020; Aiello *et al.*, 2022). Consequently, in the absence of Sen1 more DNA damage occurs, which was shown in the *sen1-3* allele that loses association to the replisome and acquires more Rad52-foci than wild type strains (Appanah *et al.*, 2020). In summary, RNase H1 is important for TRC prevention in the absence of Sen1 (Figure 28 A).

For further verification that RNase H1 indeed reacts to the replication coupled functions of Sen1, we used the *sen1-3* allele. First, we tested, if Rnh1-HA is upregulated in the *sen1-3* mutant (Figure 28 B). We could detect a subtle but significant increase in Rnh1 levels. *RNH1* deletion together with the *sen1-1* mutant is synthetic lethal at semi-permissive temperature (30 °C, Figure 17 A). If Rnh1 is important for resolving TRCs together with Sen1, *rnh1* should be synthetic sick or synthetic lethal with the *sen1-3* mutation. In unchallenged conditions *rnh1 sen1-3* does not show impaired growth, while it is synthetic sick in challenging conditions (genotoxic stress caused by 0.02 % MMS, Figure 28 C). Interestingly, the deletion of the catalytic subunit of RNase H2, *RNH201*, did not show this phenotype, again indicating that Rnh1's function in TRC resolution is unique between the two RNase H enzymes. Taken together, RNase H1 is reacting to Sen1 loss in order to prevent TRCs.

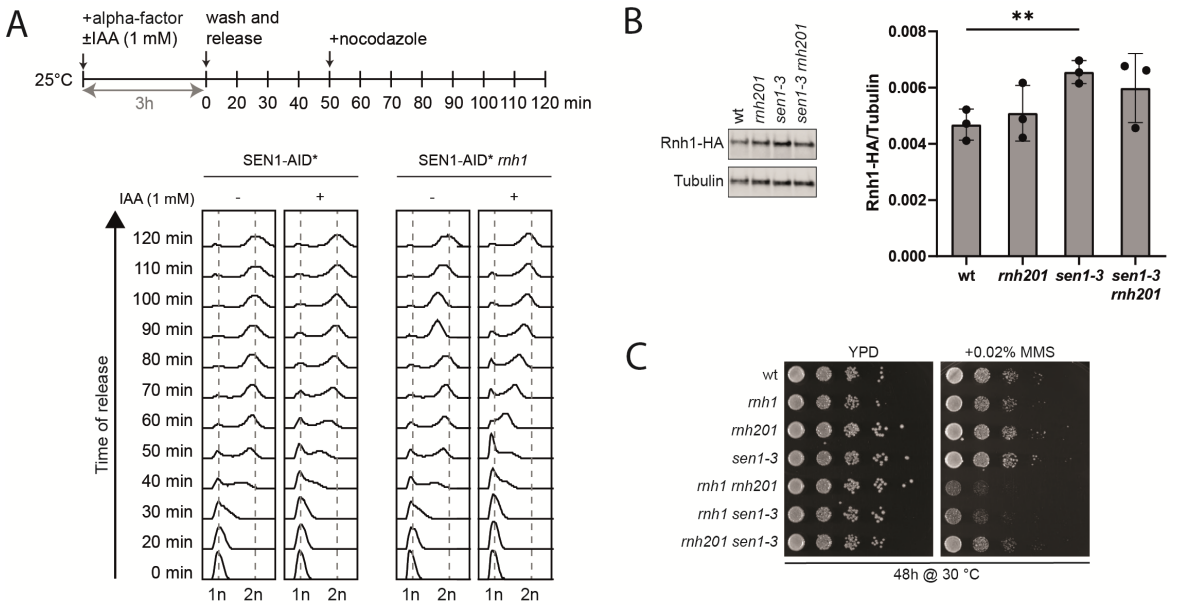

Figure 28 – RNase H1 upregulation prevents excessive transcription-replication conflicts upon Sen1-AID depletion.* ***(A)*** *S-phase progression of Sen1-AID* cells compared to Sen1-AID* rnh1 cells. Cells were arrest for 3 h in alpha-factor with parallel Sen1-AID* depletion (1 mM IAA). Cells were washed thrice in sterile ddH_2O and released at 25 °C in a time course over 2 h. Experiment performed by Ronald Wong (Helle Ulrich Laboratory)* ***(B)*** *Western blot comparing wild type Rnh1-HA levels with cells carrying the replisome binding deficient allele sen1-3. Unpaired t-test (**: p<0.01). Experiment performed by Sophia Sergi under my supervision.* ***(C)*** *Tenfold serial dilutions of the indicated budding yeast strains were spotted on YPD agar plates containing and were incubated for 72 h at 30 °C. Experiment performed by my colleague Fabio Bento.*

3.16 RNase H1 upregulation is mediated by high RNA:DNA hybrid levels

An important part of TRCs are RNA:DNA hybrids, which form after stalled RNA polymerases. Sen1 and RNase H1 are important for maintaining physiological R-loop levels. To strengthen the hypothesis that Rnh1 is upregulated due to the R-loop portion of the TRC, RNA:DNA hybrid levels were compared in wild type cells, *RNH1* deletion, depletion of Sen1-AID* or both (Figure 29 A and B). RNA:DNA hybrid levels were measured by chromatin spreads which were immuno stained using the S9.6 antibody. RNA:DNA hybrid levels were increased in both, *rnh1* and Sen1-AID*, reaching the same levels (Figure 29 A and B). No additive effect could be detected in the double mutant (Figure 29 A and B), suggesting that Rnh1 and Sen1 target the same sub-population of RNA:DNA hybrids. Importantly, overexpression of *RNH1* reduced RNA:DNA hybrids to wild type levels.

Rnh1 upregulation could be triggered by the RNA:DNA hybrids at TRCs that arise in the absence of Sen1. To test this hypothesis, a second, MYC-tagged copy of *RNH1* was introduced from a high copy plasmid. Comparing endogenous Rnh1-HA levels in the control

strains (carrying an empty vector control) and in the strains overexpressing *RNH1-MYC* showed that reduced RNA:DNA hybrids levels (mediated by *RNH1-MYC* overexpression) reduced the upregulation of the endogenous enzyme (Figure 29 C and D). This favors the hypothesis, that Rnh1 is important to resolve TRCs as the overexpression of *RNH1* reduces co-transcriptional R-loops. In summary, Rnh1 upregulation is mediated by increased RNA:DNA hybrid levels after Sen1 loss.

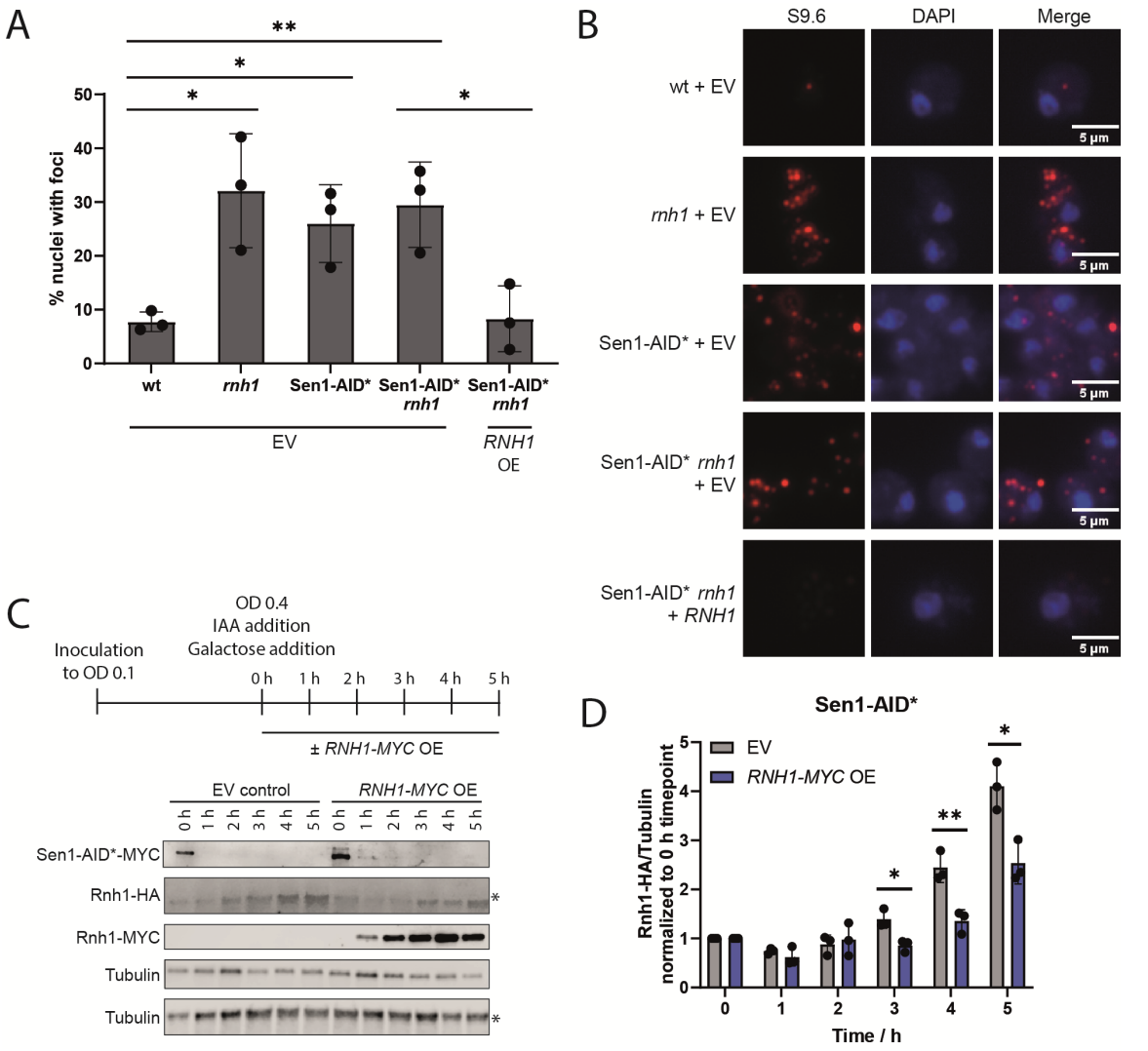

Figure 29 – High RNA:DNA hybrid levels after Sen1-AID depletion trigger RNase H1 upregulation.* ***(A)*** *RNA:DNA hybrid levels measurements in cells lacking RNH1 and that are depleted for Sen1-AID* by chromatin spreads and S9.6-antibody staining. Exponential cells in SC-Leu + 2 % raffinose were supplemented with 2 % galactose for maintenance and overexpression of the RNH1 overexpression plasmid and incubated for 1 h. 1 mM IAA were added and the cells were incubated for 5 h more. Unpaired t-test (*: p<0.05; **: p<0.01).* ***(B)*** *Example images for (A).* ***(C)*** *Western blot analysis of Rnh1-HA upregulation upon Sen1-AID* depletion in the presence of overexpressed RNase H1. Exponential cells in SC-Leu + 2 % raffinose were supplemented with 2 % galactose and 1 mM IAA and grown over a time course of 5 h with collections every hour. * indicates the loading control that belongs to the Rnh1-HA blot.* ***(D)*** *Quantification of (C). Unpaired t-test (*: p<0.05; **: p<0.01). Wt: wild type, EV: empty vector.*

4. Discussion

Genomic RNA:DNA hybrids have multiple beneficial roles, but can also be harmful. Consequently, they have to be tightly regulated. The enzyme in focus of this work, RNase H1 (Rnh1), is regulating these structures while its own regulation is not well studied. Herein, the findings from Lockhart et al. (2019) and Zimmer and Koshland (2016) were confirmed that Rnh1 is important at stabilized RNA:DNA hybrids, especially in a context of genotoxic stress. Additionally, an interplay of *RNH1* and *SEN1* regulation was found. This interdependence of the two enzymes becomes especially important during Sen1's function in the prevention of transcription-replication conflicts (TRCs).

4.1 RNase H1 targets stabilized RNA:DNA hybrids

Rnh1 binds to RNA:DNA hybrids genome-wide and only shows increased nuclease activities where hybrids are accumulated (Zimmer and Koshland, 2016). Rnh1 is important for the prevention of RNA:DNA hybrid mediated genotoxicity in these cases (Zimmer and Koshland, 2016; Lockhart *et al.*, 2019; Heuzé *et al.*, 2023). This is in accordance with overexpressed catalytic inactive *rnh1(D193N)* being non-toxic in wild type cells, while becoming toxic after the accumulation of RNA:DNA hybrids (Figure 14). It does not matter if the increase of RNA:DNA hybrids is caused by genotoxic substances or by the deletion of genes that are important for RNA:DNA hybrid regulation. The toxicity is mediated by the catalytic inactive enzyme binding to the genomic loci without resolving the RNA:DNA hybrids. The binding may prevent other RNA:DNA hybrid resolving enzymes from their action, may be a road block for the approaching replisome or both. These stabilized RNA:DNA hybrids lead to increased DNA damage, and as a consequence reduced viability of the cells (Figure 15 C). Even if the effect on cell viability is big once catalytic inactive *rnh1(D193N)* is overexpressed in cells with accumulated RNA:DNA hybrids, it has no impact on the transcriptome (Figure 16). Furthermore, the same is true for the transcriptome in case of reduced RNA:DNA hybrid levels due to overexpression of wild type *RNH1* (Figure 16). This observation was confirmed by a recent preprint, where also only negligible changes in the transcriptome were found after *in vivo* RnhA (*E. coli* RNase H1) treatment of human cells (Basille *et al.*, 2025). Together this suggests that RNase H1 may not target regulatory RNA:DNA hybrids in budding yeast. It has to be considered that the RNA sequencing experiment performed in this thesis excluded ribosomal RNA and small RNAs

like tRNAs, which are known to be targets of RNase H1 (El Hage *et al.*, 2014). Furthermore, the change of transcriptome caused by overexpressing active or catalytically inactive *RNH1* could also be subtle and the small effects could be masked by the whole RNA pool. This would make it necessary to perform nascent RNA sequencing. In this project we also did small RNA sequencing to get an overview of changes in small RNAs like tRNAs upon *RNH1* and *rnh1(D193N)* overexpression. This sequencing did not have a good quality. In a future repeat, it could be supplemented with thermostable group II intron reverse transcriptases sequencing (TGIRT-seq) which improves sequencing of e.g. tRNAs and small ncRNAs (Mohr *et al.*, 2013; Xu *et al.*, 2019).

The overexpression of the wild type *RNH1* reduced the viability only in cells treated with genotoxic chemicals (Figure 14). This indicated that, even when overexpressed, *RNH1* is not degrading RNA:DNA hybrids down to a level that is toxic to the cells. In fact, while binding to multiple genomic loci, overexpressed *RNH1* only degrades RNA:DNA hybrids in cells with high RNA:DNA hybrid levels and in these cells not at all loci it is binding to (Figure 15 A and C). This changes if DNA damage is introduced by Hydroxyurea (HU) or Methyl methanesulfonate (MMS). The toxicity can be explained by the important role of RNA:DNA hybrids at double strand breaks (DSBs). The structures are necessary for resection at DSBs, allowing repair of the break (Ohle *et al.*, 2016). After *RNH1* overexpression RNA:DNA hybrids are removed and cannot participate in DNA repair. Nonetheless, in cases where DSBs happen due to RNA:DNA hybrids, they have to be removed by RNases H (Amon and Koshland, 2016). Together, at double strand breaks RNA:DNA hybrid levels need to be tightly regulated, not allowing for changes in RNase H1 regulation caused by *RNH1* overexpression.

The binding and RNA:DNA hybrid resolution behavior of overexpressed *RNH1* described in Figure 15 A and C and illustrated in Figure 30 deserves a closer look. In a wild type scenario (Figure 30 A), Rnh1 binds to both, regions of high and low RNA:DNA hybrid levels, but does not reduce the levels of RNA:DNA hybrids. In an *rnh1 rnh201* background overexpressed Rnh1 shows an increased binding to regions that are high in RNA:DNA hybrids, actively degrading these, while there is no change in binding behavior and activity at regions with low RNA:DNA hybrid levels. Due to this behavior, regions with high levels of stabilized RNA:DNA hybrids can be called Rnh1 hotspots (in accordance with Zimmer and Koshland 2016) and regions with low RNA:DNA hybrid levels that are not degraded by Rnh1 can be

called regions of Rnh1 resistant RNA:DNA hybrids. The change in Rnh1 behavior towards 'Rnh1 hotspots' and 'regions with Rnh1 resistant RNA:DNA hybrids' raises the question how the enzyme discriminates between the different populations of RNA:DNA hybrids and what determines if it degrades the hybrid or not.

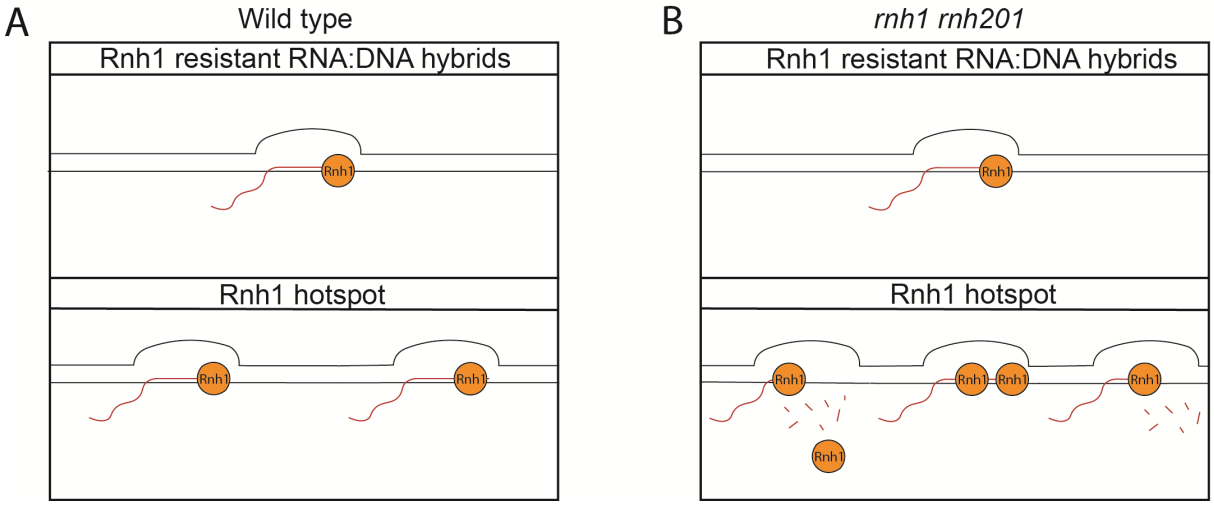

Figure 30 – RNase H1 acts at specific Rnh1 hotspots. In wild type cells Rnh1 binds to all RNA:DNA hybrid loci and has a higher local concentration around hotspot areas, but does not degrade the hybrids (Zimmer and Koshland, 2016). ***(B)*** *In rnh1 rnh201 mutants, RNA:DNA hybrid levels only increase at specific RNase H1 hotspots. These hotspots are the only regions that show lower RNA:DNA hybrid levels after RNH1 overexpression.*

4.2 RNase H1 becomes essential if Sen1 function is missing

Overexpressed Rnh1 changes its degradation behavior depending on its binding to regions of low RNA:DNA hybrid levels or regions with high levels of stabilized RNA:DNA hybrids. For studying the regulation of RNase H1, endogenous protein levels were determined in presence of different classes of RNA:DNA hybrids. RNA:DNA hybrids that are targeted by RNase H2 (Figure 6) seem likely to be targets for RNase H1, as both nucleases are often referred to as redundant when it comes to RNA:DNA hybrid resolution of hybrids longer than 3 nt (Cerritelli and Crouch, 2009; Cerritelli and El Hage, 2020).

A specific class of RNA:DNA hybrids are those stabilized by topological stress. Topoisomerase 1 (Top1) can resolve topological stress caused by positive supercoiling ahead of transcription and negative supercoiling behind the RNA polymerase (Figure 5), preventing the nascent RNA from intervening and hybridizing to the template strand. As a consequence, the deletion of *TOP1* causes increased RNA:DNA hybrid levels (El Hage *et al.*, 2010).

Pioneering work of the Aguilera lab rose awareness about the THO/TREX complex and its functions in RNA:DNA hybrid maintenance (Wellinger, Prado and Aguilera, 2006; Gómez-González *et al.*, 2011; Peña *et al.*, 2012; San Martin-Alonso *et al.*, 2021). The THO/TREX complex consists of four proteins, Hpr1, Mft1, Tho2 and Thp2 (Peña *et al.*, 2012). The THO/TREX complex is important for mRNP (Messenger Ribonucleoprotein) biogenesis and progression through S-phase (Wellinger, Prado and Aguilera, 2006; San Martin-Alonso *et al.*, 2021). Furthermore, the THO/TREX complex prevents the formation of obstacles for replication, like RNA:DNA hybrids (Gómez-González *et al.*, 2011). Loss of RNase H2, Topoisomerase 1 or components of the THO/TREX complex (Figure 4 B) does not lead to an increase in RNase H1 levels and also does not show a synthetic effect on viability when deleted (Figure 17 A and Figure 18 D - I).

Another important enzyme that regulates RNA:DNA hybrid levels is the helicase Sen1 (Figure 8). Sen1 has multiple functions, including transcription termination and prevention of transcription-replication conflicts (Alzu *et al.*, 2012; San Martin-Alonso *et al.*, 2021; Aiello *et al.*, 2022; Xie *et al.*, 2022; Xie, Libri and Porrua, 2023). Malfunctions in both can increase RNA:DNA hybrid levels in the genome. In this study, I found that the regulation of *RNH1* strongly depends on Sen1 (Figure 18 B and C). Furthermore, inactivation of Sen1 is the only condition found in which deletion of *RNH1* becomes lethal, showing that Rnh1 is essential if Sen1 is dysfunctional (Figure 17). This indicates, that Rnh1 either assists Sen1 in one of its functions or acts as a backup mechanism. Interestingly, after the deletion of *RNH1*, Sen1 is upregulated (Figure 19), indicating an intimate cross-talk between the two enzymes. This hypothesis is strengthened by the fact that Sen1-loss does not lead to increased RNase H2 levels (Figure 20).

Sen1 is an essential enzyme and the loss or malfunction causes massive read-through transcription, changes in the transcriptome and DNA damage (Figure 22; Giaever *et al.*, 2002; Mischo *et al.*, 2011; Aiello *et al.*, 2022). As a consequence, this genotoxic stress leads to cell death (Giaever *et al.*, 2002; Mischo *et al.*, 2011). The upregulation of *RNH1* is not caused by cell death *per se*, as drug mediated cell death or loss of other essential genes does not lead to its upregulation (Figure 21). These results validate that *RNH1* indeed is upregulated in order to compensate specifically for Sen1 loss.

4.3 RNase H1 transcripts are upregulated upon Sen1 loss

To fully understand why RNase H1 is upregulated upon Sen1 loss, I sought to investigate the underlying mechanism. It is possible that the upregulation happens on the biosynthesis side (more transcription or translation) or by stabilization of either the transcript or the protein. Direct analysis of transcript levels by quantitative reverse transcription PCR (qRT PCR) was not possible after depleting Sen1. Sen1 is involved in the transcription termination of all three RNA polymerases (RNAPs). RNAP II transcribes both, coding and non-coding genes (Xie, Libri and Porrua, 2023). Furthermore, Sen1 acts together with Nrd1 and Nab3 in the NNS-complex, terminating non-coding transcription (Porrua *et al.*, 2012). Even if this knowledge about RNAP II transcription termination indicates that loss of Sen1 has no impact on coding genes, all tested loci in qRT PCR showed an upregulation to a different extend, including housekeeping genes. This was also shown by Aiello *et al.* (2022), who published, that Sen1 depletion leads to genome-wide changes in the transcriptome, especially upregulating stress response genes and downregulating rDNA genes. Due to this effect, transcript levels after Sen1 depletion were measured using digital droplet PCR, giving absolute transcript numbers per cell without a need for normalization to a housekeeping gene. Additionally, the measurement of ongoing transcription through RNAP II association to the chromatin was chosen. Both showed an upregulation of *RNH1* upon Sen1 depletion (Figure 22). This effect was not specific to *RNH1*, as also all three RNase H2 subunits (*RNH201*, *RNH202* and *RNH203)* as well as *ACT1* were upregulated.

Sen1 terminates non-coding RNAP II transcription together with Nrd1 and Nab3 in the NNS complex (Porrua *et al.*, 2012). For validation that the transcriptional upregulation is caused by defects in transcription termination and not by other functions of Sen1, like deregulated RNA:DNA hybrids that allow easier transcription start, transcript levels were also monitored after depletion of Nrd1 and Nab3 (Figure 23 C and D). Again, *RNH1*, and also all three RNase H2 subunits (*RNH201*, *RNH202* and *RNH203)* as well as *ACT1* were upregulated. Interestingly, this upregulation did not cause Rnh1 protein levels to rise but lead to a decrease in Rnh1 protein. Taken together the upregulation of transcript by loss of any NNS complex member in combination with the opposite effects on protein level of Rnh1 after depletion of Nrd1 or Nab3 argues that the upregulation after Sen1 depletion is not only caused by higher transcription of the *RNH1* gene.

As the increased transcript levels after depletion of Sen1 or Nrd1 and Nab3 have different outcomes, the regulation has to happen either on a translational level or by increased protein stability. Transcription could be promoted by alternative transcription termination sides leading to longer transcripts. To test this, 3' rapid amplification of cDNA-ends (3'RACE) was carried out (Figure 23 E and F). This method allows for the detection of read-through transcription. No read-through transcription could be detected if any of the NNS complex members was degraded, indicating that alternative transcription termination is not the reason why *RNH1* is upregulated upon Sen1 depletion.

Proteins can also be upregulated due to higher stability. For RNase H1 this is not the case after Sen1 depletion (Figure 24). Many enzymes are stabilized when binding to their substrate. We used binding deficient hybrid binding domain mutants of RNase H1 in order to study the upregulation of Rnh1 after Sen1 depletion (Figure 25 F, G and H). Abolished Rnh1 chromatin binding did not inhibit the protein's upregulation upon Sen1 loss. This together with the results from Figure 24 argues that Rnh1 is not upregulated due to protein stabilization.

In summary, in the absence of Sen1 Rnh1 transcription is upregulated, but this upregulation is not specific to Rnh1. There has to be signaling after Sen1 loss that is not present after Nrd1 and Nab3 depletion that causes increased global translation. For example, different mRNA binding proteins can be recruited or the RNA itself can be modified. These changes in *SEN1* mutants could be for example caused by checkpoint activation that happens due to TRCs. These TRCs are caused by the loss or dysfunction of Sen1, which is not happening in *NRD1* mutants (Alzu *et al.*, 2012).

4.4 Upregulated RNase H1 associates with the chromatin

The upregulation of RNase H1 upon Sen1 loss does not automatically imply that the enzyme is actively binding RNA:DNA hybrids and degrading those. Overexpressed *RNH1* does not degrade all RNA:DNA hybrids it binds to, but in special hotspots it does (Figure 15 and Figure 30). Nonetheless, changes in the binding behavior are a good indicator for the activity of Rnh1 after Sen1 depletion. Herein (Figure 25 A - C), it was shown, that upregulated RNase H1 is indeed binding to chromatin genome-wide, including genes specific to RNA:DNA hybrids known to be formed after Sen1 depletion (San Martin-Alonso *et al.*, 2021). This indicates that RNase H1 indeed is targeting RNA:DNA hybrids that arise

because Sen1 cannot unwind them or prevent their formation by allowing proper transcription termination. At the same loci, the depletion of Hpr1 causes increased RNA:DNA hybrids (San Martin-Alonso *et al.*, 2021). While Sen1 RNA:DNA hybrids are S-phase specific, hybrids formed after Hpr1 depletion are highest in G1-phase and show a moderate increase in S-phase (Alzu *et al.*, 2012; San Martin-Alonso *et al.*, 2021). Furthermore it was shown in the same publications, that RNA:DNA hybrids arising after Sen1 depletion mainly cause RNA:DNA hybrids in head-on orientation with regards to the next origin of replication due to transcription on the lagging strand. In contrast, Hpr1 depletion leads to both, RNA:DNA hybrids oriented head-on and co-directional. Nonetheless, these RNA:DNA hybrids caused by Hpr1 depletion cause only little TRCs, but stall replication due to R-loop formation (San Martin-Alonso *et al.*, 2021). Interestingly, Rnh1 is recruited to the loci tested by San Martin-Alonso and colleagues after Sen1 depletion, but not after Hpr1 depletion (Figure 25 B – E, illustrated in Figure 31). Both, Sen1 and Hpr1 depletion lead to a slowed down S-phase progression (San Martin-Alonso *et al.*, 2021). It is possible, that RNase H1 is reacting to transcription-replication conflicts in a Sen1 specific manner because the presence of Sen1 is sufficient to resolve TRCs after Hpr1 depletion, hence the recruitment of RNase H1 to the conflict is not necessary. Another discriminating factor between the different conditions can be the nature of Hpr1 as part of the THO/TREX complex. As discussed under 4.3, mRNA binding proteins might be necessary for the increased translation of RNase H1. The THO/TREX complex is needed for mediating mRNP (messenger ribonucleoprotein) assembly (Peña *et al.*, 2012). In case formation of mRNA protein complexes is needed in order to upregulate Rnh1, this would explain why depletion of members of the THO/TREX complex does not lead to an upregulation of RNase H1.

In summary, Rnh1 actively goes to the loci that increase RNA:DNA hybrid levels after Sen1 depletion to resolve these, while it is not in the case of Hpr1 depletion. As Sen1 RNA:DNA hybrids are associated with slow S-phase progression (Alzu *et al.*, 2012; San Martin-Alonso *et al.*, 2021), it is possible, that Rnh1 resolves the RNA:DNA hybrid portion of the TRCs.

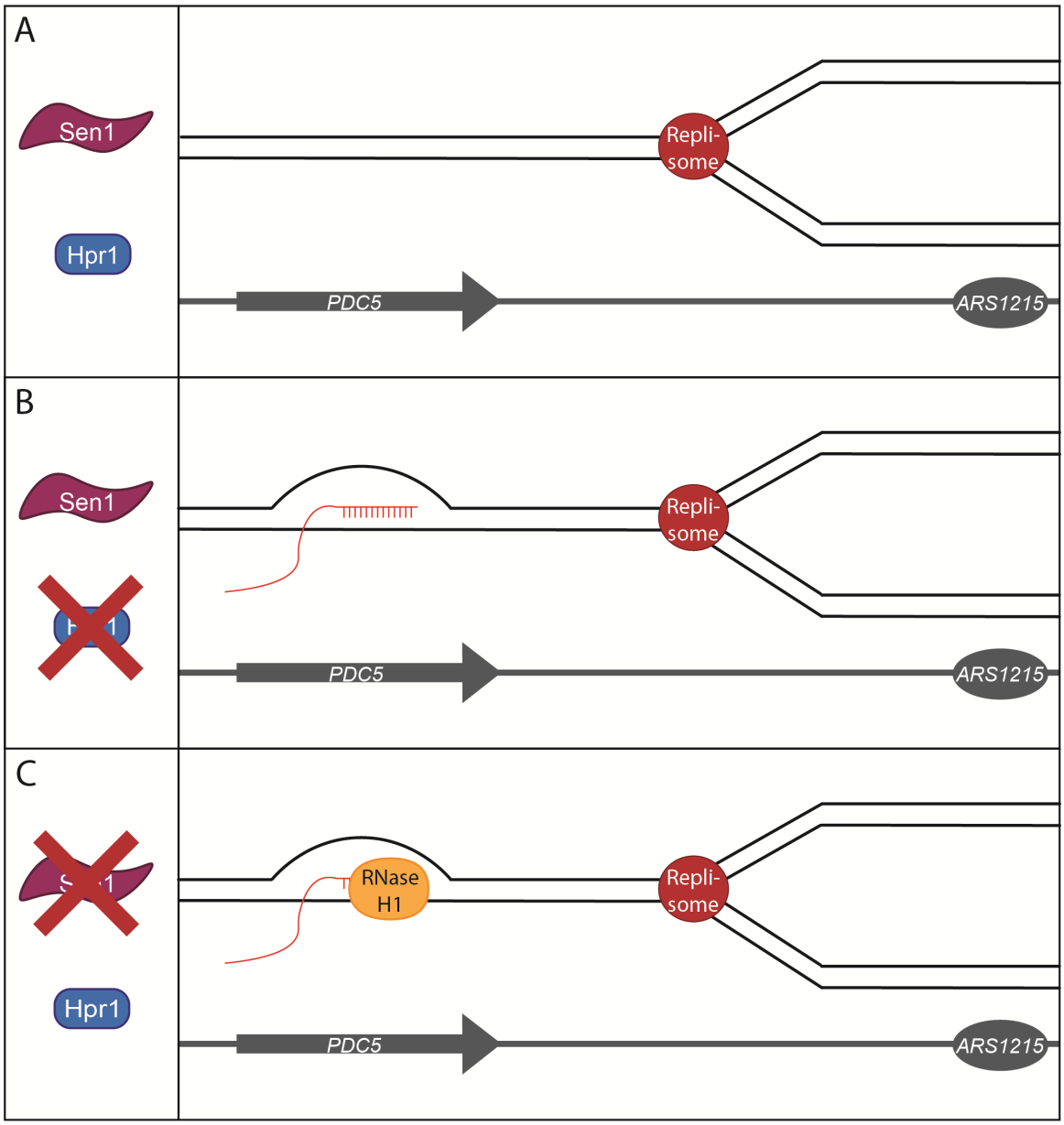

Figure 31 – RNase H1 recruitment to TRCs is Sen1 dependent. San Martin-Alonso (2021) showed, that Hpr1-AID and Sen1-AID both form RNA:DNA hybrids at the same loci. I could show that only Sen1 dependent RNA:DNA hybrids are targeted by RNase H1. The PDC5was chosen as an example region. ***(A)*** *In the presence of Sen1 and Hpr1, RNA:DNA hybrid levels are low over PDC5.* ***(B)*** *In the absence of Hpr1, RNA:DNA hybrids accumulate over the PDC5 locus. This does not induce a recruitment of RNase H1. This indicates that the presence of Sen1 is sufficient for resolving the TRC without the recruitment of RNase H1.* ***(C)*** *In the absence of Sen1 RNA:DNA hybrids accumulate over the PDC5 locus. RNase H1 is recruited in order to resolve the head-on conflict with the replisome.*

4.5 Inhibiting RNA polymerase III upregulates RNase H1

Sen1 is important for transcription termination of all three RNA polymerases (reviewed by Xie, Libri and Porrua, 2023). Rnh1 is upregulated upon Sen1 depletion probably due to RNA:DNA hybrid formation caused by faulty transcription termination at a specific RNA

polymerase or at more than one of them. The use of *rpa190-1* for inactivating RNAP I could not clarify if Rnh1 is needed in case RNAP I transcription termination is not mediated by Sen1 (Figure 26). In the chosen mutant at elevated temperatures no RNAP I transcription can occur and with that no RNA:DNA hybrids at RNAP I transcription loci can form co-transcriptionally. In case RNase H1 would be upregulated for preventing these co-transcriptional RNAP I RNA:DNA hybrids the upregulation of *RNH1* would be lost. Due to impaired ribosome assembly in the *rpa190-1* mutant, Rnh1 levels cannot be maintained at elevated temperatures, leading to decreased Rnh1 levels after the temperature shift (Figure 26). Comparing Rnh1 levels at the end point of the experiment between the double mutant with Sen1-AID* depletion and *rpa190-1* alone, an increase of Rnh1 in the absence of Sen1 can be detected that does not exceed the initial Rnh1 concentrations in the cells (Figure 26). This is why no clear conclusion can be drawn, but the experiment indicates that the upregulation of Rnh1 is not dependent on Sen1's termination function during RNAP I transcription due to the upregulation of Rnh1 when comparing the double mutant at the 2.5 h and 5 h time points. Both, Sen1 and RNases H are important for preventing conflicts between RNAP I and RNAP II at rDNA loci (Aiello *et al.*, 2022). The temperature-sensitive allele *rpa190-1* loses its catalytic activity due to the mutation in the zinc binding domain (Auld *et al.*, 1976; Wittekind *et al.*, 1988) while the RNAP I complex assembly still is functional. This indicates that in the chosen conditions conflicts between RNAP I and RNAP II or the replisome can still happen. This opens the possibility that Rnh1 is upregulated after 5 h when comparing to the 2.5 h time point in the double mutant in order to prevent TRCs at rDNA loci that arise in the absence of Sen1.

RNAP II transcribes coding genes as well as some non-coding regions. Sen1 is important for the termination of the non-coding portion of RNAP II transcribed genes (reviewed by Porrua and Libri, 2015; Xie, Libri and Porrua, 2023). Nonetheless, herein it was shown that the depletion of Sen1 and its complex members Nrd1 and Nab3 leads to dysregulated transcription (Figure 22 and Figure 23). In case both, Sen1 and the catalytic subunit of RNAP II (Rpb1) are depleted simultaneously no RNAP II transcription is happening. This would abolish Rnh1 upregulation if it is important for reducing co-transcriptional RNA:DNA hybrids arising due to faulty transcription termination. This hypothesis could not be proven or disproven as the absence of RNAP II transcription also leads to the loss of newly synthesized *RNH1* transcripts that are needed for Rnh1 translation, which is a prerequisite

of increased Rnh1 protein levels (Figure 26). In yeast, the average mRNA has a half-life of 22 min (Chia and McLaughlin, 1979) and in Figure 24 it was shown that after 45 min of inhibited translation half of the present Rnh1 is degraded due to the normal protein turnover. This explains why after the double depletion of Sen1 and Rpb1, Rnh1 levels decrease strongly and no upregulation is detectable anymore (Figure 26). As no new *RNH1* transcript can be transcribed, no upregulation of the protein is possible in the absence of Rpb1. These results do not allow to exclude Rnh1's importance in inhibiting co-transcriptional RNA:DNA hybrid formation after Sen1 depletion at RNAP II transcribed loci. It is especially noteworthy that Alzu *et al.* (2012) showed, that in a Sen1 mutant head-on conflicts of RNAP II and the replisome lead to increased RNA:DNA hybrids, indicating that these RNA:DNA hybrids might be the target of Rnh1 after Sen1 depletion. Nevertheless, the results from Figure 26 show that upregulation of Rnh1 relies on transcription and is not due to protein stabilization which was also shown in Figure 24. Without active transcription no clear conclusion in RNase H1's role in RNAP II transcription termination can be drawn.

RNAP III is important for transcription termination at tRNA genes, 5s rDNA and other non-coding RNAs (Porrua, Boudvillain and Libri, 2016). These transcripts have in common, that they are highly structured, highly transcribed and short (Porrua, Boudvillain and Libri, 2016). Transcription of RNAP III can efficiently be mediated by the transcription complex approaching a T-tract, but recently it was shown, that RNAP III transcription is also terminated in a Sen1-dependent manner (Xie *et al.*, 2022; Xie, Libri and Porrua, 2023). Sen1 in this case acts as a backup mechanism in case the primary terminator is not efficiently terminating the transcription (Xie *et al.*, 2022). Furthermore, Sen1 is important at tRNA genes in order to prevent conflicts between RNAP II and RNAP III (Aiello *et al.*, 2022).
Besides other classes of RNA, RNase H1 targets RNA:DNA hybrids at tRNA loci (El Hage *et al.*, 2014, Figure 15), a location in the genome where Sen1 is important for suppressing RNA:DNA hybrid formation and that is RNAP III transcribed. Considering these facts, it fits that inhibition of RNAP III transcription by Rpo31 depletion alone leads to an increase of Rnh1 levels, which is not as high as for Sen1 depletion, but significant (Figure 26). The double mutant does not show an additive effect but reaches the Rnh1 levels seen after depleting Sen1 alone (Figure 26). In case RNase H1 backs up Sen1's function at RNAP III, no upregulation of Rnh1 protein levels would be detectable after co-depletion of Sen1-AID* and Rpo31-AID*. It is not clear what exactly happens after depleting Rpo31. It is likely that

the transcript that is transcribed while Rpo31 depletion starts stays at the open DNA and forms an RNA:DNA hybrid. Possibly also other proteins from the RNAP III transcription complex stay bound to the genomic locus, leading to conflicts with the approaching replisome during replication or with non-terminated RNAP II transcription. This genotoxic stress could lead to a similar response as Sen1 depletion, causing RNase H1 upregulation in order to remove the RNA:DNA hybrid that causes the stress. No additivity between Sen1 and Rpo31 depletion is detectable (Figure 26). This indicated that Rnh1 is upregulated after Sen1 depletion in order to reduce RNA:DNA hybrids at RNAP III transcribed loci, which are targeted by both, Sen1 and Rnh1. These loci are known to be hotspots of transcription-replication conflicts (Tran *et al.*, 2017). Sen1, besides its transcription termination functions, travels with the replisome and prevents TRCs (Appanah *et al.*, 2020; Aiello *et al.*, 2022). Likely, Rnh1 is important for preventing these conflicts at highly transcribed loci in the absence of Sen1 by depleting the RNA:DNA hybrid portion of the conflict.

4.6 RNase H1 upregulation is caused by high RNA:DNA hybrid levels

Sen1 and RNase H1 are both important for the maintenance of physiological RNA:DNA hybrid levels. I have shown in this work, that under our used conditions after deletion of *RNH1* or depletion of Sen1-AID* RNA:DNA hybrids are indeed increased in the same amount of cells (Figure 29). Interestingly, the double mutant did not have a higher percentage of cells with detectable RNA:DNA hybrids. This suggests, that the RNA:DNA hybrids caused by deletion of *RNH1* or depletion of Sen1 have a commonality and might even be in the same locations. Another possibility is that in cases where both, RNase H1 and Sen1, are not present, RNase H2 becomes active at accumulating RNA:DNA hybrids. Furthermore, depleting RNA:DNA hybrids during Sen1 depletion slows down endogenous RNase H1 upregulation confirming that RNA:DNA hybrids are necessary for signaling towards RNase H1 upregulation. It could not be excluded in this experiment that the decreased upregulation was caused by a protein feedback of RNase H1 itself. For example, the expression of *RNH1* could be regulated by RNA:DNA hybrids forming at the genomic locus, leading to an upregulation of the protein, followed by the degradation of the RNA:DNA hybrid by RNase H1 regulating down *RNH1* transcription. For testing this, the repetition of the experiment with the catalytic inactive protein *rnh1(D193N)* would have been a proper control. This experiment gave no reproducible results due to the sickness of

these cells shown in Figure 14. Another possibility would be to overexpress either human or bacterial RNase H1 in order to tackle the question, whether or not a protein feedback exists. This experiment will be carried out in the future.

4.7 RNase H1 upregulation maintains S-phase progression in the absence of Sen1 helicase

Sen1 is important during replication in order to prevent TRCs and to retain fork progression (San Martin-Alonso *et al.*, 2021). Additionally, human RNase H1 was shown as well to prevent TRCs (Parajuli *et al.*, 2017). Interestingly, in human cells RNase H1 helps maintaining fork progression upon genotoxic stress independent of its RNA:DNA hybrid removal function (preprint, Basille *et al.*, 2025). In *E. coli* RNase HI is recruited to TRCs by the single-stranded DNA-binding protein SSB to degrade the R-loop moiety of the TRC (Wolak *et al.*, 2020). In *Leichmania major*, RNase H1 is important for maintaining replication timing and preventing DNA damage (Damasceno *et al.*, 2025). For testing whether or not the herein described phenotype of RNase H1 upregulation upon Sen1 depletion is caused by its putative role in the prevention of TRCs in budding yeast, we performed experiments in which the cells were restricted to specific cell cycle phases in order to allow or prevent replication, which is happening in S-phase. The experiments were carried out by my Master student Sophia Sergi under my supervision. We could show that replication has to be ongoing to upregulate RNase H1 in the absence of Sen1 (Figure 27 A and B). Opposite to previously published results from our lab (Lockhart *et al.*, 2019) we could show that G1-arrested cells have a lower RNase H1 content than cycling cells (Figure 27 A and B). It has to be considered, that here RNase H1 levels were determined in a Sen1-AID* degron strain while Lockhart *et al.* (2019) used wild type cells. Furthermore, a single S-phase progression is sufficient to increase RNase H1 levels above the levels detected in cells, which were not depleted from Sen1. This upregulation only happens when cells are in late S-phase or already start reaching G2/M-phase (Figure 27 C and D). In budding yeast replication of late replicating loci (for example subtelomeric regions and telomeres) can be still ongoing when mitosis starts (Ivanova *et al.*, 2020). This indicates that these regions especially rely on Sen1 and RNase H1 for resolving TRCs. Together these results show, that RNase H1 is very important during replication in the absence of Sen1. Most likely, RNase H1 acts in the prevention of TRCs by depleting the RNA:DNA hybrid fraction of the conflict. Additional

evidence can be found in data from the Koshland lab. They have shown that depletion of Sen1 during S-phase is lethal in the *rnh1 rnh201* Sen1-AID* mutant (Costantino and Koshland, 2018). The recent finding, that in human cells RNase H1 helps maintain replication fork progression independent of its RNA:DNA removal function (preprint, Basille *et al.*, 2025) goes in line with my finding, that catalytic inactive RNase H1 (D193N) can rescue the sick phenotype of *sen1-1 rnh1* back to *sen1-1* levels (Figure 17 B). For DSB repair, RNA:DNA hybrids are important in order to coordinate Rad51 recruitment (D'Alessandro *et al.*, 2018). Hence, the stabilization of RNA:DNA hybrids at TRCs by Rnh1(D193N) could be beneficial for the cells, preventing the *sen1-1 rnh1* phenotype (Figure 17). Additionally, I could show that RNase H1 does not deplete RNA:DNA hybrids in some RNA:DNA hybrid pone regions (Figure 15). The loci shown not to degrade RNA:DNA hybrids (*GCN4* and *PDC1)* are in close proximity of origins of replication and were shown by the Aguilera lab to accumulate TRCs in the absence of Sen1 (San Martin-Alonso *et al.*, 2021). Possibly, RNase H1 is not degrading RNA:DNA hybrids here in order to stabilize the RNA:DNA hybrids for allowing DNA repair. This hypothesis needs further investigation in the future.

We strengthened the finding that RNase H1 is essential in the loss of function mutant *sen1-1* with a test for viability after restricting RNase H1 expression either to G1-, S- or G2/M phase (characterization published by Lockhart *et al.* (2019) and G1 allele created by my colleague Fabio Bento) in the *sen1-1* loss of function mutant. The experiments were carried out by my Master student Sophia Sergi under my supervision. While *S-RNH1* is as sick as *RNH1* deletion in the *sen1-1* loss of function mutant at semi-permissive temperatures, *G2/M-RNH1* shows a rescue to a viability similar to the *sen1-1* mutant alone. RNase H1 becomes important during replication in the absence of Sen1 which at first glance does not fit to the rescue in G2/M-phase. The *sen1-3* mutant that loses association to the replisome shows increased DNA damage in late S-phase and this effect can be suppressed if *RNH1* is overexpressed (Appanah *et al.*, 2020). RNase H1 upregulation starts in the late S-phase, most likely for acting on persistent TRCs at late replicating origins. Like this, these TRCs are resolved before the cells enter mitosis, allowing both, mother and daughter cells to have a complete set of fully replicated chromosomes. The S-phase checkpoint guarantees that replication is completed before the cells divide. My colleague Matteo Longaretti found in his PhD work, that RNase H1 upregulation depends on the S-phase checkpoint and Rad53 in particular (unpublished data). As reviewed by Segurado and Tercero (2009), the S-phase

checkpoint is important for the stability of replication forks and late origin firing. The activation of the S-phase checkpoint relies on RPA binding of ssDNA (Segurado and Tercero, 2009), which arises upon fork stalling but is also binding to the ssDNA strand in R-loops and is important to stimulate RNase H1 function (Nguyen *et al.*, 2017). Furthermore, these findings can explain why RNase H1 is upregulated late in S-phase. Lockhart *et al.* (2019) showed, that in late S-phase the *S-RNH1* allele is expressed to a lower extent than the unrestricted allele is, while the G2/M-allele starts being expressed. This is most likely why the S-phase allele is not able to rescue the *sen1-1 rnh1* phenotype, but the G2/M-allele is.
It is not easy to interpret the phenotype of *G1-RNH1*, as the restriction of RNase H1 to G1-phase reduces viability compared to the full deletion in the *sen1-1* mutant at elevated temperatures. Sen1 is not important for prevention of RNA:DNA hybrids in G1-phase (Alzu *et al.*, 2012; San Martin-Alonso *et al.*, 2021). We have shown that RNase H1 is important in case Sen1 is absent during S-phase, so in G1-phase RNase H1 is acting independent of the phenotype seen after Sen1 depletion. Due to the used *SIC1* promotor and degron that restrict RNase H1 expression to G1-phase, the level of expression does not recreate the levels usually seen in G1-phase. In G1-phase RNase H1 expression is low (Figure 27 A and B). Higher expression caused by the cell cycle allele could lead to the depletion of physiologically important RNA:DNA hybrids, reducing cell viability. Taking together, RNase H1 is important during late S-phase, arguing for a role in assisting or backing up Sen1 in the prevention of TRCs.
We could show that RNase H1 is important for S-phase progression (Figure 28). The known slowdown of replication speed caused by Sen1 depletion (Alzu *et al.*, 2012; San Martin-Alonso *et al.*, 2021) was exacerbated in a strain with deletion of *RNH1* (Figure 28). This result argues, that RNase H1 is together with Sen1 important for preventing and or resolving TRCs. It is not clear, if RNase H1 holds a function as a backup mechanism in case Sen1 is dysfunctional or absent or if both together are needed for preventing and resolving the conflicts. Deletion of RNase H1 alone does not lead to a delay in S-phase progression (Figure 28), which goes in line with the findings from human cells in which deletion of RNase H1 did not influence the rate of fork progression (Heuzé *et al.*, 2023). These results indicate, that Sen1 is sufficient for preventing the conflicts. The role of RNase H1 in maintaining fork progression has been previously shown in human cells, where RNase H1 depletion alone slows down replication forks (Parajuli *et al.*, 2017). Furthermore,

overexpression of RNase H1 increases fork speed in human cells and decreases TRCs which are mediated by THO complex mutations in yeast (Jones *et al.*, 2013; Brown *et al.*, 2022). Interestingly, RNase H1 seems to have an effect on fork progression independently of R-loop resolution in human cells (preprint, Basille *et al.*, 2025). In the parasite *Leishmania major*, RNase H1 knock out leads to deregulated replication timing (Damasceno *et al.*, 2025). Together, we could show that RNase H1 is assisting Sen1 in its function of preventing TRCs and maintaining fork progression speed.

Furthermore, we could show that the Sen1-dependent RNase H1 phenotype depends on Sen1's functions mediated by its replisome association (Figure 28 B and C). This could be shown by exploiting the *sen1-3* allele which loses association to the replisome and to RNAP III (Appanah *et al.*, 2020; Xie *et al.*, 2022). The phenotypes here are very subtle and need further RNA:DNA hybrid stabilization by chemical treatment with genotoxic drugs. Nonetheless, RNase H1 is important in the *sen1-3* mutant in order to maintain viability. This is strengthened by the sick phenotype of the *sen1-3* mutant in the absence of Rad53 (Appanah *et al.*, 2020) where RNase H1 cannot be upregulated. Taking our data into consideration, this is happening due to the lost upregulation of RNase H1. Interestingly, we could show, that RNase H2 is not involved in resolving TRCs like RNase H1 is, as deletion of the catalytic subunit *RNH201* does not have an impact on *sen1-3* viability. Taking together, RNase H1 is important during late S-phase in the absence of Sen1 to limit damage caused by the loss of Sen1's replication coupled functions.

4.8 RNase H1 is regulated in a Sen1-dependent manner in order to prevent transcription-replication conflicts

In summary in this thesis, I could shed light on the regulation of RNase H1, which is not well studied. I found, that RNase H1 gets upregulated in cases in which the essential helicase Sen1 is depleted or dysfunctional. Furthermore, I could show with the help of my colleagues that this upregulation happens during S-phase in a Rad53-dependent manner and that in this scenario RNase H1 becomes essential in order to limit genotoxic stress. In the conditions I tested I could not detect Rad53 phosphorylation, but Alzu *et al.* (2012) were able to show that *sen1-1* cells accumulate phosphorylated Rad53 at elevated temperatures. Conflicts between replication and transcription naturally occur and need to be resolved in order to prevent genotoxic stress. It is known, that Sen1 has functions in

preventing these conflicts, even though it is discussed that Sen1 is not removing RNA:DNA hybrids in its replication coupled function, but only prevents them by maintaining correct transcription termination (Aiello *et al.*, 2022). This indicates that at TRCs the RNA:DNA hybrid portion of the conflict has to be removed by another enzyme. Aiello and colleagues (2022) introduced a role of both RNases H in resolving conflicts at the rDNA. In this work, we could narrow this interaction down to RNase H1.

In summary, in the presence of Sen1 it is the main factor for resolving TRCs, even though, RNase H1 is present and can resolve the RNA:DNA hybrid portion of the conflict in a Rad53-dependent manner (Figure 32 A). In situations where Sen1 is not present or loses its functionality, RNase H1 becomes the main factor for resolving TRCs by degrading the RNA:DNA hybrid fraction of the conflict in a Rad53-dependent manner (Figure 32 B).

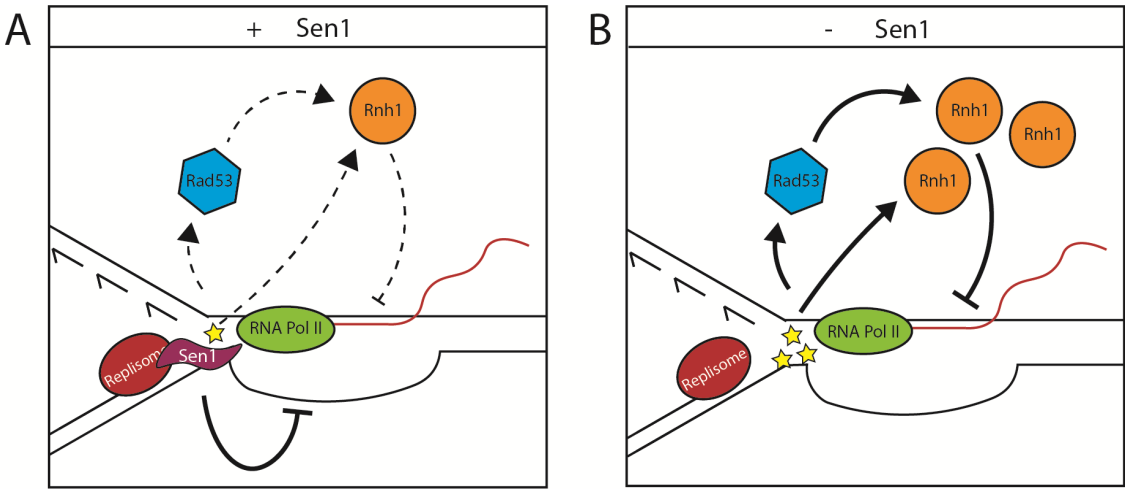

Figure 32 – RNase H1 assists Sen1 in preventing transcription-replication conflicts. ***(A)*** *In the presence of functional Sen1, genotoxic stress (Star) is low due to Sen1's function in prevention of transcription-replication conflicts. RNase H1 here assists in the prevention of conflicts in a Rad53-dependent manner but is not essential (dashed line)* ***(B)*** *In the absence of Sen1 or if it is dysfunctional, RNase H1 becomes upregulated in a Rad53-dependent manner and in order to deplete the RNA:DNA hybrid sub-portion of the conflict and prevent excessive genotoxic stress (Stars).*

Nonetheless, RNase H1 can degrade RNA:DNA hybrids at sites of TRCs. After degradation of the RNA:DNA hybrid portion of the conflict by RNase H1, the RNA polymerase is still present. The removal of the RNA polymerase can be carried out by Sen1 that is not associated with the replisome if it is present. A recent study indicated, that Rat1 and RNase H1 together can remove stalled RNA polymerases, with RNase H1 first cutting the RNA, allowing Rat1 to push off the RNA polymerase (Mérida-Cerro *et al.*, 2024). It is possible, that Rat1 and RNase H1 also at TRCs work together in the presence and absence of Sen1,

starting with RNase H1 degrading the majority of the RNA:DNA hybrid, followed by Rat1 releasing the RNA polymerase (Figure 33). Whether Sen1 or Rat is removing the RNA polymerase in TRCs is an interesting next question to study.

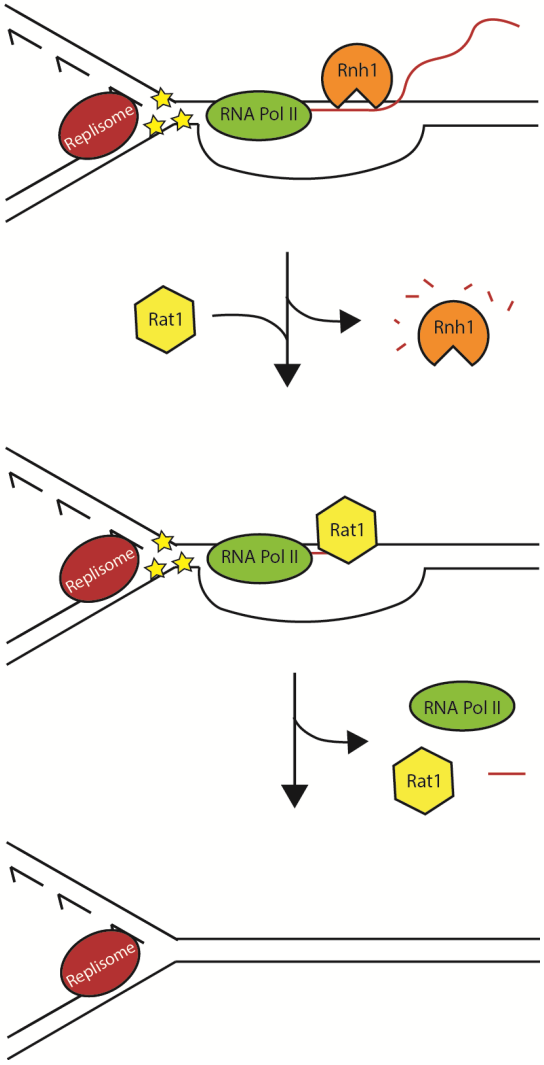

Figure 33 – Potential interplay of RNase H1 and Rat1 at TRCs. First RNase H1 degrades the RNA:DNA hybrid, followed by RNAP release by Rat1, allowing replication to proceed.

Sen1 does not only regulate conflicts between the replisome and the transcription machinery, but also between different RNA polymerases. The data presented here about RNase H1 upregulation upon inhibition of RNAP III transcription indicates, that RNase H1 might also act with Sen1 during conflicts between RNAP II and RNAP III, which Aiello and colleagues showed to be another kind of conflict Sen1 is resolving. This is a promising aspect of RNase H1 regulation and would be a nice continuation of the project. Together these findings show that Sen1 and RNase H1 are key enzymes for the prevention and resolution of TRCs.

4.9 RNase H1 vs. RNase H2 – how the difference arises

It has been a long-standing question, why two enzymes with the same function, like RNase H1 and RNase H2, are conserved from bacteria to men. Both, RNase H1 and RNase H2 can resolve RNA:DNA hybrids, while only RNase H2 has its unique function in ribonucleotide excision repair (RER). Therefore, in theory, RNase H2 alone could be sufficient to remove all RNA:DNA hybrids. It has been postulated in the field that RNase H1 is a backup mechanism in case RNA:DNA hybrid levels get very high and RNase H2 alone cannot degrade them sufficiently (Zimmer and Koshland, 2016; Lockhart *et al.*, 2019). In this work, a unique function of RNase H1 was found. It is necessary to prevent and or resolve TRCs that arise in the absence of Sen1. This leads to an upregulation of the protein in a Rad53-dependent manner. It is still unknown which is the signaling factor for this activation of RNase H1. RNase H1 binding and activation is stimulated by RPA and the interaction with RPA even leads to a change of processivity from an endonuclease into a bidirectional exonuclease (Nguyen *et al.*, 2017; Lee *et al.*, 2021). RPA, furthermore, is an important signal for checkpoint activation (Segurado and Tercero, 2009), making it a possible starting signal for RNase H1 upregulation in case TRCs happen, local high concentrations of RPA arise at the ssDNA portion of the conflict in an unscheduled manner (Alzu *et al.*, 2012).

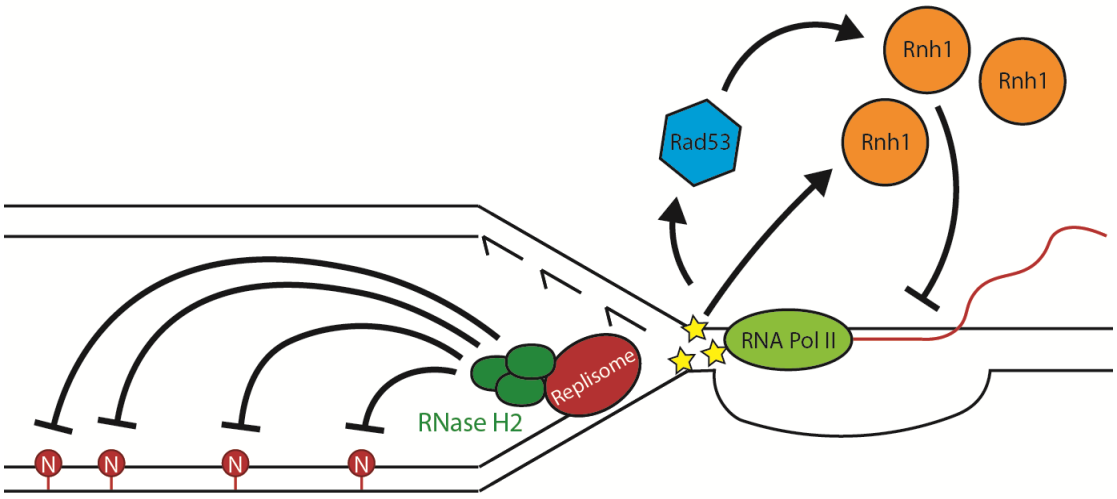

Figure 34 – During S-phase RNase H2 is mainly removing rNMPs while RNase H1 removes the R-loop portion of TRCs.

In the absence of Sen1, only RNase H1 and not RNase H2 is upregulated (Figure 18 and Figure 20). It was published that in human the interaction of RNase H1 with RPA is unique between the RNase H enzymes and none of the RNase H2 subunits interacts with RPA (Nguyen *et al.*, 2017). Together, this strengthens the idea that RNase H1 is important especially when genotoxic stress arises during a TRC. Furthermore, expression of wild type RNase H1 can suppress DNA damage signaling (gamma-H2AX foci), but not a RPA-binding deficient RNase H1 mutant (Nguyen *et al.*, 2017). Hinting once more for RNase H1's function in the prevention of TRCs. A possible dependence of RNase H1 upregulation on RPA should be verified in the future. My colleague Fabio Bento could show in his PhD thesis hat RPA directly interacts with hybrid binding domain 1 of RNase H1, but we did not study how checkpoint activation by RPA changes RNase H1 expression and activity. Furthermore, these TRCs arise in S-phase when DNA is replicated. This is the time when RNase H2 is important for RER, while it is removing R-loops during the whole cell cycle (Lockhart *et al.*, 2019). Possibly, RNase H2's function in RER is so important that all available molecules are engaged in this function, making RNase H1 evolutionary necessary for resolving transcription-replication conflicts during S-phase (Figure 34).

4.10 RNase H1 overexpression as a tool in RNA:DNA hybrid detection

Overexpression of *RNH1* is broadly used as a control when studying RNA:DNA hybrid levels (Arora *et al.*, 2014; Chan *et al.*, 2014; De Magis *et al.*, 2019; Brown *et al.*, 2022; Mérida-Cerro *et al.*, 2024). It is used for verifying that effects are indeed caused by RNA:DNA hybrids and not for example by dsRNA (Vanoosthuyse, 2018). We have also published a method for detection of telomeric RNA:DNA hybrids that includes overexpression of RNH1 and/or *rnh1(D193N)*, which is more sensitive at telomeres than DRIP (Wagner and Luke, 2022).

Especially in methods using the S9.6 antibody, the portion of signal resistant to RNase H1 is often interpreted not to be RNA:DNA hybrids and taken out of the analysis (Vanoosthuyse, 2018). The results from Figure 15 show how problematic this procedure can be, excluding RNase H1 resistant RNA:DNA hybrids from the analysis. The results confirmed data from the Koshland lab showing, that RNase H1 preferably targets RNA:DNA in hotspot regions where the hybrids are stabilized (Zimmer and Koshland, 2016). Furthermore, it could be shown, that overexpression of RNase H1 leads to increased levels

of read-through transcription, altering R-loop levels in itself (Skourti-Stathaki, Proudfoot and Gromak, 2011). Together, these results question the use of *in vivo* overexpression treatment of RNA:DNA hybrids with RNase H1 as a control for what is a real RNA:DNA hybrid in experiments using the S9.6 antibody. Especially the change in RNase H1 activity upon TRC accumulation shown in this thesis can falsify the results. Taken together, this practice is excluding a big sub-portion of RNA:DNA hybrids and might alter the RNA:DNA hybrid distribution in general. A solution to this problem would be to test, whether bacterial or human RNase H1 show a similar behavior or if they degrade all RNA:DNA hybrids. Overexpression of these enzymes could resolve the described problem. Furthermore, it should be considered to do an *in vitro* RNase H treatment instead of RNase H overexpression in experimental setups where this is possible.

5. References

Aiello, U. *et al.* (2022) 'Sen1 is a key regulator of transcription-driven conflicts', *Molecular Cell*, 82(16), pp. 2952-2966.e6. Available at: https://doi.org/10.1016/j.molcel.2022.06.021.

Aiello, U., Porrua, O. and Libri, D. (2025) 'Sen1: The Varied Virtues of a Multifaceted Helicase', *Journal of Molecular Biology*, 437(1), p. 168808. Available at: https://doi.org/10.1016/j.jmb.2024.168808.

Alzu, A. *et al.* (2012) 'Senataxin Associates with Replication Forks to Protect Fork Integrity across RNA-Polymerase-II-Transcribed Genes', *Cell*, 151(4), pp. 835–846. Available at: https://doi.org/10.1016/j.cell.2012.09.041.

Amon, J.D. and Koshland, D. (2016) 'RNase H enables efficient repair of R-loop induced DNA damage', *eLife*, 5, pp. 1–20. Available at: https://doi.org/10.7554/eLife.20533.

Appanah, R. *et al.* (2020) 'Sen1 Is Recruited to Replication Forks via Ctf4 and Mrc1 and Promotes Genome Stability', *Cell Reports*, 30(7), pp. 2094-2105.e9. Available at: https://doi.org/10.1016/j.celrep.2020.01.087.

Arora, R. *et al.* (2014) 'RNaseH1 regulates TERRA-telomeric DNA hybrids and telomere maintenance in ALT tumour cells', *Nature Communications*, 5, pp. 1–11. Available at: https://doi.org/10.1038/ncomms6220.

Arudchandran, A. *et al.* (2000) 'The absence of ribonuclease H1 or H2 alters the sensitivity of Saccharomyces cerevisiae to hydroxyurea, caffeine and ethyl methanesulphonate: implications for roles of RNases H in DNA replication and repair', *Genes to Cells*, 5(10), pp. 789–802. Available at: https://doi.org/10.1046/j.1365-2443.2000.00373.x.

Auld, D.S. *et al.* (1976) 'Yeast RNA polymerase I: A eukaryotic zinc metalloenzyme', *Biochemical and Biophysical Research Communications*, 69(2), pp. 548–554. Available at: https://doi.org/10.1016/0006-291X(76)90555-6.

Basille, A. *et al.* (2025) 'Rapid delivery of RNase H1 enables replication fork progression under stress independently of R-loop resolution'. BioRxiv. Available at: https://doi.org/10.1101/2025.02.27.640516.

Brambati, A. *et al.* (2018) 'Dormant origins and fork protection mechanisms rescue sister forks arrested by transcription', *Nucleic Acids Research*, 46(3), pp. 1227–1239. Available at: https://doi.org/10.1093/nar/gkx945.

Brown, R.E. *et al.* (2022) 'The RNA export and RNA decay complexes THO and TRAMP prevent transcription-replication conflicts, DNA breaks, and CAG repeat contractions', *PLOS Biology*. Edited by T. Paull, 20(12), p. e3001940. Available at: https://doi.org/10.1371/journal.pbio.3001940.

Browning, K.R. and Merrikh, H. (2024) 'Replication–Transcription Conflicts: A Perpetual War on the Chromosome', *Annual Review of Biochemistry*, 93(1), pp. 21–46. Available at: https://doi.org/10.1146/annurev-biochem-030222-115809.

Brüning, J.G. and Marians, K.J. (2020) 'Replisome bypass of transcription complexes and R-loops', *Nucleic acids research*, 48(18), pp. 10353–10367. Available at: https://doi.org/10.1093/nar/gkaa741.

Bubeck, D. *et al.* (2011) 'PCNA directs type 2 RNase H activity on DNA replication and repair substrates', *Nucleic Acids Research*, 39(9), pp. 3652–3666. Available at: https://doi.org/10.1093/nar/gkq980.

Buratowski, S. (2009) 'Progression through the RNA Polymerase II CTD Cycle', *Molecular Cell*, 36(4), pp. 541–546. Available at: https://doi.org/10.1016/j.molcel.2009.10.019.

Cerritelli, S.M. *et al.* (2003) 'Failure to Produce Mitochondrial DNA Results in Embryonic Lethality in Rnaseh1 Null Mice', *Molecular Cell*, 11(3), pp. 807–815. Available at: https://doi.org/10.1016/S1097-2765(03)00088-1.

Cerritelli, S.M. and Crouch, R.J. (2009) 'Ribonuclease H : the enzymes in eukaryotes', 276, pp. 1494–1505. Available at: https://doi.org/10.1111/j.1742-4658.2009.06908.x.

Cerritelli, S.M. and El Hage, A. (2020) 'RNases H1 and H2: guardians of the stability of the nuclear genome when supply of dNTPs is limiting for DNA synthesis', *Current Genetics*, 66(6), pp. 1073–1084. Available at: https://doi.org/10.1007/s00294-020-01086-8.

Chan, Y.A. *et al.* (2014) 'Genome-Wide Profiling of Yeast DNA:RNA Hybrid Prone Sites with DRIP-Chip', *PLoS Genetics*, 10(4). Available at: https://doi.org/10.1371/journal.pgen.1004288.

Chappidi, N. *et al.* (2020) 'Fork Cleavage-Religation Cycle and Active Transcription Mediate Replication Restart after Fork Stalling at Co-transcriptional R-Loops', *Molecular Cell*, 77(3), pp. 528-541.e8. Available at: https://doi.org/10.1016/j.molcel.2019.10.026.

Chédin, F. *et al.* (2021) 'Best practices for the visualization, mapping, and manipulation of R-loops.', *The EMBO journal*, p. e106394. Available at: https://doi.org/10.15252/embj.2020106394.

Chen, L. *et al.* (2017) 'R-ChIP Using Inactive RNase H Reveals Dynamic Coupling of R-loops with Transcriptional Pausing at Gene Promoters', *Molecular Cell*, 68(4), pp. 745-757.e5. Available at: https://doi.org/10.1016/j.molcel.2017.10.008.

Chia, L.-L. and McLaughlin, C. (1979) 'The half-life of mRNA in Saccharomyces cerevisiae', *Molecular and General Genetics MGG*, 170(2), pp. 137–144. Available at: https://doi.org/10.1007/BF00337788.

Choudhary, R. *et al.* (2023) 'Sen1 and Rrm3 ensure permissive topological conditions for replication termination', *Cell Reports*, 42(7), p. 112747. Available at: https://doi.org/10.1016/j.celrep.2023.112747.

Cohen, S. *et al.* (2018) 'Senataxin resolves RNA:DNA hybrids forming at DNA double-strand breaks to prevent translocations', *Nature Communications*, 9(1), p. 533. Available at: https://doi.org/10.1038/s41467-018-02894-w.

Conover, H.N. *et al.* (2015) 'Stimulation of Chromosomal Rearrangements by Ribonucleotides', *Genetics*, 201, pp. 951–961. Available at: https://doi.org/10.1534/genetics.115.181149.

Conti, B.A. *et al.* (2024) 'RTF2 controls replication repriming and ribonucleotide excision at the replisome', *Nature Communications*, 15(1), p. 1943. Available at: https://doi.org/10.1038/s41467-024-45947-z.

Costantino, L. and Koshland, D. (2015) 'The Yin and Yang of R-loop biology', *Current Opinion in Cell Biology*, 34, pp. 39–45. Available at: https://doi.org/10.1016/j.ceb.2015.04.008.

Costantino, L. and Koshland, D. (2018) 'Genome-wide Map of R-Loop-Induced Damage Reveals How a Subset of R-Loops Contributes to Genomic Instability', *Molecular Cell*, 71(4), pp. 487-497.e3. Available at: https://doi.org/10.1016/j.molcel.2018.06.037.

Crossley, M.P. *et al.* (2020) 'qDRIP: a method to quantitatively assess RNA–DNA hybrid formation genome-wide', *Nucleic Acids Research*, pp. 1–19. Available at: https://doi.org/10.1093/nar/gkaa500.

Crossley, M.P. *et al.* (2023) 'R-loop-derived cytoplasmic RNA-DNA hybrids activate an immune response', *Nature*, 613, pp. 187–194. Available at: https://doi.org/10.1038/s41586-022-05545-9.

Crossley, M.P., Bocek, M. and Cimprich, K.A. (2019) 'R-Loops as Cellular Regulators and Genomic Threats', *Molecular Cell*, 73(3), pp. 398–411. Available at: https://doi.org/10.1016/j.molcel.2019.01.024.

D'Alessandro, G. *et al.* (2018) 'BRCA2 controls DNA:RNA hybrid level at DSBs by mediating RNase H2 recruitment', *Nature Communications*, 9(1). Available at: https://doi.org/10.1038/s41467-018-07799-2.

Damasceno, J.D. *et al.* (2025) 'R-loops acted on by RNase H1 influence DNA replication timing and genome stability in Leishmania', *Nature Communications*, 16(1), p. 1470. Available at: https://doi.org/10.1038/s41467-025-56785-y.

De Magis, A. *et al.* (2019) 'DNA damage and genome instability by G-quadruplex ligands are mediated by R loops in human cancer cells', *Proceedings of the National Academy of Sciences of the United States of America*, 116(3), pp. 816–825. Available at: https://doi.org/10.1073/pnas.1810409116.

Dilley, R.L. *et al.* (2016) 'Break-induced telomere synthesis underlies alternative telomere maintenance', *Nature*, 539(7627), pp. 54–58. Available at: https://doi.org/10.1038/nature20099.

Doxtader Lacy, K.A. *et al.* (2022) 'RNA modifications can affect RNase H1-mediated PS-ASO activity', *Molecular Therapy - Nucleic Acids*, 28(June), pp. 814–828. Available at: https://doi.org/10.1016/j.omtn.2022.05.024.

El Hage, A. *et al.* (2010) 'Loss of Topoisomerase I leads to R-loop-mediated transcriptional blocks during ribosomal RNA synthesis', *Genes & Development*, 24(14), pp. 1546–1558. Available at: https://doi.org/10.1101/gad.573310.

El Hage, A. *et al.* (2014) 'Genome-Wide Distribution of RNA-DNA Hybrids Identifies RNase H Targets in tRNA Genes, Retrotransposons and Mitochondria', *PLoS Genetics*, 10(10). Available at: https://doi.org/10.1371/journal.pgen.1004716.

Feretzaki, M. *et al.* (2020) 'RAD51-dependent recruitment of TERRA lncRNA to telomeres through R-loops', *Nature* [Preprint], (October 2019). Available at: https://doi.org/10.1038/s41586-020-2815-6.

Gameiro, E. *et al.* (2025) 'Genome-wide conditional degron libraries for functional genomics', *Journal of Cell Biology*, 224(2), p. e202409007. Available at: https://doi.org/10.1083/jcb.202409007.

Gatti, V. *et al.* (2023) 'Senataxin and R-loops homeostasis: multifaced implications in carcinogenesis', *Cell Death Discovery*, 9(1), p. 145. Available at: https://doi.org/10.1038/s41420-023-01441-x.

Giaever, G. *et al.* (2002) 'Functional profiling of the Saccharomyces cerevisiae genome', *Nature*, 418(6896), pp. 387–391. Available at: https://doi.org/10.1038/nature00935.

Giannini, M. and Porrua, O. (2024) 'Senataxin: A key actor in RNA metabolism, genome integrity and neurodegeneration', *Biochimie*, 217, pp. 10–19. Available at: https://doi.org/10.1016/j.biochi.2023.08.001.

Ginno, P.A. *et al.* (2012) 'R-Loop Formation Is a Distinctive Characteristic of Unmethylated Human CpG Island Promoters', *Molecular Cell*, 45(6), pp. 814–825. Available at: https://doi.org/10.1016/j.molcel.2012.01.017.

Gómez-González, B. *et al.* (2011) 'Genome-wide function of THO/TREX in active genes prevents R-loop-dependent replication obstacles', *The EMBO Journal*, 30(15), pp. 3106–3119. Available at: https://doi.org/10.1038/emboj.2011.206.

Graf, M. *et al.* (2017) 'Telomere Length Determines TERRA and R-Loop Regulation through the Cell Cycle', *Cell*, 170(1), pp. 72–85. Available at: https://doi.org/10.1016/j.cell.2017.06.006.

Greider, C.W. and Blackburn, E.H. (1989) 'A telomeric sequence in the RNA of Tetrahymena telomerase required for telomere repeat synthesis', *Nature*, 337(6205), pp. 331–337. Available at: https://doi.org/10.1038/337331a0.

Groh, M. *et al.* (2017) 'Senataxin: Genome Guardian at the Interface of Transcription and Neurodegeneration', *Journal of Molecular Biology*, 429(21), pp. 3181–3195. Available at: https://doi.org/10.1016/j.jmb.2016.10.021.

Grunseich, C. *et al.* (2018) 'Senataxin Mutation Reveals How R-Loops Promote Transcription by Blocking DNA Methylation at Gene Promoters', *Molecular Cell*, 69(3), pp. 426-437.e7. Available at: https://doi.org/10.1016/j.molcel.2017.12.030.

Haidara, N., Giannini, M. and Porrua, O. (2022) 'Modulated termination of non-coding transcription partakes in the regulation of gene expression', *Nucleic Acids Research*, 50(3), pp. 1430–1448. Available at: https://doi.org/10.1093/nar/gkab1304.

Hamperl, S. *et al.* (2017) 'Transcription-Replication Conflict Orientation Modulates R-Loop Levels and Activates Distinct DNA Damage Responses', *Cell*, 170(4), pp. 774-786.e19. Available at: https://doi.org/10.1016/j.cell.2017.07.043.

Han, Z., Libri, D. and Porrua, O. (2017) 'Biochemical characterization of the helicase Sen1 provides new insights into the mechanisms of non-coding transcription termination', *Nucleic Acids Research*, 45(3), pp. 1355–1370. Available at: https://doi.org/10.1093/nar/gkw1230.

Hartwell, L.H. *et al.* (1973) 'Genetic Control Of The Cell Division Cycle In Yeast: V. Genetic Analysis Of *cdc* Mutants', *Genetics*, 74(2), pp. 267–286. Available at: https://doi.org/10.1093/genetics/74.2.267.

Hasanova, Z. *et al.* (2023) 'Human senataxin is a bona fide R-loop resolving enzyme and transcription termination factor', *Nucleic Acids Research*, 51(6), pp. 2818–2837. Available at: https://doi.org/10.1093/nar/gkad092.

Hatchi, E. *et al.* (2015) 'BRCA1 Recruitment to Transcriptional Pause Sites Is Required for R-Loop-Driven DNA Damage Repair', *Molecular Cell*, 57(4), pp. 636–647. Available at: https://doi.org/10.1016/j.molcel.2015.01.011.

Heuzé, J. *et al.* (2023) 'RNase H2 degrades toxic RNA:DNA hybrids behind stalled forks to promote replication restart', *The EMBO Journal*, 42(23), p. e113104. Available at: https://doi.org/10.15252/embj.2022113104.

Holt, I.J. (2019) 'The Jekyll and Hyde character of RNase H1 and its multiple roles in mitochondrial DNA metabolism', *DNA Repair*, 84(January), p. 102630. Available at: https://doi.org/10.1016/j.dnarep.2019.06.001.

Hyjek, M., Figiel, M. and Nowotny, M. (2019) 'RNases H: Structure and mechanism', *DNA Repair*, 84, p. 102672. Available at: https://doi.org/10.1016/j.dnarep.2019.102672.

Ivanova, T. *et al.* (2020) 'Budding yeast complete DNA synthesis after chromosome segregation begins', *Nature Communications*, 11(1), pp. 1–13. Available at: https://doi.org/10.1038/s41467-020-16100-3.

Janke, C. *et al.* (2004) 'A versatile toolbox for PCR-based tagging of yeast genes: new fluorescent proteins, more markers and promoter substitution cassettes', *Yeast*, 21, pp. 947–962. Available at: https://doi.org/10.1002/yea.1142.

Jones, R.M. *et al.* (2013) 'Increased replication initiation and conflicts with transcription underlie Cyclin E-induced replication stress', *Oncogene*, 32(32), pp. 3744–3753. Available at: https://doi.org/10.1038/onc.2012.387.

Jumper, J. *et al.* (2021) 'Highly accurate protein structure prediction with AlphaFold', *Nature*, 596(7873), pp. 583–589. Available at: https://doi.org/10.1038/s41586-021-03819-2.

Kielpinski, L.J. *et al.* (2017) 'RNase H sequence preferences influence antisense oligonucleotide efficiency', *Nucleic Acids Research*, 45(22), pp. 12932–12944. Available at: https://doi.org/10.1093/nar/gkz065.

Kim, N. and Jinks-Robertson, S. (2017) 'The Top1 paradox: Friend and foe of the eukaryotic genome', *DNA Repair*, 56, pp. 33–41. Available at: https://doi.org/10.1016/j.dnarep.2017.06.005.

König, F., Schubert, T. and Längst, G. (2017) 'The monoclonal S9.6 antibody exhibits highly variable binding affinities towards different R-loop sequences', *PLoS ONE*, 12(6), pp. 1–13. Available at: https://doi.org/10.1371/journal.pone.0178875.

Kramara, J., Osia, B. and Malkova, A. (2018) 'Break-Induced Replication: The Where, The Why, and The How', *Trends in Genetics*, 34(7), pp. 518–531. Available at: https://doi.org/10.1016/j.tig.2018.04.002.

Kumar, C. *et al.* (2021) 'The interplay of RNA:DNA hybrid structure and G-quadruplexes determines the outcome of R-loop-replisome collisions', *eLife*, 10, p. e72286. Available at: https://doi.org/10.7554/eLife.72286.

Lafuente-Barquero, J. *et al.* (2020) 'Harmful DNA:RNA hybrids are formed in cis and in a rad51-independent manner', *eLife*, 9, pp. 1–19. Available at: https://doi.org/10.7554/ELIFE.56674.

Lang, K.S. and Merrikh, H. (2021) 'Topological stress is responsible for the detrimental outcomes of head-on replication-transcription conflicts', *Cell Reports*, 34(9), p. 108797. Available at: https://doi.org/10.1016/j.celrep.2021.108797.

Lee, H. *et al.* (2021) 'RNase H is an exo- and endoribonuclease with asymmetric directionality , depending on the binding mode to the structural variants of RNA : DNA hybrids', (9), pp. 1–14. Available at: https://doi.org/10.1093/nar/gkab1064.

Li, Le *et al.* (2023) 'The CHCHD2/Sirt1 corepressors involve in G9a-mediated regulation of RNase H1 expression to control R-loop', *Cell Insight*, 2(4), p. 100112. Available at: https://doi.org/10.1016/j.cellin.2023.100112.

Li, Y. *et al.* (2024) 'RPA transforms RNase H1 to a bidirectional exoribonuclease for processive RNA–DNA hybrid cleavage', *Nature Communications*, 15(1), p. 7464. Available at: https://doi.org/10.1038/s41467-024-51984-5.

Lockhart, A. *et al.* (2019) 'RNase H1 and H2 Are Differentially Regulated to Process RNA-DNA Hybrids', *Cell Reports*, 29(9), pp. 2890-2900.e5. Available at: https://doi.org/10.1016/j.celrep.2019.10.108.

Maestroni, L. *et al.* (2020) 'RPA and Pif1 cooperate to remove G-rich structures at both leading and lagging strand', *Cell Stress*, 4(3), pp. 48–63. Available at: https://doi.org/10.15698/cst2020.03.214.

Malig, M. *et al.* (2020) 'Ultra-deep Coverage Single-molecule R-loop Footprinting Reveals Principles of R-loop Formation', *Journal of Molecular Biology*, 432(7), pp. 2271–2288. Available at: https://doi.org/10.1016/j.jmb.2020.02.014.

Manzo, S.G. *et al.* (2018) 'DNA Topoisomerase I differentially modulates R-loops across the human genome', *Genome Biology*, 19(1), pp. 1–18. Available at: https://doi.org/10.1186/s13059-018-1478-1.

Marnef, A. and Legube, G. (2021) 'R-loops as Janus-faced modulators of DNA repair', *Nature Cell Biology*, 23, pp. 305–313. Available at: https://doi.org/10.1038/s41556-021-00663-4.

Matsui, M. *et al.* (2020) 'USP42 enhances homologous recombination repair by promoting R-loop resolution with a DNA–RNA helicase DHX9', *Oncogenesis*, 9(6), p. 60. Available at: https://doi.org/10.1038/s41389-020-00244-4.

Mazina, O.M. *et al.* (2017) 'Rad52 Inverse Strand Exchange Drives RNA-Templated DNA Double-Strand Break Repair', *Molecular Cell*, 67(1), pp. 19-29.e3. Available at: https://doi.org/10.1016/j.molcel.2017.05.019.

Mazina, O.M. *et al.* (2020) 'Replication protein A binds RNA and promotes R-loop formation', *The Journal of biological chemistry*, 295(41), pp. 14203–14213. Available at: https://doi.org/10.1074/jbc.RA120.013812.

McElhinny, S.A.N. *et al.* (2010) 'Genome instability due to ribonucleotide incorporation into DNA', *Nature Chemical Biology*, 6(10), pp. 774–781. Available at: https://doi.org/10.1038/nchembio.424.

Mérida-Cerro, J.A. *et al.* (2024) 'Rat1 promotes premature transcription termination at R-loops', *Nucleic Acids Research*, 52(7), pp. 3623–3635. Available at: https://doi.org/10.1093/nar/gkae033.

Michelini, F. *et al.* (2017) 'Damage-induced lncRNAs control the DNA damage response through interaction with DDRNAs at individual double-strand breaks', *Nature Cell Biology*, 19(12), pp. 1400–1411. Available at: https://doi.org/10.1038/ncb3643.

Mischo, H.E. *et al.* (2011) 'Yeast Sen1 helicase protects the genome from transcription-associated instability', *Molecular Cell*, 41(1), pp. 21–32. Available at: https://doi.org/10.1016/j.molcel.2010.12.007.

Mischo, H.E. *et al.* (2018) 'Cell-Cycle Modulation of Transcription Termination Factor Sen1', *Molecular Cell*, 70(2), pp. 312-326.e7. Available at: https://doi.org/10.1016/j.molcel.2018.03.010.

Misino, S. *et al.* (2022) 'TERRA increases at short telomeres in yeast survivors and regulates survivor associated senescence (SAS)', *Nucleic Acids Research*, 50(22), pp. 12829–12843. Available at: https://doi.org/10.1093/nar/gkac1125.

Mohr, S. *et al.* (2013) 'Thermostable group II intron reverse transcriptase fusion proteins and their use in cDNA synthesis and next-generation RNA sequencing', *RNA*, 19(7), pp. 958–970. Available at: https://doi.org/10.1261/rna.039743.113.

Monteuuis, G. *et al.* (2019) 'Non-canonical translation initiation in yeast generates a cryptic pool of mitochondrial proteins', *Nucleic Acids Research*, 47(11), pp. 5777–5791. Available at: https://doi.org/10.1093/nar/gkz301.

Morawska, M. and Ulrich, H.D. (2013) 'An expanded tool kit for the auxin-inducible degron system in budding yeast', *Yeast*, 30, pp. 341–351. Available at: https://doi.org/10.1002/yea.

Mukhopadhyay, P. *et al.* (2024) 'Approaches for Mapping and Analysis of R-loops', *Current Protocols*, 4(4), p. e1037. Available at: https://doi.org/10.1002/cpz1.1037.

Nguyen, H.D. *et al.* (2017) 'Functions of Replication Protein A as a Sensor of R Loops and a Regulator of RNaseH1', *Molecular Cell*, 65(5), pp. 832-847.e4. Available at: https://doi.org/10.1016/j.molcel.2017.01.029.

Niehrs, C. and Luke, B. (2020) 'Regulatory R-loops as facilitators of gene expression and genome stability', *Nature Reviews Molecular Cell Biology*, 21(3), pp. 167–178. Available at: https://doi.org/10.1038/s41580-019-0206-3.

O'Connell, K., Jinks-Robertson, S. and Petes, T.D. (2015) 'Elevated Genome-wide instability in yeast mutants lacking RNase H activity', *Genetics*, 201(3), pp. 963–975. Available at: https://doi.org/10.1534/genetics.115.182725.

Ohle, C. *et al.* (2016) 'Transient RNA-DNA Hybrids Are Required for Efficient Double-Strand Break Repair', *Cell*, 167(4), pp. 1001-1013.e7. Available at: https://doi.org/10.1016/j.cell.2016.10.001.

Ortega, P. *et al.* (2021) 'DNA-RNA hybrids at DSBs interfere with repair by homologous recombination', *eLife*, 10, p. e69881. Available at: https://doi.org/10.7554/eLife.69881.

Parajuli, S. *et al.* (2017) 'Human ribonuclease H1 resolves R-loops and thereby enables progression of the DNA replication fork', *Journal of Biological Chemistry*, 292(37), pp. 15216–15224. Available at: https://doi.org/10.1074/jbc.M117.787473.

Peña, Á. *et al.* (2012) 'Architecture and nucleic acids recognition mechanism of the THO complex, an mRNP assembly factor: Structure and function of the THO complex', *The EMBO Journal*, 31(6), pp. 1605–1616. Available at: https://doi.org/10.1038/emboj.2012.10.

Porrua, O. *et al.* (2012) 'In vivo SELEX reveals novel sequence and structural determinants of Nrd1-Nab3-Sen1-dependent transcription termination', *EMBO Journal*, 31(19), pp. 3935–3948. Available at: https://doi.org/10.1038/emboj.2012.237.

Porrua, O., Boudvillain, M. and Libri, D. (2016) 'Transcription Termination: Variations on Common Themes', *Trends in Genetics*, 32(8), pp. 508–522. Available at: https://doi.org/10.1016/j.tig.2016.05.007.

Porrua, O. and Libri, D. (2015) 'Transcription termination and the control of the transcriptome: Why, where and how to stop', *Nature Reviews Molecular Cell Biology*, 16(3), pp. 190–202. Available at: https://doi.org/10.1038/nrm3943.

Promonet, A. *et al.* (2020) 'Topoisomerase 1 prevents replication stress at R-loop-enriched transcription termination sites', *Nature Communications*, (2020), pp. 1–12. Available at: https://doi.org/10.1038/s41467-020-17858-2.

Rao, S. *et al.* (2024) 'Senataxin RNA/DNA helicase promotes replication restart at co-transcriptional R-loops to prevent MUS81-dependent fork degradation', *Nucleic Acids Research*, p. gkae673. Available at: https://doi.org/10.1093/nar/gkae673.

Rawal, C.C. *et al.* (2020) 'Senataxin Ortholog Sen1 Limits DNA:RNA Hybrid Accumulation at DNA Double-Strand Breaks to Control End Resection and Repair Fidelity', *Cell Reports*, 31(5), p. 107603. Available at: https://doi.org/10.1016/j.celrep.2020.107603.

Renaudin, X. *et al.* (2021) 'BRCA2 deficiency reveals that oxidative stress impairs RNaseH1 function to cripple mitochondrial DNA maintenance', *Cell Reports*, 36(5), p. 109478. Available at: https://doi.org/10.1016/j.celrep.2021.109478.

Ribeiro De Almeida, C. *et al.* (2018) 'RNA Helicase DDX1 Converts RNA G-Quadruplex Structures into R-Loops to Promote IgH Class Switch Recombination', *Molecular Cell*, 70(4), pp. 650-662.e8. Available at: https://doi.org/10.1016/j.molcel.2018.04.001.

Rivosecchi, J. *et al.* (2019) 'Senataxin homologue Sen1 is required for efficient termination of RNA polymerase III transcription', *The EMBO Journal*, 38(16), pp. 1–14. Available at: https://doi.org/10.15252/embj.2019101955.

Roy, S. *et al.* (2024) 'The Smc5/6 complex counteracts R-loop formation at highly transcribed genes in cooperation with RNase H2', *eLife*, 13, p. e96626. Available at: https://doi.org/10.7554/eLife.96626.

Sagi, T. *et al.* (2024) 'RNA–DNA hybrids on protein coding genes are stabilized by loss of RNase H and are associated with DNA damages during S-phase in fission yeast', *Genes to Cells*, 29(11), pp. 966–982. Available at: https://doi.org/10.1111/gtc.13157.

San Martin-Alonso, M. *et al.* (2021) 'Harmful R-loops are prevented via different cell cycle-specific mechanisms', *Nature Communications*, 12(1), p. 4451. Available at: https://doi.org/10.1038/s41467-021-24737-x.

Santos-Pereira, J.M. *et al.* (2013) 'The Npl3 hnRNP prevents R-loop-mediated transcription-replication conflicts and genome instability', *Genes & Development*, 27(22), pp. 2445–2458. Available at: https://doi.org/10.1101/gad.229880.113.

Sanz, L.A. *et al.* (2016) 'Prevalent, Dynamic, and Conserved R-Loop Structures Associate with Specific Epigenomic Signatures in Mammals', *Molecular Cell*, 63(1), pp. 167–178. Available at: https://doi.org/10.1016/j.molcel.2016.05.032.

Segurado, M. and Tercero, J.A. (2009) 'The S-phase checkpoint: targeting the replication fork', *Biology of the Cell*, 101(11), pp. 617–627. Available at: https://doi.org/10.1042/BC20090053.

Silva, S., Guillén-Mendoza, C. and Aguilera, A. (2022) 'RNase H1 Hybrid-Binding Domain-Based Tools for Cellular Biology Studies of DNA–RNA Hybrids in Mammalian Cells', in A. Aguilera and A. Ruzov (eds) *R-Loops*. New York, NY: Springer US (Methods in Molecular Biology), pp. 115–125. Available at: https://doi.org/10.1007/978-1-0716-2477-7_8.

Singer, M.S. and Gottschling, D.E. (1994) '*TLC1* : Template RNA Component of *Saccharomyces cerevisiae* Telomerase', *Science*, 266(5184), pp. 404–409. Available at: https://doi.org/10.1126/science.7545955.

Skourti-Stathaki, K., Proudfoot, N.J. and Gromak, N. (2011) 'Human Senataxin Resolves RNA/DNA Hybrids Formed at Transcriptional Pause Sites to Promote Xrn2-Dependent Termination', *Molecular Cell*, 42(6), pp. 794–805. Available at: https://doi.org/10.1016/j.molcel.2011.04.026.

Smolka, J.A. *et al.* (2021) 'Recognition of RNA by the S9.6 antibody creates pervasive artifacts when imaging RNA:DNA hybrids', *Journal of Cell Biology*, 220(6), p. e202004079. Available at: https://doi.org/10.1083/jcb.202004079.

Stoy, H. *et al.* (2023) 'Direct visualization of transcription-replication conflicts reveals post-replicative DNA:RNA hybrids', *Nature Structural & Molecular Biology*, 30(3), pp. 348–359. Available at: https://doi.org/10.1038/s41594-023-00928-6.

Sui, Y. *et al.* (2022) 'Ribodysgenesis: sudden genome instability in the yeast *Saccharomyces cerevisiae* arising from RNase H2 cleavage at genomic-embedded ribonucleotides', *Nucleic Acids Research*, 50(12), pp. 6890–6902. Available at: https://doi.org/10.1093/nar/gkac536.

Sun, H. *et al.* (2023) 'Okazaki fragment maturation: DNA flap dynamics for cell proliferation and survival', *Trends in Cell Biology*, 33(3), pp. 221–234. Available at: https://doi.org/10.1016/j.tcb.2022.06.014.

Suzuki, Y. *et al.* (2010) 'An Upstream Open Reading Frame and the Context of the Two AUG Codons Affect the Abundance of Mitochondrial and Nuclear RNase H1', *Molecular and Cellular Biology*, 30(21), pp. 5123–5134. Available at: https://doi.org/10.1128/MCB.00619-10.

Tan-Wong, S.M., Dhir, S. and Proudfoot, N.J. (2019) 'R-Loops Promote Antisense Transcription across the Mammalian Genome', *Molecular Cell*, 76(4), pp. 600-616.e6. Available at: https://doi.org/10.1016/j.molcel.2019.10.002.

Tran, P.L.T. *et al.* (2017) 'PIF1 family DNA helicases suppress R-loop mediated genome instability at tRNA genes', *Nature Communications*, 8(1), p. 15025. Available at: https://doi.org/10.1038/ncomms15025.

Vanoosthuyse, V. (2018) 'Strengths and Weaknesses of the Current Strategies to Map and Characterize R-Loops', *Non-Coding RNA*, 4(2), p. 9. Available at: https://doi.org/10.3390/ncrna4020009.

Visintin, R., Prinz, S. and Amon, A. (1997) 'CDC20 and CDH1: A Family of Substrate-Specific Activators of APC-Dependent Proteolysis', *Science*, 278(5337), pp. 460–463. Available at: https://doi.org/10.1126/science.278.5337.460.

Wach, A. *et al.* (1994) 'New Heterologous Modules for Classical or PCR-based Gene Disruptions in Saccharomyces cerevisiae', *Yeast*, 10, pp. 1793–1808. Available at: https://doi.org/10.1002/yea.320101310.

Wagner, C.B. and Luke, B. (2022) 'DNA–RNA Hybrids at Telomeres in Budding Yeast', *Methods in Molecular Biology*, 2528, pp. 145–157. Available at: https://doi.org/10.1007/978-1-0716-2477-7_10.

Wahba, L. *et al.* (2011) 'RNase H and Multiple RNA Biogenesis Factors Cooperate to Prevent RNA : DNA Hybrids from Generating Genome Instability', *MOLCEL*, 44(6), pp. 978–988. Available at: https://doi.org/10.1016/j.molcel.2011.10.017.

Wahba, L. *et al.* (2016) 'S1-DRIP-seq identifies high expression and polyA tracts as major contributors to R-loop formation', *Genes and Development*, 30(11), pp. 1327–1338. Available at: https://doi.org/10.1101/gad.280834.116.

Wahba, L., Gore, S.K. and Koshland, D. (2013) 'The homologous recombination machinery modulates the formation of RNA-DNA hybrids and associated chromosome instability', *eLife*, 2:e00505, pp. 1–20. Available at: https://doi.org/10.7554/eLife.00505.

Wang, K. *et al.* (2021) 'Genomic profiling of native R loops with a DNA-RNA hybrid recognition sensor.', *Science advances*, 7(8), pp. 1–18. Available at: https://doi.org/10.1126/sciadv.abe3516.

Wellinger, R.E., Prado, F. and Aguilera, A. (2006) 'Replication Fork Progression Is Impaired by Transcription in Hyperrecombinant Yeast Cells Lacking a Functional THO Complex', *Molecular and Cellular Biology*, 26(8), pp. 3327–3334. Available at: https://doi.org/10.1128/MCB.26.8.3327-3334.2006.

Wen, X. *et al.* (2024) 'Senataxin deficiency disrupts proteostasis through nucleolar ncRNA-driven protein aggregation', *Journal of Cell Biology*, 223(7), p. e202309036. Available at: https://doi.org/10.1083/jcb.202309036.

Winzeler, E.A. *et al.* (1999) 'Functional Characterization of the *S. cerevisiae* Genome by Gene Deletion and Parallel Analysis', *Science*, 285(5429), pp. 901–906. Available at: https://doi.org/10.1126/science.285.5429.901.

Wittekind, M. *et al.* (1988) 'Isolation and characterization of temperature-sensitive mutations in RPA190, the gene encoding the largest subunit of RNA polymerase I from Saccharomyces cerevisiae.', *Molecular and Cellular Biology*, 8(10), pp. 3997–4008. Available at: https://doi.org/10.1128/MCB.8.10.3997.

Wolak, C. *et al.* (2020) *Interaction with single-stranded DNA-binding protein localizes ribonuclease HI to DNA replication forks and facilitates R-loop removal*, *Molecular Microbiology*. Available at: https://doi.org/10.1111/mmi.14529.

Wu, H., Lima, W.F. and Crooke, S.T. (2001) 'Investigating the Structure of Human RNase H1 by Site-directed Mutagenesis', *Journal of Biological Chemistry*, 276(26), pp. 23547–23553. Available at: https://doi.org/10.1074/jbc.M009676200.

Xie, J. *et al.* (2022) 'An integrated model for termination of RNA polymerase III transcription', *Science Advances*, 8(28), pp. 19–22. Available at: https://doi.org/10.1126/sciadv.abm9875.

Xie, J., Libri, D. and Porrua, O. (2023) 'Mechanisms of eukaryotic transcription termination at a glance', *Journal of Cell Science*, 136(1), pp. 1–7. Available at: https://doi.org/10.1242/jcs.259873.

Xu, C. *et al.* (2021) 'R-loop resolution promotes co-transcriptional chromatin silencing', *Nature Communications*, 12(1), p. 1790. Available at: https://doi.org/10.1038/s41467-021-22083-6.

Xu, H. *et al.* (2019) 'Improved TGIRT-seq methods for comprehensive transcriptome profiling with decreased adapter dimer formation and bias correction', *Scientific Reports*, 9(1), p. 7953. Available at: https://doi.org/10.1038/s41598-019-44457-z.

Yan, Q. *et al.* (2019) 'Mapping Native R-Loops Genome-wide Using a Targeted Nuclease Approach', *Cell Reports*, 29(5), pp. 1369-1380.e5. Available at: https://doi.org/10.1016/j.celrep.2019.09.052.

Yang, S. *et al.* (2023) 'Helicases in R-loop Formation and Resolution', *Journal of Biological Chemistry*, 299(11), p. 105307. Available at: https://doi.org/10.1016/j.jbc.2023.105307.

Yi, C. *et al.* (2023) 'A pan-cancer analysis of RNASEH1, a potential regulator of the tumor microenvironment', *Clinical and Translational Oncology*, 25(8), pp. 2569–2586. Available at: https://doi.org/10.1007/s12094-023-03142-4.

Yu, K. *et al.* (2003) 'R-loops at immunoglobulin class switch regions in the chromosomes of stimulated B cells', *Nature Immunology*, 4(5), pp. 442–451. Available at: https://doi.org/10.1038/ni919.

Yu, Z. *et al.* (2020) 'DDX5 resolves R-loops at DNA double-strand breaks to promote DNA repair and avoid chromosomal deletions', *NAR Cancer*, 2(3), p. zcaa028. Available at: https://doi.org/10.1093/narcan/zcaa028.

Zardoni, L. *et al.* (2021) 'Elongating RNA polymerase II and RNA:DNA hybrids hinder fork progression and gene expression at sites of head-on replication-transcription collisions', *Nucleic Acids Research*, 49(22), pp. 12769–12784. Available at: https://doi.org/10.1093/nar/gkab1146.

Zhang, J. *et al.* (2024) 'The ARID1A-METTL3-m6A axis ensures effective RNase H1-mediated resolution of R-loops and genome stability', *Cell Reports*, 43(2), p. 113779. Available at: https://doi.org/10.1016/j.celrep.2024.113779.

Zhao, H. *et al.* (2018) 'RNase H eliminates R-loops that disrupt DNA replication but is nonessential for efficient DSB repair', *EMBO reports*, 19(5), pp. 1–10. Available at: https://doi.org/10.15252/embr.201745335.

Zheng, K.W. *et al.* (2017) 'Superhelicity Constrains a Localized and R-Loop-Dependent Formation of G-Quadruplexes at the Upstream Region of Transcription', *ACS Chemical Biology*, 12(10), pp. 2609–2618. Available at: https://doi.org/10.1021/acschembio.7b00435.

Zimmer, A.D. and Koshland, D. (2016) 'Differential roles of the RNases H in preventing chromosome instability', *Proceedings of the National Academy of Sciences of the United States of America*, 113(43), pp. 12220–12225. Available at: https://doi.org/10.1073/pnas.1613448113.